The emergence of visual responses in the developing retinotectal system *in vivo*

Joram Jacob van Rheede



Thesis submitted for the degree of Doctor of Philosophy

University College
University of Oxford
Trinity term 2013

Abstract

The emergence of visual responses in the developing retinotectal system in vivo

Joram Jacob van Rheede
University College, Oxford

Submitted for the degree of Doctor of Philosophy
Trinity Term 2013

Patterned neuronal activity driven by the sensory environment plays a key role in the development of precise synaptic connectivity in the brain. It is well established that the action potentials ('spikes') generated by individual neurons are crucial to this developmental process. A neuron's spiking activity is jointly determined by its synaptic inputs and its intrinsic excitability. It is therefore important to ask how a neuron develops these attributes, and whether the emergence of spiking might itself be governed by activity-dependent processes. In this thesis, I address these questions in the retinotectal system of Xenopus laevis.

First, I investigate the extent to which visuospatial information is available to the developing retinotectal system. I show that the eyes of developing Xenopus larvae are hyperopic at the onset of vision, but rapidly grow towards correct vision. Despite its imperfect optics, the Xenopus eye is able to generate spatially restricted activity on the retina, which is evident in the spatial structure of the receptive fields (RFs) of tectal neurons. Using a novel method to map the visually driven spiking output and synaptic inputs of the same tectal neuron *in vivo*, I show that neuronal spiking activity closely follows the spatiotemporal profile of glutamatergic inputs.

Next, I characterise a population of neurons in the developing optic tectum that does not fire action potentials, despite receiving visually evoked glutamatergic and γ-aminobutyric acid (GABA)ergic synaptic inputs. A comparison of visually spiking and visually non-spiking neurons reveals that the principal reason these neurons are 'silent' is that they lack sufficient glutamatergic synaptic excitation.

In the final section of the thesis, I investigate whether visually driven activity can play a role in the 'unsilencing' of these silent neurons. I show that non-spiking tectal neurons can be rapidly converted into spiking neurons through a visual conditioning protocol. This conversion is associated with a selective increase in glutamatergic input and implicates a novel, spike-independent form of synaptic potentiation. I provide evidence that this novel plasticity process is mediated by GABAergic inputs that are depolarising during early development, and can act in synergy with N-methyl-D-aspartate receptors (NMDARs) to strengthen immature glutamatergic synapses. Consistent with this, preventing the depolarising effects of GABA or blocking NMDARs abolished the activity-dependent unsilencing of tectal neurons.

These results therefore support a model in which GABAergic and glutamatergic transmitter systems function synergistically to enable a neuron to recruit the synaptic excitation it needs to develop sensory-driven spiking activity. This represents a transition with important consequences for both the functional output and the activity-dependent development of a neuron.

Acknowledgements

First of all I have to thank Dr. Colin Akerman, who is a brilliant scientist, and a fantastic supervisor and mentor. I greatly admire his ability distil the essence out of every scientific story and to find the story hidden in every data set. I have learnt, and continue to learn, a lot from him. I have also never had more useful, more constructive or more thorough feedback, although I currently have a love / hate relationship with his attention to detail.

I am greatly indebted to Dr. Blake Richards who showed me the ropes and paved the way for *in vivo* recordings of visual responses in the Xenopus optic tectum – you did all the hard work! I also don't know whether to thank or curse you for setting such a bloody high standard. Specifically, data collection and analysis for Figures 3.1-3.3 were carried out jointly, and Dr. Richards designed the computer simulation of a tectal neuron used in Figure 4.4 and provided data used in Figure 4.1d and Figure 5.3.

I should also thank my co-supervisor Dr. Karri Lämsä, who was always available for helpful discussions and useful advice.

The other members of the Akerman lab have made it a pleasure to work here and have provided their insights, inspiration and plenty of excuses to go for a drink, and they have not been shy about demanding cake. I might have to thank Joe in particular for being a nocturnal companion during the final formative moments of this thesis and suffering through my caffeine-fuelled progress reports.

Thanks also to Dr. Deborah Clarke and the organising committee of the MSc and 4-year Doctoral programme in Neuroscience, for this fantastic opportunity and for making this course such a rewarding experience, academically and otherwise. Which brings me to the next point - thanks to the whole MSc Neuro gang, who have made it tremendously fun to hang around in Oxford for all this time. Patchclamp!

The Wellcome Trust provided generous funding for this research.

Dr. Jeremy Taylor provided fixed retinal tissue that was used for the anatomical measurements in Chapter 3.

I should also recognise my mentors, official or otherwise, at the University of Utrecht: Prof. Frans Verstraten and Dr. Jocelyn Ballantyne, who have been inspiring and supportive, and Dr. Ignace Hooge, who is rarely correct but usually right.

I owe many drinks to Mike for generally keeping me sane during the past year (or just making me look sane by comparison… or all three), for making sure that there is always some project or other brewing in the house, and for generally injecting some rock 'n roll into everything.

Layla, for putting up with my capricious mistress Science and my thesis beard, for being incredibly supportive and never failing to find some spare time in the mighty filofax. You are amazing.

En natuurlijk mijn ouders, Jurriën en Anne, de hele prettig gestoorde bende thuis (ja, dat zijn jullie, Jannick, Jafeth, Jiddon en Jenthe), en ook de opa's en oma's De Weerd en Van Rheede, voor alle aanmoediging van afstand en omdat jullie ervoor zorgen dat het altijd weer voelt alsof ik nooit ben weggeweest.

Table of Contents

Abstract I

Acknowledgements II

Table of contents III

List of figures V

Chapter 1
Introduction **1**
1.1 The development of precise connectivity in the visual system 2
1.2 Integration of synaptic inputs and spike generation during development 9
1.3 Synapse formation and plasticity 16
1.4 The aims of this thesis 22

Chapter 2
Methods **24**
2.1 Animals 24
2.2 Focal length measurements 24
2.3 Eye measurements 25
2.4 Estimating image resolution 25
2.5 *In vivo* preparation for electrophysiology 27
2.6 Visual stimulation 27
2.7 Electrophysiological recordings 29
2.8 Recording spiking output, synaptic inputs and intrinsic excitability of the same tectal neuron *in vivo* 30
2.9 Assessment of intrinsic excitability 31
2.10 Conversion of visually non-spiking tectal neurons 31
2.11 Assessing the effect of GABAergic responses 32
2.12 Recording visually evoked NMDAR currents 33
2.13 Detection of glutamatergic and GABAergic PSCs 34
2.14 Spike detection and defining visually spiking and non-spiking neurons 34
2.15 RF maps 35
2.16 Assessment of instructive RF change 35
2.17 Computer simulations of developing tectal neurons 36
2.18 Data analysis and statistics 37

Chapter 3
Visuospatial information in the developing retinotectal system at the onset of vision **38**
3.1 Tadpole eyes undergo a developmental emmetropisation 40
3.2 Visuospatial information is present in synaptic inputs to tectal neurons and can lead to spatially specific output at the onset of vision 46
3.3 Glutamatergic inputs are the major driver of tectal neuron spiking activity at the onset of vision 51
3.4 Discussion 56

Chapter 4
A population of non-spiking neurons in the developing optic tectum **60**
4.1 A population of visually non-spiking neurons in the developing optic tectum 61
4.2 Visually non-spiking tectal neurons have weak glutamatergic synaptic drive 63
4.3 Spatiotemporal organisation of synaptic inputs to non-spiking neurons 69
4.4 Discussion 71

Chapter 5
Visually driven unsilencing of non-spiking tectal neurons **76**
5.1 Visually non-spiking neurons can be rapidly converted into spiking neurons 79
5.2 Increased glutamatergic input underlies tectal neuron unsilencing 85
5.3 The unsilencing of tectal neurons requires depolarising GABAergic inputs and NMDA receptor activation 88
5.4 Discussion 93

Chapter 6
General discussion **97**
6.1 Experimental findings 97
6.2 The development of emmetropic vision 100
6.3 The availability of visuospatial information to the optic tectum 101
6.4 Silent neurons in the developing tectum 102
6.5 The relationship between spiking output and synaptic input in the developing optic tectum 103
6.6 The emergence of visual spiking activity in tectal neurons 106
6.7 A postsynaptic mechanism for activity-dependent unsilencing of silent neurons 107
6.8 Implications for activity-dependent development in the optic tectum 109
6.9 Concluding remarks 112

Appendix I
The onset of vision in Xenopus laevis **113**

Appendix II
Cell types in the developing optic tectum of Xenopus laevis **115**

References **118**

List of figures

Chapter 2
Methods

2.1 Experimental setup 27

Chapter 3
Visuospatial information in the developing retinotectal system at the onset of vision

3.1 The focal length of developing Xenopus laevis lenses decreases during early development 40
3.2 Xenopus laevis eyes undergo a developmental emmetropisation 42
3.3 The image forming properties of developing Xenopus eyes show a developmental improvement at the onset of vision 44
3.4 Tectal neurons can exhibit spatially restricted spiking RFs at the onset of vision 47
3.5 Tectal neurons can exhibit spatially restricted glutamatergic RFs at the onset of vision 48
3.6 Tectal neurons can exhibit spatially restricted GABAergic RFs at the onset of vision 49
3.7 Spiking, glutamatergic and GABAergic RFs are spatially matched at the onset of vision 52
3.8 Glutamatergic inputs are the most important contributors to spike timing at the onset of vision 54

Chapter 4
A population of non-spiking neurons in the developing optic tectum

4.1 A large proportion of developing tectal neurons receives visually evoked synaptic input but does not generate visually evoked spikes 61
4.2 Non-spiking tectal neurons are excitable and have voltage-gated currents similar to those of spiking neurons 63
4.3 Visually non-spiking neurons receive weaker glutamatergic synaptic input, but similar GABAergic synaptic input 65
4.4 Weak glutamatergic synaptic input accounts for the absence of visual spiking 67
4.5 Visually non-spiking neurons can have spatially restricted RFs 69
4.6 Visually evoked glutamatergic synaptic input arrives later to visually non-spiking neurons 71

Chapter 5
Visually driven unsilencing of non-spiking tectal neurons

5.1 Visual conditioning can convert visually non-spiking neurons into visually spiking neurons 80

5.2 Emergent spiking RFs of converted neurons can be spatially coherent 81
5.3 The conversion from visually non-spiking to visually spiking does not reflect the spatial properties of the conditioning stimulus 83
5.4 The conversion from visually non-spiking to visually spiking does not involve changes in intrinsic excitability 85
5.5 The conversion from visually non-spiking to visually spiking involves the recruitment of stronger glutamatergic input 86
5.6 A proposed mechanism for the recruitment of AMPAR-mediated glutamatergic input in visually non-spiking neurons 88
5.7 Visually non-spiking neurons exhibit depolarising GABAergic responses and NMDAR currents 90
5.8 Conversion of non-spiking neurons into visually spiking neurons is dependent on depolarising GABAergic responses and NMDAR activation 91

Appendix I
The onset of vision in Xenopus laevis

A1 The onset of vision in Xenopus laevis 113

Appendix II
Cell types in the developing optic tectum of Xenopus laevis

A2 Cell types in the developing optic tectum of Xenopus laevis 116

Chapter 1

Introduction

The brain is characterised by precise patterns of synaptic connectivity between neurons. From local circuits to long-range projections, this precise connectivity underlies the remarkable computational power of the brain. How such an intricate system of synaptic connections can develop has intrigued biologists ever since the complexity of the nervous system was first visualised (Ramón y Cajal 1909). While unfolding genetic programs and molecular gradients are essential for the guidance of long-range projections to their targets, various forms of neuronal activity provide developmental triggers and instructions for refining the strength and patterns of synaptic connectivity. Such neuronal activity ranges from spontaneous oscillations to sensory inputs driven by the environment. The influence of neuronal activity during development is most readily studied in the developing sensory systems of the brain, where activity can be experimentally controlled and manipulated simply by changing stimuli in the environment. Moreover, synaptic connections are generally systematically ordered throughout sensory pathways, which endow mature neurons with defined receptive fields (RFs), such that they respond only to a particular part of sensory space. This means that the state of a developing neuron's RF can be used as a readout of whether that neuron has established the appropriate pattern of synaptic connectivity.

In this thesis I investigate the influence of visually driven activity on the emergence of neuronal responses in the developing retinotectal system of Xenopus laevis. The retinotectal system is the animal's principal visual pathway, and has long been a model system for investigations into the establishment of precise neuronal connectivity during development (Gaze et al. 1972; Cline 1991; Debski & Cline 2002; Richards, Aizenman, et al. 2010a; Ruthazer & Cline 2004). The optic tectum receives visual inputs from the retina as soon as the axons of retinal ganglion cells make contact with developing tectal neurons ((Holt & Harris 1983), Chapter 3). This

makes Xenopus particularly well suited for studying the interaction of developing circuitry with neuronal activity driven by visual experience. Furthermore, the retinotectal system has been shown to be highly plastic during development, and neural activity can influence several properties of developing retinotectal circuitry, such as the morphology of retinal ganglion cell axons, the dendritic morphology of tectal neurons and the strength of synaptic connections (O'Rourke et al. 1994; Rajan & Cline 1998; Ruthazer et al. 2003; Tao & Poo 2005; L. I. Zhang et al. 1998; L. I. Zhang et al. 2000). To help place the findings of this thesis in the context of this previous work, a timeline of developmental events related to the onset of vision in the retinotectal system of Xenopus laevis has been provided in Appendix I.

First, I investigate the extent to which visuospatial information is available to the developing optic tectum, to determine whether it can provide a source of patterned activity to guide neuronal circuit development at the onset of vision. Second, I characterise a population of developing tectal neurons that receives visual synaptic input but remains silent, in the sense that these neurons do not generate any action potential output. Third, I investigate whether visually driven, patterned activity can play a role in the developmental 'unsilencing' of such silent neurons. I then propose and test a mechanism by which this unsilencing process might occur. These studies build upon a large body of work investigating the activity-dependent development of precise neuronal connectivity, the balancing of inhibitory and excitatory synaptic inputs with neuronal excitability, and the formation and plasticity of developing synapses. In this Chapter, I will introduce these themes and describe the work that has led up to the current study, as well as the outstanding issues that I aim to address experimentally.

1.1 The development of precise connectivity in the visual system

One of the reasons the visual system is attractive for studying the development of synaptic connectivity is that information is represented in orderly 'maps', which reflect the spatial organisation of the input stage of the visual system - the retina. Moreover, there is a natural correspondence between the position and shape of visual stimuli and the spatial location of the retinal photoreceptors that they activate. Therefore, a particular visual stimulus will produce a predictable pattern of activation in retinotopically organised visual areas. Retinotopic maps are found in brain structures throughout the visual pathway of vertebrates, such as the visual cortex (Talbot & Marshall 1941), the lateral geniculate nucleus (LGN) of the thalamus (Kaas

et al. 1972) and the superior colliculus (Cooper et al. 1953; Apter 1945), as well as its non-mammalian equivalent, the optic tectum (Gaze 1958; Gaze et al. 1974). These topographic maps are thought to play a fundamental role in sensory processing (Kaas 1997), providing an efficient wiring solution for local comparisons and allowing for the natural superposition of multisensory representations of space (e.g. in the superior colliculus; (Knudsen 1982)). The problem of how such precise connectivity develops has been a long-standing problem in the study of the nervous system.

Molecular mechanisms for establishing visuotopic connectivity

There is substantial evidence that developing nervous systems rely on molecular cues and gradients to establish initial topographic connectivity (McLaughlin & O'Leary 2005). This 'chemoaffinity' hypothesis was first articulated by Roger Sperry (Sperry 1963) based on work that examined the regeneration of retinotectal connectivity after optic nerve section. Various other *in vivo* experiments investigating patterns of growth and regeneration corroborated this hypothesis (Bonhoeffer & Gierer 1984). *In vitro* experiments using membranes derived from the target structures showed that there are chemical cues that affect retinal ganglion cell axons differentially, and as a function of their source within the retina (Walter, Henke-Fahle, et al. 1987a; Walter, Kern-Veits, et al. 1987b). Later research efforts have identified the molecules that generate chemical gradients in the brain, such as the Eph/ephrin family of receptors and ligands, which can account for much of the targeting of retinal axons in the retinotectal system (McLaughlin & O'Leary 2005).

Such molecular mechanisms ensure that topographic maps are already present throughout the visual pathway before the onset of visual experience. Consistent with this, retinotopically organised RFs were observed in the visual cortex of visually inexperienced or deprived kittens by Hubel and Wiesel (Hubel & Wiesel 1963). Indeed, a retinotopic map that is present before the onset of vision has since been described in primary visual cortex (Allman & Kaas 1971; Cang et al. 2005), the lateral geniculate nucleus of the thalamus (Kaas et al. 1972; Jeffery 1985; Pfeiffenberger et al. 2006), the mammalian superior colliculus (Chalupa & Snider 1998; King et al. 1998; Simon & O'Leary 1992) and the optic tectum of amphibia such as Xenopus (Sakaguchi & Murphey 1985), where neuronal RFs were also found to be retinotopically organised at the onset of vision (Gaze et al. 1974; Holt & Harris 1983).

However, there is evidence that initial connectivity is not yet fully refined (e.g. (Simon & O'Leary 1992; Cline 1998)). Retinal ganglion cell axons initially extend beyond their final location in the retinotopic map in the mammalian superior colliculus and, in amphibians, initial axonal branching is more widespread than in the adult (McLaughlin & O'Leary 2005). After initial connectivity is established, synaptic connections undergo a period of restructuring (McLaughlin & O'Leary 2005; Cline 1998). An added factor in the developing amphibian retinotectal system is that the tectum undergoes considerable expansion over development, with neurogenesis occurring particularly on the caudal side of the map, while retinal expansion is concentric. The retinotopic map of the amphibian tectum therefore needs to continuously shift over development to keep up with these changes (Gaze et al. 1979). It is hard to account for such refinement or changes by means of static molecular gradients alone, suggesting that there are other, more dynamic processes, which guide map development beyond 'chemoaffinity'.

Neuronal activity guides the development of precise connectivity

A variety of studies have shown that there is more to the development of topographically organised visual response properties than just molecular cues. In most developing visual systems that have been studied, synaptic connectivity is refined by neuronal activity (Huberman et al. 2008; L. C. Katz & Shatz 1996; McLaughlin & O'Leary 2005). It was already appreciated by Hebb (Hebb 1949) that a mechanism that could detect correlated activity between neurons, and strengthen only those connections that contributed to responses in the postsynaptic neuron, could be a powerful tool for refining synaptic connectivity. Theoretical work later confirmed that correlated activity within a neural pathway could be an effective way for topographic maps to self-organise (Willshaw & Malsburg 1976), such that local correlations in activity (e.g. correlated activity amongst adjacent retinal ganglion cells) could help neurons in the target structure (e.g. the optic tectum or LGN) to select the correct synaptic inputs.

The first evidence that neuronal activity contributes to the refinement of synaptic connectivity came from investigations into the effects of visual deprivation. Numerous studies indicated that the development of response properties in the developing visual system was abnormal in visually deprived animals (Movshon & Van Sluyters 1981). In particular, the pioneering work of Hubel and Wiesel (Wiesel & Hubel 1963a; Hubel & Wiesel 1963; Wiesel & Hubel 1963b; Wiesel

& Hubel 1965; Hubel & Wiesel 1965; Hubel & Wiesel 1962) indicated that visual experience played an important role in the development of response properties throughout the visual system. Such studies led to the view that early visual experience has an important role in refining connectivity. Intriguingly however, a large number of response properties seemed to develop without visual experience. Visually inexperienced (rather than long term deprived) animals were found to often resemble adult animals both in terms of their ocular dominance, orientation selectivity and retinotopy (Hubel & Wiesel 1962; Hubel & Wiesel 1963). Moreover, the severity of defects in LGN development first postulated by Wiesel and Hubel (Wiesel & Hubel 1963a) was, upon later inspection, found to be rather subtle (Guillery 1973). This suggested that many properties develop before the onset of visual experience, even if the sensory environment may have an impact at later stages of development. This pointed towards a role for another kind of activity-dependent process, which operated before the onset of vision and was therefore likely to be intrinsically generated. Indeed, a body of research emerged studying the effects of pharmacological blockade of activity, in which total abolition of retinal activity was shown to have much more profound effects than visual deprivation alone. It was found that using tetrodotoxin (TTX) to block activity in the developing retina before birth abolished layering of the LGN (Shatz & Stryker 1988), blocked the refinement of the retinocollicular projection (O'Leary, Fawcett, et al. 1986b), and prevented the formation of ocular dominance columns (Stryker & Harris 1986). It was therefore realised that both intrinsically generated and extrinsically generated patterns of activity had a role to play in the refinement of connectivity.

What is the role of such neuronal activity during development? The roles of activity in development can be broadly divided into 'permissive' and 'instructive' (Crair 1999). On the one hand, the presence of activity may simply act as a trigger or promoter for certain developmental processes to occur, without directing their outcome. In such cases, activity is said to be *permissive*. However, if the outcome of plasticity is dependent on the specific pattern of activity, the process can be considered to be *instructive*. What distinguishes instructive mechanisms is that they provide the developing system with information about their origin (Crair 1999). If that origin is another developing structure, such as the retina, this information can be used by the target structure to refine its retinotopic organisation. Moreover, if patterned activity is driven by the environment, this allows the developing brain to 'learn' from, and adapt its response properties to, the properties of this environment. Below, I will describe some of the progress

that has been made in understanding the roles of intrinsically and extrinsically driven activity in the development of visual pathways.

Intrinsically generated activity and retinal waves

Various forms of intrinsically generated neuronal activity have been described during visual system development (Feller 1999) and such activity is thought to play a role in refining initially coarse connectivity before the onset of visual experience (L. C. Katz & Shatz 1996). Evidence for this came from the effect of pharmacological blockade of retinal activity with TTX before the onset of visual experience. Unlike visual deprivation, this manipulation had a profound effect on the refinement of retinogeniculate and retinocollicular projections (Shatz & Stryker 1988; O'Leary, Crespo, et al. 1986a), as well as on the formation of ocular dominance columns in cortex (Stryker & Harris 1986), and pointed towards a role for spontaneous retinal activity in establishing appropriate connectivity patterns. Correlated patterns of activity were soon observed in the developing retina (Meister et al. 1991; Galli & Maffei 1988; Maffei & Galli-Resta 1990; Wong et al. 1993) and sparked a large body of research into the source and function of these 'retinal waves' (Wong 1999; Firth et al. 2005).

Subsequent investigations have shown that retinal waves propagate throughout the visual pathway (Ackman et al. 2012). They have been found to play a crucial role in the refinement of RFs in the retina (Sernagor & Grzywacz 1996) and the superior colliculus (McLaughlin et al. 2003), as well as the segregation of inputs from the different eyes in the lateral geniculate nucleus (Stellwagen & Shatz 2002; Penn et al. 1998) and the visual cortex (L. C. Katz & Crowley 2002). The waves represent an instructive process that introduces local correlations between retinal ganglion cell activity, which are thought to help shape topographic maps and eye segregation through competitive mechanisms between inputs (Butts et al. 2007; Butts 2002). Such activity provides an effective developmental mechanism for the refinement of topographic maps, overcoming the limitations of the initial processes guided by molecular gradients and informing central parts of the visual pathway about retinal topography.

A role for visually driven activity

If intrinsically generated activity provides a mechanism for setting up a precise correspondence between sensory receptors and their targets in the brain, then what is the role of visual

experience? The work of Hubel and Wiesel on the effect of monocular deprivation, in particular, had proved that there was an important role for visual experience in the development of response properties of the visual system (Wiesel & Hubel 1963b; Wiesel & Hubel 1965). The pioneering work of Blakemore and colleagues (Blakemore & Cooper 1970; Blakemore & Van Sluyters 1975) then showed that it is not just the presence or absence of visual experience that impacts development, but that the statistical properties of the environment also actively influence properties of the visual system. Hubel and Wiesel had shown that neurons in visual cortex respond selectively to edges of a particular orientation, and that there was normally an equal representation of all orientations (Hubel & Wiesel 1962). Blakemore and colleagues observed that by biasing the statistical properties of the visual environment, in this case by overrepresenting edges of a certain orientation, it was possible to influence the tuning of cortical neurons (Blakemore & Cooper 1970; Blakemore & Van Sluyters 1975). The implications of this finding were that visual experience could exercise an instructive role in circuit development, such that the response properties of neurons in the developing brain become more tuned to the visual environment that the animal experiences.

Moreover, it was later demonstrated that the development of a number of features of the visual system is not accomplished by intrinsically generated activity patterns, but requires visual experience. In the developing ferret, for example, early visual experience is required for the development of direction selectivity and for the maturation of orientation selectivity (Li et al. 2006; White et al. 2001; Li et al. 2008)**.** More generally, the importance of the visual environment was supported by findings that development is accelerated if the animal is presented with an enriched environment (Cancedda et al. 2004) and synaptic plasticity processes are initiated rapidly after eye opening (Lu & Constantine-Paton 2004). While the most striking examples of plasticity have been reported during developmental critical periods, even the adult visual cortex can undergo structural and functional plasticity driven by visual experience (Sawtell et al. 2003; H.-Y. He et al. 2006).

Extrinsically and intrinsically driven activity may contribute to a different extent in different species. In the retinotectal system of frogs and fish, aspects of visual system development that have been shown to depend on intrinsic activity patterns in other species, such as the refinement of the tectal map (Schmidt & Eisele 1985; Schmidt & Buzzard 1993), have been

shown to require visual experience. In the Xenopus retinotectal system, the refinement of synaptic inputs to developing tectal neurons (i.e. their reduction in RF size) is dependent on visual activity (Tao & Poo 2005), and visual stimulation has been shown to both induce direction selectivity in tectal neurons (Engert et al. 2002) and selectively modify visuospatial properties of RFs (Vislay-Meltzer et al. 2006; Richards, Voss, et al. 2010b). In fact, a recent paper suggests that patterned activity driven by the visual environment may play an even more important role in the emergence of response properties in the retinotectal system of Xenopus: it was found that the developing Xenopus retina does not exhibit the intrinsically generated retinal waves that underlie the refinement of visual system connectivity in other species (Demas et al. 2012).

The availability of visual information to the developing nervous system

An obvious constraint upon the extent to which sensory experience can influence visual system development is the nature of the visual information that the system can encode. This is a sometimes underappreciated aspect of sensory-driven plasticity, but nevertheless important when studying visually driven development. Blurred vision, for instance, can have a profound effect on sensory-driven development (Kiorpes et al. 1987). There is evidence that the eyes may not be very good at relaying information to visual areas around the developmental onset of vision. Studies conducted in developing kittens indicate that during the early postnatal period, vasculature that supports the developing lens degrades the image available to the retina (Thorn et al. 1976; Freeman & Lai 1978). Additionally, the optical abilities of the eye's refractive surfaces (cornea and lens) are initially imperfect, but show improvement over the course of early development (Thorn et al. 1976; Freeman & Lai 1978; Freeman et al. 1978). The period of greatest improvement, in fact, corresponds to the onset of a critical period of visually driven plasticity (Thorn et al. 1976). In non-mammals such as chick and zebrafish too, the image-forming properties of the lens are not sufficiently developed to project a focused image onto the retina at early developmental stages (Easter & Nicola 1996; Wallman et al. 1981). By itself, such imperfect input may still be a source of information for the developing system – even visual experience through closed eyelids can provide patterned activity to guide development (Akerman et al. 2002). However, the limits of the sensory input stage necessarily influence the extent to which a developing system can learn from its environment.

In this thesis, I study visual activity-dependent development in the retinotectal system of Xenopus laevis. Despite the fact that developing Xenopus larvae are used to study activity-dependent development from the time their retinal ganglion cell axons arrive in the optic tectum, little is known about the ability of the eye to project an image onto the retina at this time. This is a particularly relevant question given the observation that zebrafish are severely hyperopic at early developmental stages (Easter & Nicola 1996). Furthermore, a number of seminal studies demonstrating plasticity in the retinotectal system of Xenopus have been conducted in a preparation where the lens was removed and images were directly projected onto the retina. For instance, studies investigating the size and alignment of glutamatergic and GABAergic RFs of tectal neurons (Tao & Poo 2005), the visually driven development of direction selectivity (Engert et al. 2002), and asymmetric RF modifications (Mu & Poo 2006) were all carried out by effectively bypassing the animal's lens. Other studies have investigated plasticity processes through direct electrical stimulation (e.g. (L. I. Zhang et al. 1998; Tao et al. 2001; Zhou et al. 2003)) or have used full field illumination (L. I. Zhang et al. 2000), which also eliminate the problem posed by the optics of the developing eye. There is some evidence that patterned visual stimuli can lead to instructive plasticity in the retinotectal system through intact eyes (Richards, Voss, et al. 2010b), but the extent to which visuospatial information is available to this developing system has not been well characterised.

The capacity of the retina to generate an appropriate response to light is also a crucial factor to consider when investigating the activity-dependent development of the visual system. In Xenopus, visual responses in the tectum can be recorded as soon as the axons of retinal ganglion cells arrive, around stages 39-40 (Holt & Harris 1983). This is coincident with the first light-evoked responses in the retina (Witkovsky et al. 1976). However, the extent to which the earliest retinal output translates into the first synaptic inputs that converge upon tectal neurons is not well understood. In this thesis, I will characterise the availability of visuospatial information in the synaptic inputs of tectal neurons of Xenopus laevis at the onset of vision. I address the ability of the developing eye to form a sharp image on the retina, as well as the availability of visuospatial information carried by synaptic inputs to tectal neurons, and how such inputs combine to give rise to the first visually driven action potentials in the tectum.

1.2 Integration of synaptic inputs and spike generation during development

Action potentials, or 'spikes', are the fundamental currency of neuronal computation. The operation performed by a neuron to translate its pattern of synaptic inputs into spiking output is therefore of great importance for any neuron's function. In addition to this important role in information processing, however, the spiking activity of a neuron plays a central role in synaptic plasticity processes. Hebbian plasticity requires activity of both the presynaptic neuron and the postsynaptic neuron (Hebb 1949). Indeed, the first experimentally demonstrated long-term modification of synaptic strength (Bliss & Lømo 1973; Bliss & Gardner-Medwin 1973) was shown to require postsynaptic depolarisation (Gustafsson et al. 1987; Gustafsson & Wigström 1988). Postsynaptic spiking in particular has proved important for the induction of changes in synaptic strength (Linden 1999). More recently, the importance of the precise timing of postsynaptic spikes in neuronal plasticity mechanisms has become apparent (L. I. Zhang et al. 1998; Markram et al. 1997; Magee & Johnston 1997). This seminal work has established that it is not just the presence of postsynaptic spikes, but also the precise timing of these spikes in relation to synaptic inputs, which is important in determining how synaptic strength is altered. The generation of spikes, therefore, is very important to a developing neuron, not only to participate in neuronal information processing, but also to enable the neuron to participate in activity-dependent plasticity processes.

A neuron's spiking output is jointly determined by its intrinsic excitability and its synaptic inputs. To what extent each of these factors contributes to spiking output throughout early brain development remains an open question for several reasons. First, developing neurons may still be in the process of acquiring mature intrinsic excitability (Spitzer & Ribera 1998; Spitzer 2002). Second, there is reason to believe that the balance of synaptic excitation and inhibition may be different during development. The formation and maturation of synaptic contacts is a gradual process and γ-aminobutyric acid (GABA)ergic inputs, which are the major source of inhibition in the mature brain, can have depolarising and even excitatory effects on developing neurons (Ben-Ari 2002). Below, I discuss the changing nature of intrinsic excitability and synaptic transmission over the course of development and their relevance to neuronal spiking output.

The development and regulation of intrinsic excitability

To be able to support action potentials a neuron first needs to develop the ability to support

the ionic currents that underlie the action potential (Hodgkin & Huxley 1952), which it does by expressing the appropriate voltage-gated ion channels (Hille 2001). Electrical excitability develops early in newborn neurons (Spitzer 1991; Spitzer & Ribera 1998), but can be adjusted and modified by neuronal activity (Turrigiano et al. 1999; Turrigiano et al. 1994) and therefore continues to play a key role in controlling neuronal output. It has been argued that this provides neurons with a powerful homeostatic mechanism to maintain their output levels as synaptic weights change (Davis & Bezprozvanny 2001; Turrigiano & Nelson 2004). In most mature neurons, the generation of action potentials relies chiefly on a rapid, depolarising, TTX-sensitive sodium (Na^+) current mediated by voltage-gated Na^+ channels that activate upon depolarisation (the spike threshold), and a potassium (K^+) current mediated by voltage-sensitive K^+ channels that repolarises the neuron (Hille 2001; Johnston & S. M.-S. Wu 1999; Bean 2007). The rapid inward Na^+ current generates the fast rising phase of the action potential, which is quickly inactivated and followed by the K^+ currents that serve to repolarise the neuron and allow the Na^+ current to deinactivate. There is a great diversity in the expression of the different voltage-gated ion channels across the central nervous system, leading to a range of spike thresholds and a large diversity in the dynamics of active membrane responses (Llinás 1988; Bean 2007).

Studies in developing Xenopus neurons have indicated that electrical excitability develops soon after neuronal differentiation (within 8 hours of the final round of DNA synthesis, (Baccaglini & Spitzer 1977; Lamborghini 1980; Hartenstein 1989)). Initial action potentials, however, are different in nature to those that mediate fast neurotransmission in mature neurons. They are characterised by a much longer time course (tens or even hundreds of milliseconds) and are mainly carried by fluxes of calcium (Ca^{2+}) ions (Spitzer & Ribera 1998). These Ca^{2+}-dependent action potentials lead to elevated intracellular Ca^{2+} levels, which initiate intracellular cascades and may trigger the onset of a number of maturational events (Spitzer 2006). It is only over the course of subsequent development that the faster, TTX sensitive voltage-gated Na^+ current associated with the mature action potential appears (Spitzer & Ribera 1998; Spitzer 2002).

During later development, however, and even in the adult, the intrinsic properties of the membrane are not static. There is evidence that neurons can adjust their intrinsic properties in an activity-dependent manner (W. Zhang & Linden 2003; Daoudal & Debanne 2003). These

changes can be homeostatic responses to a change in synaptic excitation or inhibition, serving to keep neuronal firing rate within an informative range (Turrigiano & Nelson 2004; Turrigiano et al. 1999; Pratt & Aizenman 2007), while other mechanisms can serve to cause long-lasting increases or decreases in neuronal output. For instance, studies in developing Xenopus have suggested that a period of enhanced visual stimulation can lead to long term increases in the excitability of tectal neurons, thereby improving their ability to respond to visual stimuli (Aizenman et al. 2003). In this thesis, I explore whether such changes in intrinsic excitability contribute to the emergence of visual responses in tectal neurons.

Synaptic integration of glutamatergic and GABAergic inputs

In the mature CNS, glutamate is the principal mediator of fast synaptic excitation**.** Glutamate release by the presynaptic neuron leads to activation of ionotropic glutamate receptors, the most prominent of which are the α-amino-3-hydroxy-5-methyl-4-isoxazolepropionic acid receptors (AMPARs) and N-methyl-D-aspartate receptors (NMDARs) (Dingledine et al. 1999; Nakanishi 1992). Upon activation by glutamate, AMPARs become permeable to Na^+ and K^+ ions (Dingledine et al. 1999), triggering an influx of Na^+-ions into the neuron that leads to depolarisation of the postsynaptic membrane - an excitatory postsynaptic potential (EPSP). Activation of NMDARs triggers an influx of both Na^+ and Ca^{2+} ions, the latter of which is a potent trigger for various intracellular cascades (Ghosh & Greenberg 1995). NMDARs have a non-linear current-voltage relationship due to their block by extracellular magnesium (Mg^{2+}) ions at the resting membrane potential (Mayer et al. 1984). This precludes NMDAR-mediated excitation of the neuron and entry of Ca^{2+} ions, unless the neuron is already depolarised. For this reason, NMDAR-mediated Ca^{2+} entry has been described as a coincidence detector of excitatory synaptic inputs. The influx of positive ions when postsynaptic AMPARs and NMDARs are activated raises the membrane potential, and can trigger spike generation if the postsynaptic depolarisation reaches the spike threshold, i.e. the point at which voltage-gated Na^+ channels activate in sufficient quantity to initiate the action potential.

GABA, on the other hand, is the main mediator of fast inhibitory neurotransmission in the mature CNS (Sivilotti & Nistri 1991) and acts on the ionotropic $GABA_A$ receptor ($GABA_AR$) to trigger an influx of Cl^- ions into the neuron (Kaila 1994). Such an influx of negative ions hyperpolarises the neuron, producing an inhibitory postsynaptic potential (IPSP), and counteracting the

excitatory actions of glutamatergic inputs. GABAergic inputs can also activate $GABA_B$ receptors ($GABA_B$Rs), which are metabotropic and can affect synaptic transmission by influencing the flux of ions through K^+ and Ca^{2+} channels (Bormann 1988; Bowery 1989).

Whether or not a neuron reaches its spike threshold depends on the spatiotemporal interaction of EPSPs, IPSPs and the intrinsic properties of the neuron. EPSPs and IPSPs can be additive, allowing the outcome of their interaction to be determined from a simple summation of their effects (Eccles 1961). However, non-linear effects can occur, particularly if the conductances triggered by the inhibitory input are large, thereby decreasing the resistance of the neuronal membrane and leading to a 'shunting' effect (Blomfield 1974; Fatt & B. Katz 1953; Hao et al. 2009). In this case, IPSPs can act as a divisor rather than a subtractor of excitation. The spatial distribution of glutamatergic and GABAergic inputs on the cell body and dendrites also impacts how inputs are integrated (London & Häusser 2005). Finally, the relative timing of synaptic activity can have a major impact on spiking outcome. For instance, the relative amount of 'shunting' versus 'additive' inhibition can change over the course of a GABAergic response (Staley & Mody 1992; Gao et al. 1998; Gulledge & Stuart 2003), and if inhibition is significantly delayed it may no longer be able to prevent spiking. This means there is a complex interplay between synaptic activity and spiking output.

The temporal interaction of glutamatergic and GABAergic inputs is controlled by the synaptic circuitry that underlies excitation and inhibition. Broadly speaking, inhibitory circuits can be divided into 'feedback' and 'feedforward'. Feedback inhibition occurs when activity in a given area excites the inhibitory interneurons within the same area, which then serves to inhibit further activity. By nature, such inhibition always occurs after the first neuronal activity. Meanwhile, excitatory afferent input to an area can simultaneously activate local inhibitory interneurons and excitatory neurons. Such afferent, or feedforward, inhibition allows a set of inputs to exert more precise control over the activity within the target area (Mountcastle 1957; Mountcastle & Powell 1959; Buzsáki 1984). Hence, feedforward inhibition ensures that excitatory input can be rapidly followed by an appropriate inhibitory counterpart, limiting the time window for the summation of excitatory inputs and narrowing the time window for spiking activity (Pouille & Scanziani 2001). Indeed, rather than simply decreasing the spiking output of a given neuron, GABAergic transmission seems to be responsible for precise regulation of spike timing and

spike patterns.

A feedforward circuit is present in the developing retinotectal system of Xenopus (Akerman & Cline 2006). While limiting the time window for summation of excitatory inputs appears to be one of the main functions for feedforward inhibitory circuits, a study of visually driven plasticity in the Xenopus retinotectal system found that GABAergic inputs can also serve to decorrelate tectal spiking activity (Richards, Voss, et al. 2010b). This role for GABAergic inputs was found to be crucial for stimulus-instructed plasticity in the developing retinotectal system.

Excitation / inhibition balance during circuit development

While GABA is the major inhibitory neurotransmitter in the mature CNS, GABAergic inputs can depolarise developing neurons (Ben-Ari et al. 1989; Mueller et al. 1984; Ben-Ari 2002; Ben-Ari et al. 2007). This developmental reversal of GABA's effect on the postsynaptic neuron is explained by a changing transmembrane gradient for chloride (Cl^-), which alters the reversal potential for the Cl^--permeable $GABA_AR$ (Owens et al. 1996). Mature neurons have low intracellular Cl^-, primarily due to the expression of the K^+/Cl^- cotransporter KCC2 that moves Cl^- out of the neuron. In contrast, immature neurons lack KCC2 and instead express the Na^+-K^+-$2Cl^-$ cotransporter NKCC1 that raises intracellular Cl^- (Delpire 2000; Fiumelli & Woodin 2007). Activation of the $GABA_AR$ in immature neurons therefore leads to a Cl^- efflux. This results in a depolarising effect on the postsynaptic membrane potential and can even result in an excitatory effect of GABAergic inputs (resulting in spiking activity) if the reversal potential for $GABA_ARs$ lies above the spike threshold (Chen et al. 1996).

When GABAergic inputs are depolarising there are a number of ways glutamatergic and GABAergic inputs can interact. First, if the $GABA_AR$ reversal potential lies above the spike threshold of the neuron, GABAergic inputs can have an excitatory effect, and can summate with glutamatergic inputs to increase spiking output. However, if the $GABA_AR$ reversal potential lies below the spike threshold (but still above the neuron's resting membrane potential), two things can occur. If the GABAergic conductance depolarises the neuron but is not so large as to significantly alter the total membrane resistance of the neuron, GABAergic inputs can summate with glutamatergic inputs and facilitate spike generation (Gao et al. 1998; Gulledge & Stuart 2003). If, however, the GABAergic conductance does have a significant effect on total

membrane resistance, GABAergic inputs will depolarise the membrane, but still reduce the probability of spiking activity as a result of the shunting effect (Staley & Mody 1992). Importantly, depolarisation mediated by $GABA_A$Rs will also interact with voltage-sensitive proteins in the postsynaptic membrane, including the voltage-sensitive Mg^{2+} block of NMDARs (Leinekugel et al. 1997).

The developmental shift in the effect of GABA means that the balance of excitation and inhibition to a developing neuron is dynamic. Moreover, it is interesting to note that the effect of GABA on the postsynaptic neuron is a feature of each individual neuron, and depends on how that neuron regulates its intracellular Cl^- levels (Martina et al. 2001). This means that within the same developing structure, GABAergic inputs could have quite different effects upon different neurons, and serves to illustrate that the actions of GABA are complex, particularly during development.

The changes to glutamatergic and GABAergic inputs, and the fact that intrinsic membrane properties may still be maturing, present a challenge for understanding the integration of synaptic inputs in developing neurons. In this thesis I investigate the nature of the first externally driven (i.e. visually evoked) glutamatergic and GABAergic activity in the developing tectum and relate this to the spiking output of tectal neurons. A difficulty in addressing the question of the interaction of excitatory and inhibitory inputs in a physiologically relevant manner is that the measurement of the size of individual postsynaptic currents can only be carried out by clamping a neuron's membrane potential at a given voltage. This precludes measurement of the neuronal membrane potential and its possible spiking output in response to those same inputs. Therefore, to investigate the input-output relationship of developing tectal neurons, I have developed a protocol that allows me to record both the synaptic inputs and the spiking output of the same tectal neuron in response to multiple repeats of a set of visual stimuli. This has allowed me to investigate how synaptic inputs relate to visually driven spiking output in individual neurons *in vivo*.

Non-spiking neurons and the emergence of spiking activity

Given the expression of the appropriate voltage-gated channels and sufficient synaptic excitation, a neuron will fire one or more action potentials. Spiking output is thought to be a

neuron's most important contribution to information processing and therefore most studies in sensory neuroscience have focused on spiking activity as an indicator of a neuron's stimulus selectivity. This may also be partly due to the relative ease of recording action potentials compared to recording subthreshold synaptic inputs. It has been argued, however, that this has led to a bias towards focusing on active, or even very active, neurons (Shoham et al. 2006). Much less is therefore known about neurons that do not fire action potentials in response to particular stimuli, even though their silence could potentially be informative. Is a neuron silent because it receives no excitation, or is it in fact being actively inhibited?

It is estimated that this bias towards active neurons could mean that a large proportion of the neuronal population is electrophysiologically overlooked (Shoham et al. 2006). This issue may be even more relevant in studies of the developing brain, where the population of silent neurons could be higher. During development, there must be a point when each differentiated neuron becomes active and starts to fire stimulus-related spikes. Yet, remarkably little is known about this stage in neuronal maturation. While there have been numerous studies charting the development of intrinsic excitability of neurons (Spitzer & Ribera 1998; Spitzer 2002) or the development and maturation of synaptic inputs (Vaughn 1989; Cohen-Cory 2002; Cline 2001), the functional consequences of these processes on the output of a neuron have remained largely unexplored, and the transition of a neuron from a passive developmental unit into an active contributor to the network has not been studied experimentally. In this thesis**,** I address this issue by characterising the synaptic inputs and intrinsic excitability of a population of non-spiking neurons in the developing optic tectum of Xenopus laevis, and investigate the possibility that the emergence of spiking responses in this population may be dependent on neuronal activity.

1.3 Synapse formation and plasticity

How does a neuron acquire the appropriate synaptic inputs to develop its desired response properties? As described above, there are a number of processes that will guide axons and dendrites towards their targets, but what governs the actual formation of synaptic contacts? This question has sparked a large body of research. It has initially been informed to a large extent by observations at the neuromuscular junction, which proved to be an attractive model due to its size, relative simplicity and accessibility (Sanes & Lichtman 1999; Sanes & Lichtman

2001). More recently, and particularly due to the advent of *in vivo* imaging techniques, it has become feasible to study the dynamics of synaptogenesis in the developing central nervous system (Cline 2001; Cline & Haas 2008; Cohen-Cory 2002; Meyer et al. 2003; Niell et al. 2004).

The first requirement for the establishment of a synaptic contact is the proximity of an axon from a putative presynaptic neuron, and a process (typically a dendrite) or soma of a putative postsynaptic neuron. It has been shown in *in vivo* studies that developing axons and dendrites possess highly motile filopodia, which extend and retract on a rapid time scale, sampling their environment for potential synaptic partners. The formation of an initial contact is thought to rely on a class of cell-cell adhesion molecules (Yamagata et al. 2003; Washbourne 2004), which establish a physical interaction between the motile filopodia of axons and dendrites. After contact is established, presynaptic vesicle components rapidly accumulate at the site (Ahmari et al. 2000; Friedman et al. 2000). In the postsynaptic neuron too, a rapid sequence of events is required for synaptogenesis. Proteins associated with the postsynaptic density and glutamate receptor components rapidly accumulate at the developing postsynaptic site (Washbourne et al. 2002; Ahmari et al. 2000; Friedman et al. 2000). Many more synapses are initially established than are maintained, consistent with the idea that neurons possess mechanisms to 'decide' whether to keep or discard a developing synapse (Cohen-Cory 2002).

There is mounting evidence that the establishment, maintenance and maturation of synaptic contacts is influenced by neuronal activity (Zito & Svoboda 2002; Goda & Davis 2003; Cohen-Cory 2002). The motility of axons and dendrites itself has been shown to be affected by whether synapses are formed (Niell et al. 2004; Meyer & Smith 2006; Ben Fredj et al. 2010; Cline 2001) and by neuronal activity (O'Rourke et al. 1994; Rajan & Cline 1998; Ruthazer et al. 2003). Consistent with this, activation of postsynaptic glutamate receptors has been implicated in stabilising dendritic branches (Haas et al. 2006; Sin et al. 2002) and there is evidence that this is mediated by Ca^{2+} entry into the neuron (G. Wu & Cline 1998; Lohmann et al. 2002). As will become clear in the section below, this evidence supports a model in which synaptogenesis can be regulated by the activity-dependent maturation of signalling at nascent synapses.

The maturation of glutamatergic synaptic transmission

Once a synaptic contact is established, glutamate receptors are rapidly recruited to the nascent synapse. It is now becoming clear that the membrane of a nascent glutamatergic postsynaptic site is high in NMDARs but low in AMPARs (Durand et al. 1996; Liao et al. 1995; Isaac et al. 1995; Liao et al. 1999; Isaac et al. 1997; Petralia et al. 1999; G. Y. Wu et al. 1996). This means that during early development, glutamatergic neurotransmission is relatively ineffective at the resting membrane potential. However, due to the presence of NMDARs, transmission at these 'silent' synapses can occur when the neuron is depolarised. Over the course of development, such synapses acquire more AMPAR-mediated glutamatergic excitation in an activity-dependent manner, via a process that is thought to be mediated by Ca^{2+} entry following NMDAR activation (Durand et al. 1996; Liao et al. 1995; Isaac et al. 1995; Liao et al. 1999; Isaac et al. 1997; Petralia et al. 1999; G. Y. Wu et al. 1996). This does suggest, however, that a source of postsynaptic depolarisation is required in order for a developing neuron to acquire mature glutamatergic synapses.

As discussed above, GABAergic inputs can have a depolarising effect on developing neurons. Moreover, the formation of GABAergic and glutamatergic synapses appears to be sequential (Tyzio et al. 1999; Khazipov et al. 2001), such that the GABAergic neurotransmitter system becomes operational before the glutamatergic system. This has led to the hypothesis that the GABAergic system may act as a pioneer neurotransmitter that contributes to the maturation of the glutamatergic system. More specifically, it has been proposed that early depolarising GABAergic inputs could enable nascent glutamatergic synapses to recruit more AMPARs (Ben-Ari et al. 2007; Ben-Ari 2002; Ben-Ari et al. 1997; Leinekugel et al. 1997; Akerman & Cline 2007). In particular, evidence from the hippocampus suggests that large, intrinsically generated GABAergic depolarisations are common in the developing brain and could act in synchrony with glutamate release to activate the NMDAR and lead to Ca^{2+} increases in developing neurons (Leinekugel et al. 1997; Garaschuk et al. 1998).

Experimental evidence is now accumulating in support of this theory. Depolarising GABAergic inputs and NMDAR activation have been found to be required for the maturation of glutamatergic synapses in developing cortex. Forcing the effect of $GABA_AR$ activation to be prematurely hyperpolarising prevents the normal maturation of glutamatergic synaptic transmission, which can be rescued by introducing a mutant form of the NMDAR that is Ca^{2+}-permeable at

the resting membrane potential (Wang & Kriegstein 2008; Wang & Kriegstein 2011). In the adult brain, the integration of newborn neurons into the local synaptic circuits of the dentate gyrus has also been found to require depolarising GABAergic transmission (Ge et al. 2005). Interestingly, while the main focus has been on the role of intrinsically generated GABAergic activity in the maturation of the glutamatergic system, recent studies have shown that enriched environments also generate GABA-mediated effects upon the developing glutamatergic system (S. He et al. 2010; Chancey et al. 2013). This suggests that not only intrinsically generated, but also environmentally driven activity can play a role in the maturation of glutamatergic synaptic transmission.

Work in this thesis takes advantage of the fact that the developing Xenopus optic tectum receives stimulus-evoked activity from the retina at a time when GABAergic transmission can have depolarising effects on tectal neurons (Akerman & Cline 2006) and the maturation of glutamatergic transmission is still in progress (G. Y. Wu et al. 1996). One explicit aim is to test the possibility that visually evoked, depolarising GABAergic inputs can drive the maturation of glutamatergic synaptic transmission in the developing optic tectum. It has already been observed that premature expression of the KCC2 Cl^- transporter (making GABAergic inputs more hyperpolarising) interferes with the normal development of glutamatergic transmission (Akerman & Cline 2006). It was also noted that GABAergic depolarisation observed in the tectum would be well placed to relieve the Mg^{2+} block of the NMDAR at developing glutamatergic synapses (Akerman & Cline 2006; Akerman & Cline 2007). In this thesis, I test this possibility directly, by exploring the effect of a brief period of enhanced visual stimulation on neurons that appear to have immature glutamatergic input. Because the appropriate selection of experimental visual stimuli allows for control over the pattern of activity on the retina, this experimental approach also enables me to investigate whether the activity-dependent maturation of glutamatergic transmission represents a permissive or an instructive process. Moreover, I characterise for the first time the impact of this process on the functional output of developing neurons.

Modulating the strength of developing synapses – LTP

The developmental changes in neuronal connectivity described above have illustrated that activity can cause long-term changes in the efficacy of synaptic transmission. The mechanisms by which this occurs have been the subject of a long line of scientific inquiry. Experimentally, both

potentiation and depression of synapse efficacy can be induced by stimulation protocols (Bear & Malenka 1994). Bliss and colleagues first demonstrated an activity-dependent long-lasting change in synaptic efficacy (Bliss & Lømo 1973; Bliss & Garner-Medwin 1973), reporting that burst stimulation of afferent fibres can lead to a persistent increase in the ability of those fibres to excite the postsynaptic region. This long-term potentiation, or LTP, has gained prominence as a potential biological basis for learning and memory (Bliss & Collingridge 1993). Moreover, it provided developmental neuroscience with a potential set of mechanisms that could underlie the establishment and refinement of synaptic connectivity during development.

Postsynaptic depolarisation was found to be required for the induction of LTP (Gustafsson et al. 1987; Gustafsson & Wigström 1988), which made it an attractive mechanism to underlie the type of plasticity rule proposed by Donald Hebb (Hebb 1949) - i.e. a mechanism to strengthen synaptic inputs that contributed to postsynaptic spiking. Indeed, not just postsynaptic depolarisation, but postsynaptic spiking in particular was found to have important consequences for expression of synaptic plasticity (Linden 1999). The NMDAR was soon put forward as a putative mediator of this new phenomenon (Collingridge & Bliss 1987) because the voltage-dependence of the receptor (Mayer et al. 1984; Nowak et al. 1984) made it an ideal coincidence detector (Kelso et al. 1986; Sastry et al. 1986; Gustafsson & Wigström 1988).

In the classic form of LTP, postsynaptic NMDAR activation leads to postsynaptic expression of LTP (Kauer et al. 1988)**.** This expression of LTP is dependent on elevated postsynaptic Ca^{2+} (Malenka, Kauer, Perkel & Nicoll 1989a), which is thought to exert its actions through activation of Ca^{2+}-calmodulin-dependent protein kinase II (CaMKII) (Malenka, Kauer, Perkel, Mauk, et al. 1989b). CaMKII can remain active for long periods of time once activated, which can account for the long term effects of brief bursts of stimulation (Lisman et al. 2002). The CaMKII-dependent expression of LTP seems to be in part mediated by postsynaptic AMPAR trafficking, leading to more AMPARs in the postsynaptic membrane and therefore a larger EPSP in response to glutamate (Malinow & Malenka 2002). It may be noted that the mechanism proposed here is very much like the mechanism that is thought to underlie the developmental ‘unsilencing’ of synapses and the maturation of glutamatergic transmission described above. Indeed, the unsilencing of synapses has been proposed as the main process underlying LTP (Kerchner & Nicoll 2008), although this remains an active area of research. While the bulk

of this work has been carried out in the rodent hippocampal formation, the potency of LTP has been demonstrated throughout the developing brain. Notably, LTP can be observed at thalamocortical inputs in somatosensory (Crair & Malenka 1995) and visual (Artola & Singer 1987; Heynen & Bear 2001) sensory pathways. It has also been shown that LTP can account for visually driven plasticity within the primary visual cortex (Cooke & Bear 2010).

Spike timing dependent plasticity

While the induction protocols for LTP and LTD classically relied upon multiple rounds of burst stimulation, there are mechanisms that can generate long-lasting changes in synaptic efficacy from relatively small numbers of correlated pre- and postsynaptic events. Precise pairing of pre- and postsynaptic spikes was found to be a very effective inducer of LTP (Magee & Johnston 1997). Moreover, such a protocol could induce LTD if the spike timing of the pre- and postsynaptic neuron was switched (Markram et al. 1997). This crucial spike timing dependence of the direction of plasticity was first explored *in vivo* in the developing retinotectal system of Xenopus (L. I. Zhang et al. 1998). This seminal study revealed a synaptic plasticity function that maximises potentiation if an input arrives just before a postsynaptic spike, and maximises depression if an input arrives just after the postsynaptic spike. Later work in other systems has shown that indeed, such spike timing dependent plasticity (STDP) can occur if physiological patterns of spiking are used (Froemke & Dan 2002). STDP, therefore, is an effective mechanism by which synaptic inputs that contribute to postsynaptic spiking behaviour are strengthened, while synaptic inputs that do not contribute to postsynaptic spiking are weakened. This satisfies the criteria for Hebbian plasticity and makes STDP an attractive mechanism for mediating instructive forms of learning during development.

Further studies in the Xenopus retinotectal system have shown that STDP rules can account for the emergence of a number of interesting visual response properties. First, it has been shown that visually driven modification of tectal neuron RFs relies on spike timing (Tao & Poo 2005; Vislay-Meltzer et al. 2006). Second, STDP rules can account for the development of direction selectivity in the tectum (Engert et al. 2002; Mu & Poo 2006). Third, the pruning of recurrent excitatory synaptic circuitry in the optic tectum shows STDP-like properties (Pratt et al. 2008). Such processes appear to be necessary for normal development, as exemplified by the observation that tectal neurons with impaired spiking output fail to refine their response

properties (Dong & Aizenman 2012).

The molecular mechanisms proposed for STDP and LTP show considerable overlap, with the NMDAR still playing a prominent role. In fact, one of the mechanisms proposed for LTP and STDP is akin to the 'unsilencing' or AMPAfication of silent synapses, although its mechanistic details are still subject of debate (Lisman & Spruston 2005). From a developmental perspective, however, this raises the fundamental question of how STDP can occur if glutamatergic neurotransmission is not able to drive postsynaptic spiking. This is an appropriate point to reiterate the importance of how and when a developing neuron acquires the ability to exhibit stimulus-dependent spiking activity. In this thesis, I explore how a developing neuron can develop the ability to spike in response to visual stimuli and thereby develop the ability to participate in STDP.

1.4 The aims of this thesis

1. To characterise the potential for visual information to guide neuronal circuit development in the developing retinotectal system of Xenopus laevis (Chapter 3) by investigating:
    I. Whether the optical properties of developing eyes of Xenopus laevis are adequate for projecting a focused image onto the retina.
    II. To what extent visuospatial information is available to a developing tectal neuron.
    III. The relationship between the visual synaptic inputs and the spiking output of developing tectal neurons at the onset of vision.
2. To investigate a population of developing tectal neurons that receives visually evoked synaptic inputs, yet does not spike (Chapter 4), and to establish:
    I. Whether these neurons differ in terms of their intrinsic excitability.
    II. Whether these neurons receive quantitatively different synaptic inputs.
    III. Whether there are differences in the spatiotemporal distribution of visual inputs between visually spiking and non-spiking neurons.
3. To investigate how visually non-spiking tectal neurons may become 'unsilenced' during development (Chapter 5) and thereby establish:
    I. Whether the transition to becoming a spiking neuron is an activity-dependent process.

II. Which changes underlie the transition from visually non-spiking to visually spiking.

III. A cellular mechanism for the activity-dependent unsilencing of tectal neurons.

Chapter 2

Methods

2.1 Animals

All experiments were carried out in accordance with UK Home Office regulations. Wild-type Xenopus laevis embryos were generated from an in-house breeding colony purchased from the European Xenopus Resource Centre (University of Portsmouth) and raised in modified Barth's saline solution ('rearing solution', in mM: 87.6 NaCl, 1 KCl, 2.3 $NaHCO_3$, 14.9 HEPES, 0.3 $CaNO_3 4H_2O$, 0.8 $MgSO_4 7H_2O$, 0.6 $CaCl_2 6H_2O$; with 10 µg/ml penicillin streptomycin) on a 14-h/10-h light/dark cycle at 18°C. The animals' developmental stages were characterised according to the commonly used staging criteria (Nieuwkoop & Faber 1956). Under the rearing conditions described, animals went through stages 40-44 between 4 and 6 days post fertilisation. All drugs and chemicals were obtained from Sigma (St. Louis, MO) unless otherwise stated.

2.2 Focal length measurements

To measure the focal lengths of tadpole lenses, a customised experimental design was used, modified from a previous study in zebrafish (Easter & Nicola 1996) and similar to that employed by Land & Stirling (Land & Stirling 1975) in their study of *Xenopus* optical development. Tadpoles of stages 38-48 were placed in rearing solution containing a lethal dose of 0.5% (weight/volume) of the anaesthetic tricaine methanesulfonate (MS-222). Following confirmation of death, each eye was removed and the lens was then excised using fine forceps. In order to measure the size of lenses and their focal length, the lenses were placed in a small well of rearing solution and positioned on a microscope stage directly above a convex glass lens of focal length 25 mm (Comar Optics; Cambridge, UK). The corner of a microscope stage graticule was placed 25 mm below the convex lens, thereby placing the image of the graticule at optical infinity relative to the animal's lens (Figure 3.1a). The microscope objective was first focused onto the animal's lens and the position of the microscope objective in the Z-axis was

measured. The microscope objective was then moved upwards in the Z-axis until the image of the graticule formed by the animal's lens could be seen (Figure 3.1b). The focal length of the animal's lens was taken as the difference in the Z-axis between the animal's lens and the point at which the image of the graticule formed by the animal's lens was in sharpest focus. These experiments were performed upon excised lenses, because it was found that the pigmented scleral surface of the eye did not allow for clear observation of the image of the graticule. While this could influence measurements of focal length, it was found that the lenses could be removed without damage (Figure 3.1b). Therefore the measurements should provide a good estimate of the focal length in the absence of any accommodation caused by alteration of the lens shape in the intact eye.

2.3 Eye measurements

Measurements of lens radius were taken from images obtained during the focal length measurements. To measure pupil diameter and eye width, animals were sacrificed as described above and placed in liquid 1% UltraPure low melting point agarose (Invitrogen Ltd.; Paisley, UK). Following hardening of the agarose, the gel was cut to form flat surfaces on all sides of the animal. Eye widths were measured with the animal's dorsal side facing upwards and pupil diameters were measured with the animal's lateral side facing upwards. To measure the density of photoreceptor cells and the width of pigment cells in the eye, Bouin-fixed cresyl violet stained wax sections (10 μm thickness) were used. These were generously provided by Dr. Jeremy Taylor (University of Oxford). Photoreceptor densities were measured in sagittal sections and pigment epithelia widths were measured in horizontal sections. By comparing the mean eye widths measured in fixed tissue and fresh tissue, the tissue shrinkage associated with fixation was estimated to be less than 20%. This would have a negligible impact on the overall estimate of the distance from the lens to the photoreceptor mosaic, as the pigment epithelia only represents approximately one tenth of this distance (Figure 3.2). The photoreceptor density was defined as the number of photoreceptors found in a randomly selected square patch of the retina, 50 μm x 50 μm in size. This served as a reasonable estimation of overall photoreceptor density, as the Xenopus retina does not have a foveal region or visual streak (Wilhelm & Gabriel 1999). Cones and rods were not distinguished in the density estimates.

2.4 Estimating image resolution

To estimate the image forming properties of eyes, the measurements of the focal length of the lens and eye size over development were used to calculate the number of photoreceptors that a point source of light would be predicted to illuminate at a given distance from the eye. This calculation was made using the following equation:

1)

$$C = D\left(\frac{X}{Y} - \frac{X}{f} + 1\right)$$

Where *C* is the diameter of the circle of light produced by the point source on the photoreceptors, *D* is the pupil diameter, *X* is the distance from the lens to the photoreceptor mosaic, *Y* is the distance of the point source of light from the animal, and *f* is the focal length of the lens. Note that for an emmetropic eye $X = f$, and thus equation (1) reduces to a rearrangement of the equation for the hyperfocal distance (i.e. the distance at which all objects are at an acceptable focus as defined by *C*) (Kingslake 1951). Also, if an object is at optical infinity (i.e. $Y = \infty$) then equation (1) reduces to the same equation used by Land & Stirling (Land & Stirling 1975) to calculate the diameter of the blur circle.

Equation (1) was obtained by taking advantage of the fact that for an eye that is hyperopic (or emmetropic) the following is true:

2)

$$\frac{D}{C} = \frac{f'}{f' - X}$$

Where *f'* is the distance from the lens to the location behind the eye where the image is fully focused. Moreover, for any lens it holds true that:

3)

$$\frac{1}{Y} + \frac{1}{f'} = \frac{1}{f}$$

Taking equation (3) and solving for *f'* produces:

4)

$$f' = \frac{Yf}{Y - f}$$

Equation (4) can then be used to replace *f'* in equation (2). Using this replacement and solving for *C*, equation (1) is obtained. To relate the diameter of the illumination disc (*C*) to the number of photoreceptors, the area of a circle with diameter *C* was divided by the mean photoreceptor area that was measured.

2.5 *In vivo* preparation for electrophysiology

Stage 40–44 Xenopus laevis embryos were anaesthetised in buffered artificial cerebrospinal fluid (ACSF; in mM: 115 NaCl, 3 $CaCl_2$, 2 KCl, 1.5 $MgCl_2$, 5 HEPES, 0.01 Glycine, 10 $_D$-Glucose) containing 0.01% MS-222 and stabilised on an immersed Sylgard platform in the recording chamber using insect pins (Figure 2.1a). The brain was exposed by making an incision to the top of the head, along the dorsal midline, and the tectal lobes were separated to expose the neurons lining the ventricle wall. After the dissection was complete, the ACSF with MS-222 was rinsed out with two washes of fresh ACSF. To prevent movement during the recordings, ACSF with 3–4 µg/ml of the neuromuscular blocker α-bungarotoxin (Invitrogen Ltd., Paisley, UK) was washed in and an incision was made in the embryo's tail to facilitate the drug's access to the bloodstream.

2.6 Visual stimulation

The position of the animal in the recording chamber was such that one of its eyes directly faced a square screen that covered approximately 90x90 degrees of the eye's central visual field (Figure 2.1a). A LED projector (Samsung SP-P310ME) with a 12 cm focal length convex lens (Comar Optics, Cambridge, UK) was positioned on the other side of the screen to allow for the presentation of visual stimuli. Visual stimuli were generated with custom-made software programmed in C++ using the OpenGL and GLUT libraries (Blake A. Richards, Akerman Lab). The RF mapping protocol used throughout this thesis consisted of 4 full field flashes, followed by square stimuli (11.25 x 11.25 degrees of visual space) that were flashed at one of 64 locations defined by dividing the screen into an 8x8 grid. The stimuli consisted of white

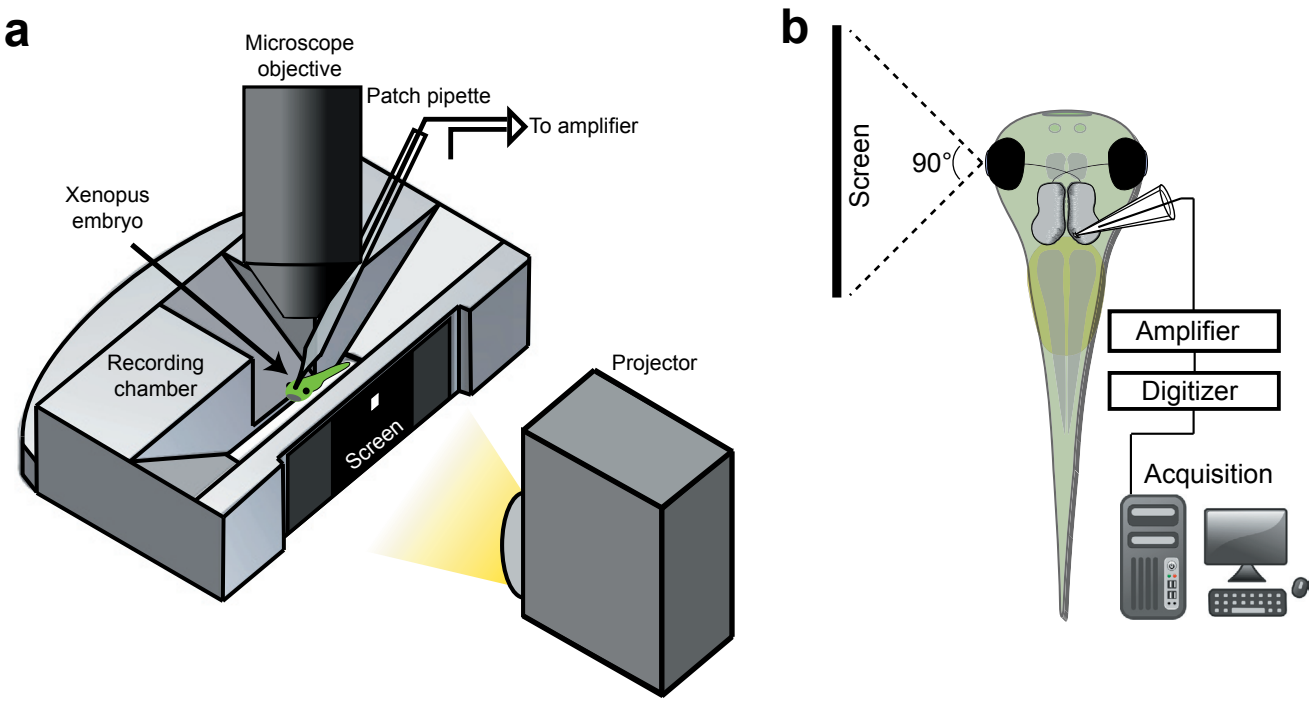


Figure 2.1: Experimental setup
a) A schematic representation of the experimental setup. A Xenopus embryo was positioned on a platform in the recording chamber filled with artificial cerebrospinal fluid (ACSF) and held in place with insect pins. One of its eyes faced a screen that covered approximately 90 x 90 degrees of its central visual field. The exposed tectum was visualised using a microscope immersion objective, which enabled visually guided targeting of tectal neurons with a patch pipette. The patch pipette was used to record visual responses from individual tectal neurons while visual stimuli were projected onto the screen by an LED projector. **b)** Dorsal view of the Xenopus embryo indicating the position of the patch pipette on the caudal to medial ventricular surface of the exposed tectal lobe contralateral to the visual stimulation. The recorded signal was sent to an amplifier (Multiclamp 700B) and an analog-to-digital board (Digidata 1440A), and acquired using PClamp 10 software (Molecular Devices).

squares on a black background, as it was previously found that this stimulus polarity produces the most robust responses in developing tectal neurons (Tao & Poo 2005). The maximum luminance of the image projected onto the screen was 13,000 cd/m^2, and the minimum was 22.9 cd/m^2, giving a contrast ratio of 568:1. Stimuli were presented at the different locations in a pseudorandom order and each stimulus was presented for 1.25 s, followed by 1.25 s during which the screen went black. The conditioning stimulus used in Chapter 5 consisted of a white bar (width 10 degrees) presented on a black background, which moved at a constant speed (90 visual degrees/s) from one edge of the screen to the other. The direction of the drifting bar was one of the 4 cardinal directions and this conditioning stimulus was repeated with a frequency of either 0.4 or 0.2 Hz for 15 minutes. To determine whether neurons had visually evoked NMDA receptor (NMDAR)-mediated currents (Figure 5.7) a simple full field flash stimulus was used. This stimulus consisted of cycles of bright full screen illumination for 2.5s, followed by 2.5s during which the screen went black.

2.7 Electrophysiological recordings

Patch pipettes with a tip resistance of 5-10 MΩ were pulled from borosilicate glass capillaries with filament (1.2 mm outer diameter, 0.69 mm inner diameter, Warner Instruments, Hamden, CT, USA) using a horizontal puller (P-97, Sutter, Novato CA, USA) and back-filled with an artificial intracellular solution. For the cell-attached recordings followed by whole cell characterisation of synaptic currents, the intracellular solution was either cesium-methanesulfonate based (in mM: 90 $CsCH_3O_3S$, 5 $MgCl_2$, 20 TEA, 10 EGTA, 20 HEPES, 2 Na_2ATP, 0.3 NaGTP, 3 QX-314 (Tocris Cookson Ltd., Bristol, UK)) or potassium (K^+) gluconate based to allow for assessment of excitability and voltage-gated currents (in mM: 110 K^+-gluconate, 8 KCl, 5 NaCl, 1.5 $MgCl_2$, 20 HEPES, 0.5 EGTA, 4 Na_2ATP, 0.3 NaGTP). For the gramicidin perforated patch recordings, a high chloride (Cl^-) pipette solution was used to monitor whether the perforated patch was still intact (in mM: 114 KCl, 1.5 $MgCl_2$, 20 HEPES, 10 EGTA, 2 Na_2ATP, 0.3 NaGTP) (Akerman & Cline 2006). Gramicidin (Calbiochem, Merck Millipore, Billerica, MA, USA) was dissolved in dimethylsulfoxide (DMSO) to achieve a stock solution of 10 mg / ml. This stock solution was added to the internal solution on the day of recording to achieve a final concentration of 80 µg / ml. Prior to filling the pipette, the solution was vortexed for 1 min, sonicated for 30 s, and filtered with a 0.45 pore cellulose acetate membrane filter (Nalgene, Rochester, NY, USA). The osmolarity of pipette solutions was adjusted to 250 mOsm with CsOH for the Cs^{2+}-based

pipette solution, and with KOH for the K^+-gluconate and KCl-based pipette solutions. For loose patch cell-attached recordings, the pipette was filled with ACSF (as above).

Recordings were made from tectal neurons that were exposed by gently disrupting the ventricular surface, in the caudal to medial region of the tectal lobe contralateral to the eye receiving visual stimulation (Figure 2.1b). For some notes on the types of tectal neurons likely to be targeted in this manner, see Appendix II. The electrical signal was amplified by a Multiclamp 700B amplifier controlled by Multiclamp commander software (Molecular Devices, Sunnyvale, CA). The signal was then digitised at 10 kHz via a Digitata 1440A analog-to-digital board (Molecular Devices) and acquired using Clampex software version 10.1 (Molecular Devices). During recordings, series resistance was compensated at 90% (predictive and corrective). Membrane potential measurements were corrected for the liquid junction potential of the pipette solution and the ACSF (14.6 mV for the K^+-gluconate based pipette solution). All experiments were carried out at room temperature (20-22 °C). Whole cell recordings that had an access resistance of over 60 MΩ were excluded from the data set and the majority of neurons had an access resistance well below this value with a mean of 30.1 ± 0.9 MΩ. Neurons that displayed an unstable baseline or fired non-stimulus related spikes that are indicative of a damaged membrane were also excluded from the data set. Developing tectal neurons of stage 40-44 animals had a mean resting membrane potential of -60.1 ± 1.6 mV (estimated from the membrane resistance and holding current at -75 mV), a mean membrane capacitance of 17.6 ± 0.4 pF, and a mean membrane resistance of 1.43 ± 0.10 GΩ. None of these properties were significantly different between the populations of visually spiking and visually non-spiking tectal neurons described in Chapter 4 ($p > 0.05$).

2.8 Recording spiking output, synaptic inputs and intrinsic excitability of the same tectal neuron *in vivo*

For the *in vivo* electrophysiological experiments reported in Chapters 3 and 4, the experimental procedure was as follows: First, a gigaseal was established with the tectal neuronal membrane. In this cell-attached configuration, the spiking responses of the neuron were recorded in response to 3 repeats of the visual RF mapping stimulus. Next, suction was applied to the pipette to break through the cell membrane into whole cell mode. In the subset of recordings where the pipette solution was K^+-gluconate based, the intrinsic excitability of the neurons

was first assessed using a current injection protocol in current clamp, followed by a voltage step protocol in voltage clamp (see below). Subsequently, to find the glutamatergic and GABAergic reversal potentials, the membrane potential was first raised and lowered during the presentation of a full field flash stimulus and the visually evoked postsynaptic currents (PSCs) were monitored. The GABAergic reversal potential was estimated as the most positive membrane potential at which no outward component of the PSC was visible. Conversely, the glutamatergic reversal potential was defined as the most negative membrane potential at which no more inward current was observed. In case the visually evoked PSCs in response to the full field flash stimulus were too small to allow for an accurate estimation of these points, the default values of -65mV and 0 mV were used for the GABAergic and glutamatergic reversal potentials, respectively. Glutamatergic responses were then recorded to 3 repeats of the RF mapping stimulus at the GABAergic reversal potential, and GABAergic responses were recorded to 3 repeats of the RF mapping stimulus at the glutamatergic reversal potential.

2.9 Assessment of intrinsic excitability

For neurons recorded with a K^+-gluconate based pipette solution, the neuron's ability to spike in response to a current injection protocol was assessed in whole cell current clamp mode. This protocol consisted of a set of 200 ms current injections ranging from 20 pA to 180 pA, in increments of 20 pA. Spike number was defined as the number of sharp peaks in the membrane response. Spike threshold was calculated by determining the point of inflection in the membrane potential response, where active currents were first detected. Returning to voltage clamp, measurements of voltage-gated conductances were made by subjecting the neuron to a series of voltage steps, from a baseline of -75 mV. The command voltages ranged from -95 to -5 mV in increments of 10 mV. The hyperpolarising voltage steps were used to estimate the membrane conductance and used to perform leak subtraction. This facilitated measurements of the voltage gated conductances that were activated by depolarising steps.

2.10 Conversion of visually non-spiking tectal neurons

Experiments in Chapter 5 investigated whether visually non-spiking neurons could be driven to start spiking as a result of visual conditioning *in vivo*. For these experiments, the protocol was as follows: The loose cell-attached patch recording configuration was established with a tectal neuron, and responses to 3 repeats of the RF mapping protocol were recorded. If the

neuron displayed clear visual spikes in response to the RF mapping protocol, the recording was aborted and a new neuron was targeted. If the neuron did not exhibit visual spiking activity, the animal was exposed to a visual conditioning protocol consisting of a repeated drifting white bar on a black background (see above). The animal was exposed to this stimulus for 15 minutes, after which responses to 3 repeats of the RF mapping protocol were recorded once more. Offline analysis was used to confirm whether the neuron qualified as 'visually non-spiking' based on the first 3 repeats of the RF mapping protocol. A neuron was classified as 'converted' if it changed from being visually non-spiking to visually spiking following the conditioning protocol. Animals were not exposed to the conditioning protocol more than twice, to prevent saturation of plasticity. For a number of experiments, the NKCC1 blocker bumetanide (100 µM, Tocris Cookson Ltd., Bristol, UK) or the NMDAR antagonist APV (Tocris Cookson Ltd., Bristol, UK) were applied to the bath solution to investigate the role of depolarising GABAergic inputs and NMDARs, respectively. Bumetanide was added to the bath by adding 50 µl of a dimethylsulfoxide (DMSO) based stock solution.

To be able to characterise the intrinsic excitability and synaptic currents of converted neurons, a subset of experiments were performed in gigaseal mode, instead of the loose patch configuration. In these cases the first part of the protocol was identical to that described above, except that the RF mapping protocols were shortened to 1 - 2 repeats. The protocol was shortened because it was found that extending the recording time beyond 25 minutes greatly increased the incidence of spontaneous gigaseal rupture. After the neuron had been subjected to the pre-conditioning RF mapping protocol, the conditioning protocol and the post-conditioning RF mapping protocol, the recording configuration was changed to whole cell mode. This allowed for a characterisation of the intrinsic excitability, voltage gated currents and glutamatergic and GABAergic inputs. This was performed as described above, with the exception that responses were only recorded to single repeats of the RF mapping protocol to ensure that all necessary data could be collected before deterioration of the patch.

2.11 Assessing the effect of GABAergic responses

To investigate the effect of GABAergic inputs on visually spiking and visually non-spiking tectal neurons, I used gramicidin perforated patch clamp recordings. Gramicidin perforated patch recordings allow for electrical access to the neuron without disturbing intracellular Cl^- levels,

thus maintaining the reversal potential of the neuron's $GABA_A$ receptors (Akerman & Cline 2006; Ebihara et al. 1995; Kyrozis & Reichling 1995). For these experiments, the spiking output of the tectal neuron was first recorded to allow for offline classification of the neuron as visually spiking or visually non-spiking. This was achieved by recording responses to the RF mapping protocol immediately after formation of the gigaseal and thus before perforation of the membrane patch (i.e. effectively in cell-attached mode). After the RF mapping protocol, a decrease in access resistance was monitored as a sign of membrane perforation. Puffs of 100 µM GABA were then delivered at the cell soma using a Picospritzer III (Parker Hannifin Corporation, Cleveland, OH, USA). Due to the *in vivo* nature of this study and the presence of a heartbeat, it was extremely challenging to establish perforated patch recordings with an access resistance that would permit an accurate quantification of the $GABA_AR$ reversal potential in voltage clamp. In all cases, the neuronal membrane ruptured before the access resistance decreased below 100 MΩ. Therefore, to classify the effect of $GABA_AR$ activation on the membrane as either 'depolarising' or 'hyperpolarising', I assessed only the direction of the membrane potential response to GABA puffs in current clamp mode. To assess the effect of $GABA_AR$ activation, the resting membrane potential was measured just prior to the GABA puff and the integrated membrane potential response was measured during the 2 seconds immediately following the puff. If the membrane potential response was negative GABAergic inputs were deemed to be hyperpolarising, whereas if the integrated membrane potential response was positive, GABAergic inputs were deemed to be depolarising.

2.12 Recording visually evoked NMDAR currents

To confirm the presence of NMDAR-mediated currents, neurons were first classified as visually non-spiking by recording in gigaseal cell-attached configuration (see above). The recording configuration was then changed to whole cell mode, which enabled measurements of different synaptic currents. First, AMPA receptor (AMPAR)-mediated glutamatergic responses to a visual full-field flash stimulus were recorded at the GABAergic reversal potential. Next, the membrane potential was moved to +25 mV, where a combined current mediated by AMPA, NMDA and $GABA_A$-receptors ($GABA_ARs$) could be observed (Figure 5.7c). Local application of the $GABA_AR$ antagonist SR95531 (50 µM, Tocris Cookson Ltd., Bristol, UK) was used to abolish the $GABA_AR$-mediated component of this combined current, leaving a current mediated by NMDARs and AMPARs. To confirm that a component of this current was NMDAR-mediated, the NMDAR

antagonist APV (1 mM) was applied locally to the optic tectum. Local drug application was achieved using patch pipettes containing the pharmacological agent dissolved in ACSF plus a fluorescent dye (Alexa 594, Invitrogen Ltd., Paisley, UK). When required, positive pressure was applied to the pipette, and flow was monitored under epifluorescent illumination.

2.13 Detection of glutamatergic and GABAergic PSCs

To assess responsiveness to visual RF stimuli, a PSC detection algorithm was used. Only PSCs recorded between 50 ms and 500 ms following stimulus presentation were used to assess visual responsiveness. The baselined signal that had been acquired at 10 kHz was convolved with a 15 sample (1.5 ms) flat smoothing window (moving average) to eliminate high frequency noise. A PSC was defined as a deflection lasting a minimum of 2 ms, with an amplitude of at least 8 standard deviations from the baseline for glutamatergic currents, or 5 standard deviations from the baseline for GABAergic currents. These thresholds were found to capture the vast majority of PSCs and yield the least false positives. Different threshold values were used for glutamatergic and GABAergic PSCs because of differences in signal noise associated with holding the neuron at different membrane potentials. A neuron was considered to receive visually evoked PSCs if there was at least 1 RF location where a PSC could be detected for at least 2 out of 3 repeats of the RF mapping stimulus. Only neurons that were considered to receive both glutamatergic and GABAergic visually evoked PSCs were included in the data set. PSCs were converted into postsynaptic conductances by dividing by the driving force. Synaptic responses were quantified as the total integrated synaptic conductance (pS*s) during the first 500 ms following stimulus presentation, and only ‘responsive’ RF locations (i.e. PSCs detected on at least 2 out of 3 repeats) were used to determine the mean glutamatergic and GABAergic response amplitude for a neuron.

2.14 Spike detection and defining visually spiking and non-spiking neurons

Spikes were identified using a custom spike detection algorithm. The trace was first convolved with a 5 sample (0.5 ms) flat smoothing window (moving average) to eliminate high frequency noise. The noise distribution was approximated with a Gaussian fit. A spike was defined as an upward deviation of over 5 standard deviations from the noise distribution followed by a downward deviation of over 5 standard deviations, with a total duration of at least 5 samples (0.5 ms). A neuron was considered to be ‘visually spiking’ if there was evidence for significantly

time-locked spiking responses to stimulus 'OFF' events. This was investigated by constructing a post-stimulus time histogram of spike events and determining whether there was a nonrandom distribution of spike times with respect to the visual stimulus. To capture even very sparsely spiking neurons, a sliding window was used to sum all responses over a 350 ms time window, and the peak of this summed response was determined during the first 500 ms following stimulus presentation. If the peak of this summed response was significantly different from the mean of the distribution of peaks obtained from a bootstrap procedure generating 10,000 random distributions of the same number of spike events ($p < 0.05$), the neuron was classified as 'visually spiking'. A neuron that did not meet this criterion was considered to be 'visually non-spiking'. Spiking responses were quantified as the spike count at a given RF location recorded during the first 500 ms following stimulus presentation.

2.15 RF maps

To construct RF maps, visual responses were arranged in an 8x8 grid according to the location of the square flashes that evoked them (See Chapter 3, Figures 3.4-6 for examples). This sampling of visual space was sensitive enough to pick up different RF structures – in older (stage 48-49) animals RFs with more than one 'centre' could sometimes be distinguished (unpublished observations). Spiking RF maps were generated from the spike count in the first 500 ms after stimulus 'OFF' events for each RF location. Synaptic RF maps were generated from the integrated synaptic conductance (pS*s) recorded during the first 500 ms following stimulus 'OFF' events. To estimate the spatial information available to tectal neurons, a 2-dimensional Gaussian surface was fit to the RF maps for each cell, using the following equation:

$$G(x) = Ae^{(x-\mu)^T \Sigma^{-1} (x-\mu)}$$

Where A is the height of the Gaussian surface (in pS·s), x is a 2-element vector that ranges over locations in visual space (in visual degrees), μ is the 2-element centre of the RF (in visual degrees), and Σ is the 2 x 2 covariance matrix (in visual degrees squared). The RF centre was defined as the maximum of this Gaussian fit, and the RF was deemed 'coherent' if there was a significant negative Spearman's rank correlation between distance from the RF centre and response size. To investigate whether the rank correlation coefficient was significant, it was

compared to a distribution of correlation coefficients obtained from 10,000 shuffled RFs obtained by randomly redistributing the values for the different RF locations. To determine the minimum width of these Gaussian surfaces at half their maximum, an eigenvector decomposition of Σ was determined, and the width of the curve along the eigenvector direction corresponding to the smaller of the two eigenvalues was calculated.

2.16 Assessment of instructive RF change

In order to assess whether the visual conditioning stimulus had been instructive in inducing RF changes in neurons that converted to visually spiking (Chapter 5, Figure 5.3), I investigated whether there was systematic change along the direction of movement of the conditioning stimulus (and used the orthogonal direction as a control). All RFs were aligned according to the direction of movement of the conditioning stimulus, which is referred to as the 'conditioned direction'. RF change values were normalised to range from 0 to 1. For each RF, the RF change along the conditioned direction and the RF change along the orthogonal direction were calculated, resulting in two vectors of RF change for each neuron. To test whether there was evidence for systematic changes along either the conditioned direction or the orthogonal direction, I first determined the extent to which the position along each direction could explain the variance in change along that direction. This resulted in an r^2-value for each direction, where a high r^2-value would indicate that there was a systematic effect of position along this direction, and a low r^2-value would indicate no such effect. To assess the likelihood of observing a particular r^2-value by chance, a bootstrap procedure was used. The two vectors of RF change obtained for each RF were randomly shuffled and new means were calculated along both directions. The r^2-value associated with these shuffled means was then calculated, and this procedure was repeated 10,000 times. To obtain a p-value, the r^2-value obtained from the experimental data was compared to the distribution of 'shuffled' r^2-values. A significant result here ($p < 0.05$) would indicate an instructive effect of the visual stimulus on the RF change.

2.17 Computer simulations of developing tectal neurons

To systematically investigate the effects of changing glutamatergic synaptic input amplitudes and spike threshold on the spiking output of tectal neurons (Chapter 4, Figure 4.4) a single compartment neuronal model was built in Matlab 7.12 (Mathworks Inc.) on a PC running Ubuntu Linux 12.10. The model neuron received both glutamatergic and GABAergic synaptic inputs

and was defined as having spiked if the membrane potential of the compartment reached threshold. Each simulation was initialised with experimental data collected from the whole cell recordings. Resting membrane potential (V_{rest}), glutamatergic reversal potential (E_{glut}), and GABAergic reversal potential (E_{GABA}) were set to -60 mV, 0 mV and -60 mV, respectively. Membrane capacitance (C_m) and input resistance (R_{in}) were sampled randomly from truncated normal distributions with means and standard deviations of 17.6 ± 2.8 pF and 1.4 ± 0.6 GΩ, respectively. 1.25 s long glutamatergic and GABAergic conductance traces from the whole cell recordings were randomly sampled with replacement, and used to drive the synaptic inputs (G_{glut} and G_{GABA}) of the model. To achieve particular glutamatergic input strengths the G_{glut} traces were scaled. The neuron's membrane potential was initialised to V_{rest} and was then updated at each time-step using the Euler method according to the equation: $C_m(V(t)/dt) = (1/R_{in})(V_{rest} - V) + G_{glut}(E_{glut} - V) + G_{GABA}(E_{GABA} - V)$, where $V(t)$ is the voltage of the model neuron at time t. 500 simulations with unique membrane capacitance, input resistance, and synaptic samples were run for each value of spike threshold (ranging from -37 mV to -44 mV) and glutamatergic input strength (ranging from 1 pS·s to 25 pS·s). The spike probability for each combination of input parameters was defined as the percentage of the 500 simulations that reached spike threshold.

2.18 Data analysis and statistics

Data were analysed in Matlab (Mathworks; Natick, MA). All data are reported in the text as mean plus or minus standard error of the mean. All fits to the data were performed using the Matlab Curve-Fitting Toolbox. Statistical tests of differences in means were performed with two-tailed Student's *t*-tests and are unpaired unless otherwise noted. Statistical tests of the significance of r^2-values (coefficients of variation) were performed with Student's *t*-tests unless otherwise noted.

Chapter 3

Visuospatial information in the developing retinotectal system at the onset of vision

In Chapter 1, I reviewed the importance of activity-dependent processes in general, and sensory-driven neuronal activity in particular, for the development and refinement of neuronal circuitry. Sensory-driven plasticity processes allow a developing system to adapt to the properties of the environment, so that the range of response sensitivities in a system is adjusted to reflect the statistical properties of the sensory environment (Blakemore & Cooper 1970; Blakemore & Van Sluyters 1975). The retinotectal system of Xenopus laevis has been a favoured model for research into such activity-dependent development (Cline 1991; Debski & Cline 2002; Richards, Aizenman, et al. 2010a; Ruthazer & Cline 2004). It is the animal's principal visual pathway and it has become clear that neuronal activity can influence various properties of retinotectal circuitry, including the axonal morphology of retinal ganglion cells, the dendritic morphology of tectal neurons and their functional synaptic connectivity (Tao & Poo 2005; O'Rourke et al. 1994; Rajan & Cline 1998; Ruthazer et al. 2003; Zhang et al. 1998; Zhang et al. 2000). The retinotectal system is highly plastic during development and relatively brief periods of sensory stimulation have been shown to affect response properties of tectal neurons, such as their receptive field (RF) position, RF size and direction selectivity (Tao & Poo 2005; Engert et al. 2002; Lien et al. 2006; Mu & Poo 2006; Richards, Voss, et al. 2010b; Vislay-Meltzer et al. 2006).

The availability of visual information to the developing retinotectal system of Xenopus may be of particular importance in this animal. Whereas the retinae of mammals and sauropsids display spontaneous waves of activity that influence circuit development throughout the visual system (Galli & Maffei 1988; Meister et al. 1991; Penn et al. 1998; Sernagor & Grzywacz 1996; Stellwagen & Shatz 2002; Wong et al. 1993; Ackman et al. 2012), the retinae of developing Xenopus do not display such spontaneous correlated activity (Demas et al. 2012). Developing

Xenopus embryos, therefore, must rely on correlated activity that is driven by the visual environment. Moreover, due to the *ex utero* nature of their development, Xenopus embryos are already using sensory input to guide behaviours such as visual avoidance (Dong et al. 2009). This highlights that the Xenopus visual system must become functional early in development and suggests that the animal's retinotectal system learns from its visual environment at the same time that the animal is using its visual system to interact with the environment.

The ability of the developing visual system to obtain information about the sensory environment depends upon the ability of the developing eye to project a focused image on the retina. This is a function of the optical properties of the lens, the size of the eye, and the size of the pupil. If an eye is able to focus parallel incoming rays of light (i.e. from optical infinity) onto the retinal photoreceptor layer when the eye is in a relaxed state, then the eye is considered to exhibit correct vision (emmetropia). If the lens focuses the image in front of the retina, the eye is near-sighted (myopic), whereas if the projected image lies beyond the retina, the eye is considered to be far-sighted (hyperopic). In other species it has been observed that during early development, the optics of the eye may be inadequate for the projection of a focused image onto the retina (Easter & Nicola 1996; Wallman et al. 1981; Freeman & Lai 1978; Thorn et al. 1976). Therefore, to study visually driven plasticity in Xenopus, it is important to understand to what extent visuospatial information is available to the retinotectal system at the stages of development under investigation.

In addition to the optical properties of the eye, it is important to understand the early functional connectivity of the developing Xenopus visual system. By characterising both the arrangement of synaptic inputs to individual tectal neurons and their spiking output, it is possible to investigate how these developing neurons convert synaptic inputs into action potential output. Previous work indicates that excitatory synaptic inputs from the retina first reach the optic tectum at stages 39-40 (around 4 days after fertilisation) and immediately lead to visual responses in the tectum (Holt & Harris 1983). The retinal inputs give rise to broadly tuned glutamatergic and GABAergic synaptic RFs in tectal neurons, which become more refined and more overlapping over time (Tao & Poo 2005). It has been reported that visually driven glutamatergic inputs to tectal neurons initially have a broad temporal profile, with polysynaptic recurrent excitatory circuitry within the tectum making up the major part of synaptic excitation (Pratt et al. 2008).

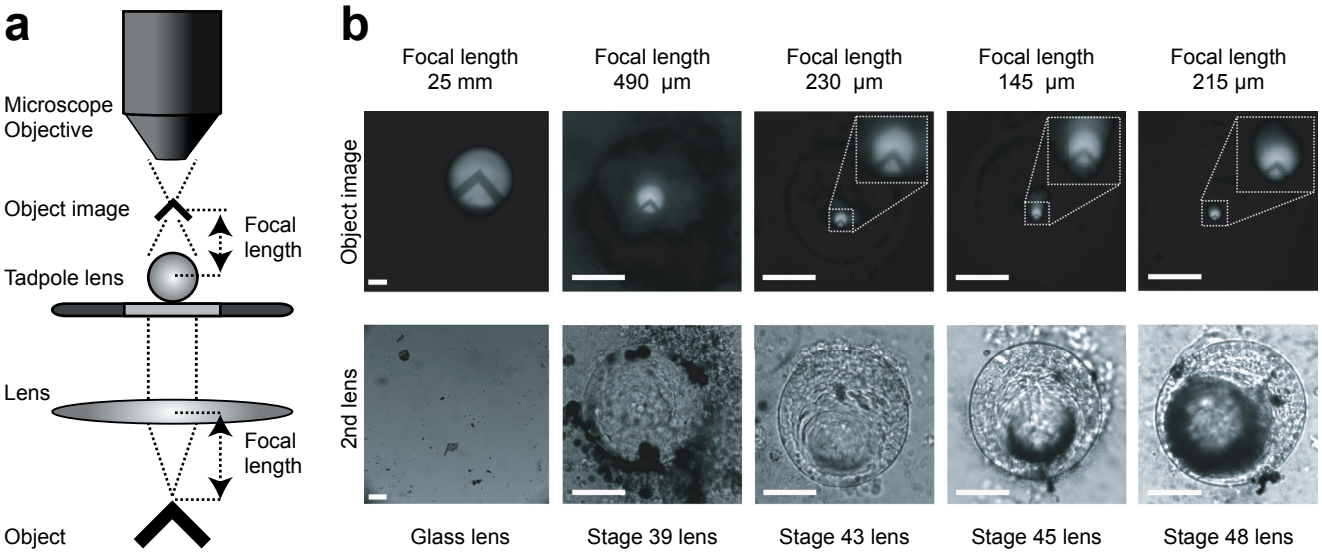
Over development, the glutamatergic inputs acquire a faster time course and spiking responses of tectal neurons become more tightly time-locked to the stimulus. While such glutamatergic inputs are thought to have a clear role in the excitation of tectal neurons, the role of local GABAergic inputs within the tectum is less clear-cut. It has been reported that there is already a feedforward inhibitory circuit in place in the developing tectum at the onset of vision (Zhang et al. 1998; Zhang et al. 2000; Akerman & Cline 2006). However, like in other developing systems (Ben-Ari 2002; Ben-Ari et al. 2007), the recruitment of local GABAergic inputs can have a depolarising effect on developing tectal neurons (Akerman & Cline 2006), which means that GABAergic inputs may be excitatory or facilitate, attenuate or inhibit spike generation (Gao et al. 1998; Chen et al. 1996; Gulledge & Stuart 2003; Staley & Mody 1992). The observation that blocking $GABA_A$ receptors ($GABA_A$Rs) during early tectal development results in altered spiking patterns and prevents stimulus-instructed plasticity, but does not alter overall levels of spiking, further argues for a complex role for GABAergic inputs in the shaping of stimulus-related spiking in the tectum (Richards, Voss, et al. 2010b).

In this Chapter I set out to determine the potential for the tectum to undergo visually driven plasticity at early developmental stages and through intact eyes by investigating:

1. Whether the optics of the eyes of developing Xenopus embryos are able to focus an image of the visual environment onto the retina.
2. To what extent visuospatial information is present in the input and output of developing tectal neurons.
3. How the spatiotemporal properties of the synaptic inputs of tectal neurons relate to their spiking output.

3.1 Tadpole eyes undergo a developmental emmetropisation

Retinal inputs begin to arrive in the optic tectum of Xenopus laevis tadpoles by developmental stages 39-40 (Holt & Harris 1983) and visually driven activity can drive synaptic plasticity from this point onwards (Zhang et al. 2000). Hence, the inputs from the retina have the potential to instruct the refinement of tectal circuitry at the earliest stages of the animal's sighted life (Dunfield & Haas 2009; Engert et al. 2002; Richards, Voss, et al. 2010b; Vislay-Meltzer et al. 2006; Zhang et al. 2000). However, in other species such as zebrafish and chicken, it has been shown that the lens does not correctly focus images onto the retina at early stages

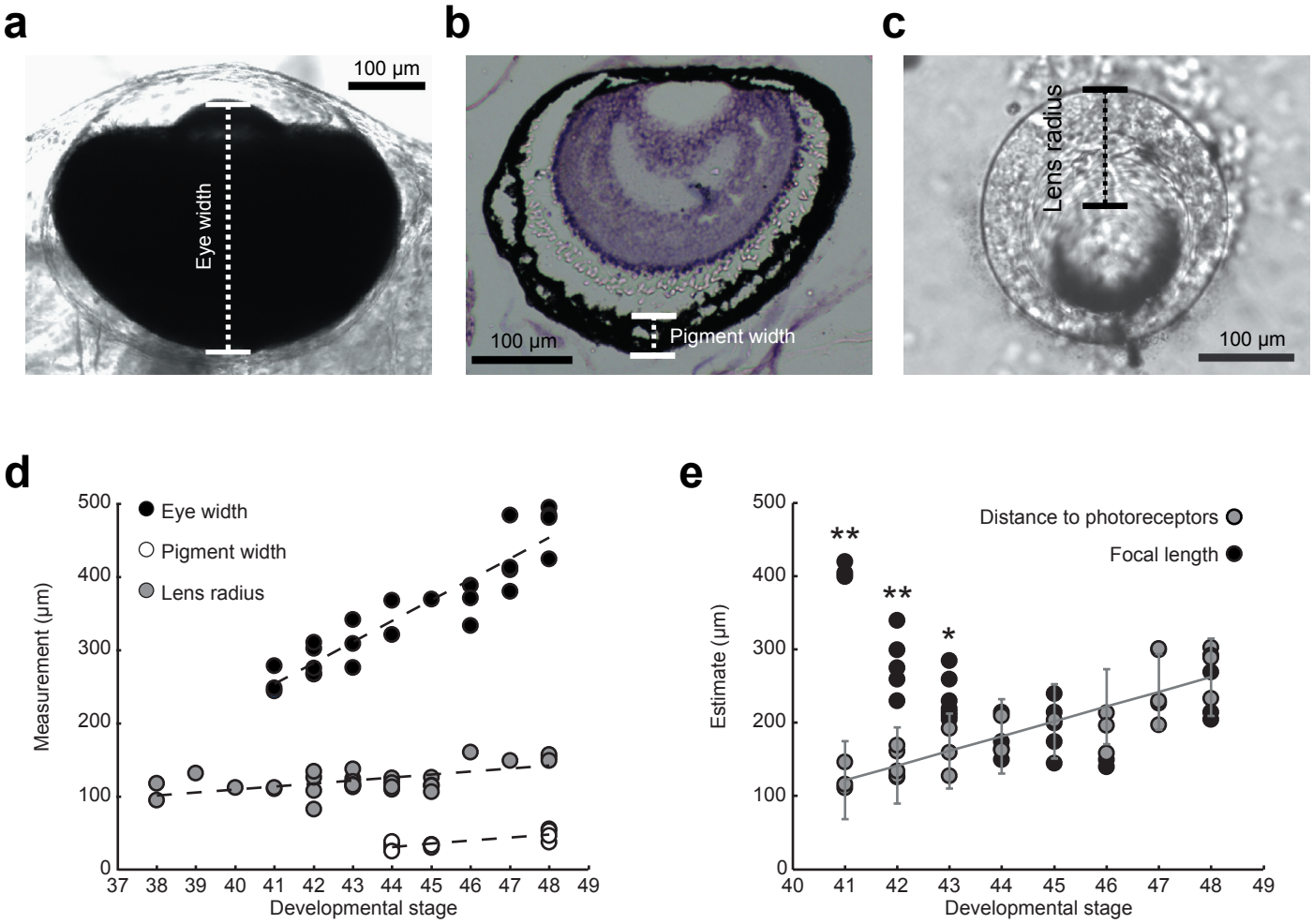


3.1 The focal length of developing Xenopus laevis lenses decreases during early development
a) The focal length of larval Xenopus lenses was measured in a bespoke optical experiment. The condenser of a microscope was removed and replaced with a simple glass convex lens with a known focal length. A small object (the corner of a microscope stage graticule) was placed below this lens at its focal distance, thereby placing the object at 'optical infinity' with respect to the microscope stage. An excised Xenopus tadpole lens was then placed on the stage. Because the object was at optical infinity relative to the position of this tadpole lens, the image that the tadpole lens formed of the object was located at exactly the focal length of the tadpole lens. By first focusing on the tadpole lens and then measuring how far the microscope objective had to be raised until the 'object image' was brought into focus, the focal length of the tadpole lens could be determined. **b)** Example images of lenses from tadpoles at various stages of development (bottom row) and the object images that they formed (top row) are shown. The images on the far left are from a reference glass lens of focal length 25 mm (used for calibration). Note the decrease in focal length from stages 39 to 45. Scale bars are all 100 µm.

of development, as young animals exhibit hyperopia (Easter & Nicola 1996; Wallman et al. 1981). To determine whether this is the case in embryonic Xenopus laevis, a bespoke optical experiment was conducted to measure the focal lengths of tadpole lenses over different stages of development (Figure 3.1a, see also Methods).

The focal lengths of 33 tadpoles ranging from stages 38-48 (3 – 16 days after fertilisation) were measured by the method illustrated in Figure 3.1a. Using a small graticule and a glass lens of known focal length, an image of the graticule was projected onto the tadpole lens at optical infinity, under a microscope objective. The focal length of the tadpole lens could be estimated by adjusting the z-axis of the microscope, starting at the point where the lens was in focus and stopping when the image projected by the tadpole lens was in focus (Figure 3.1b). The distance travelled in the z-axis then corresponded to the focal distance of the tadpole lens. At developmental stages 38-40**,** the focal length of the lens was found to be relatively large (483 ± 41 µm, n = 3 animals). This was followed by a sharp decrease in focal length over the next developmental stages, with a mean of 284 ± 19 µm (n = 15) for animals between stages 41-43 and a mean of 179 ± 10 µm (n = 11) for animals of stages 44-46. Animals at stages 47-48 showed a modest increase in focal length, with a mean of 247 ± 23 µm (n = 4). This indicates that there is an initial period of rapid shortening of the focal length of the lens, followed by a slight increase in focal lengths beyond stage 45, which may correspond to the growth of the eye.

To determine how this developmental change in the focal length of the lens impacted the ability of the lens to project images onto the retina, the distance from the centre of the lens to the photoreceptor mosaic was estimated. The estimate was based on three anatomical measurements: The width of the animal's eye (from the back of the pigment epithelium to the front edge of the lens, Figure 3.2a), the width of the pigment epithelium layer (Figure 3.2b), and the radius of the animal's lens (Figure 3.2c). The distance to the photoreceptors at a given developmental stage could then be estimated by calculating the mean width of the eye, minus the radius of the lens and the pigment epithelium layer. There was a significant linear increase in eye width over stages 41-48 (Figure 3.2d, black dots; n = 25 animals, $r^2 = 0.86$, $p < 0.001$), from 258 ± 11 µm at stage 41 (n = 3 animals) to 472 ± 16 µm at stage 48 (n = 4 animals). The width of the pigment epithelium and lens radius showed similar growth. Over stages 44-48 (n



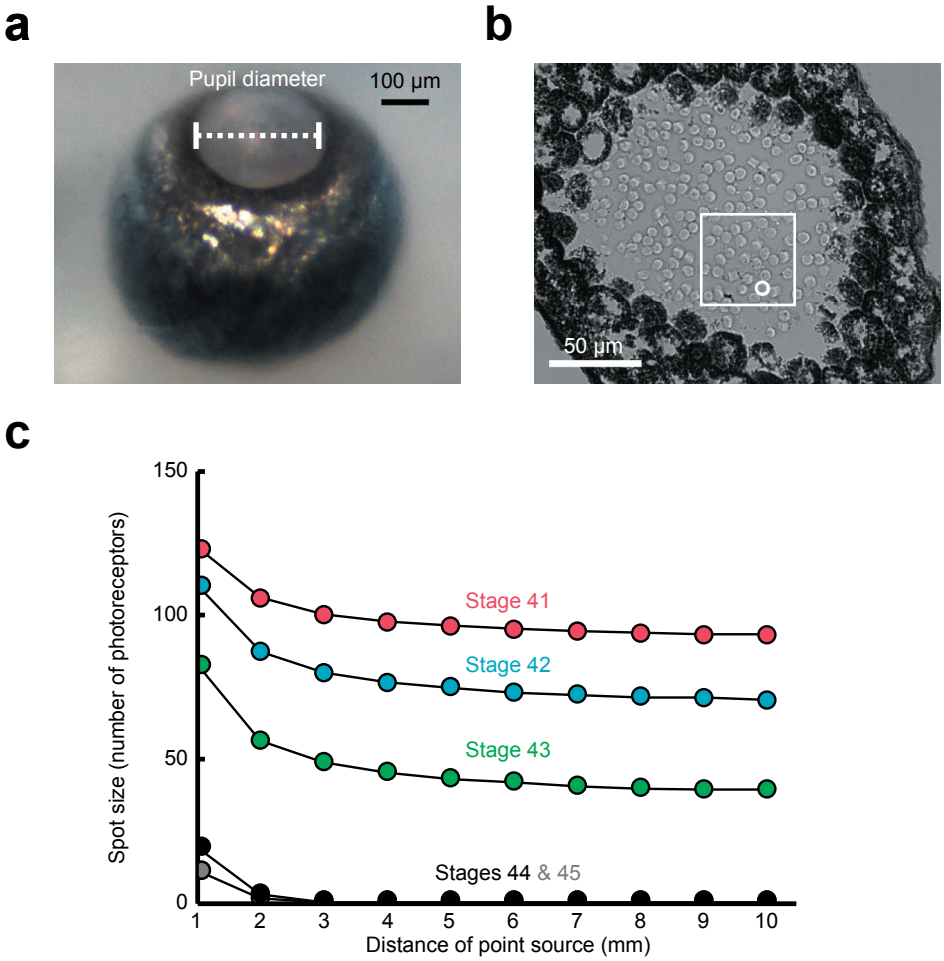
3.2 Xenopus laevis eyes undergo a developmental emmetropisation

a) The width of the eye was measured from the front edge of the lens to the back of the eye, as shown in this dorsal view of a stage 48 animal. **b)** The width of the layer of pigment epithelium at the back of the eye was measured in fixed horizontal sections of tadpole eyes, illustrated here for a stage 48 animal. **c)** The lens radius was measured from dissected lenses, as shown here for a lens from a stage 45 animal. **d)** The eye width (black, n = 25), pigment layer width (white, n = 13), and lens radius (grey, n = 30) were measured across development and are plotted here against the stage of the animal. The corresponding dashed lines show lines of best fit for each measurement (eye width: $r^2 = 0.86$, $p < 0.001$, pigment layer width: $r^2 = 0.69$, $p < 0.001$, lens radius: $r^2 = 0.37$, $p < 0.001$). **e)** The values obtained in 'd' were used to calculate the distance from the center of the lens to the back of the photoreceptors for animals between stages 41 and 48. This is plotted here as grey data points with an accompanying line of best fit and error bars indicating the standard error in predicting the data (n = 25). These values could then be compared with the focal lengths of lenses measured at the corresponding stages (black data points: n = 30). Note the convergence of the lens focal lengths with the distance from the lens to the photoreceptors, indicating a developmental emmetropization. The difference between the focal lengths and the distance from the lens to the photoreceptors was significantly different for animals at stages 41, 42, and 43, and was no longer significant at later stages (**$p < 0.001$ and *$p < 0.01$, $p > 0.05$ for all others).

= 13 animals) the width of the pigment epithelium increased from 33 ± 2 µm at stage 44 (n = 5 animals) to 49 ± 4 µm at stage 48 (Figure 3.2d, white dots; n = 4 animals, $r^2 = 0.69$, $p < 0.001$). Lens radius increased from 115 ± 8 µm at stages 38-40 (n = 4 animals) to 154 ± 2 µm at stage 48 (Figure 3.2d, grey dots; n = 3 animals, $r^2 = 0.37$, $p < 0.001$).

To estimate the distance from the centre of the lens to the photoreceptors over stages 41-48, the linear fits of the lens radius and pigment epithelium were subtracted from the measurements of eye width (Figure 3.2e, grey dots and line). Comparing these estimates with the values obtained for the focal lengths of the lens at different stages, it was observed that the mean focal lengths were significantly larger than the estimated distance from the lens to the photoreceptors at stage 41 ($p < 0.001$), stage 42 ($p < 0.001$) and stage 43 ($p = 0.009$), but not at any of the older stages ($p > 0.05$). These data indicate that tadpoles are hyperopic at early developmental stages, but that their eyes undergo a rapid process of emmetropisation similar to the one observed in other species (Easter & Nicola 1996; Wallman et al. 1981). Consequently, the ability of the eye to focus images on the retina emerges around stage 44-45. After the initial decrease, focal length increases at stages 46-48 in line with the observed increases in eye width, which may serve to maintain emmetropia as the animal grows.

While it was found that tadpoles are hyperopic at early developmental stages, the lens might nevertheless be able to project an image onto the retina during this period. Such a blurred image could still provide the animal with spatial information, to be passed on to the tectum to guide neural development. I therefore sought to determine the resolving power of developing Xenopus eyes at different developmental stages given the above observations about the focal length and eye width of embryos. To do so, it was necessary to determine the diameter of the pupil and the density of photoreceptor cells over development, as both of these factors influence the effective resolving power of the eye (see Methods). The diameter of the pupil was measured in the naso-temporal axis for 23 animals between stages 41-48 (Figure 3.3a). Pupil diameter increased linearly from 144 ± 5 µm at stage 41 (n = 2 animals) to 294 ± 7 µm at stage 48 (n = 4 animals, $r^2 = 0.87$, $p < 0.001$). Conversely, measurements of photoreceptor density on sagittal sections of fixed tadpole eyes from 26 animals (Figure 3.3b) did not show any developmental change, with a mean photoreceptor density of 47 ± 3.9 photoreceptors/2500 μm^2 at stage 44 (n = 8 animals), 43 ± 2 photoreceptors/2500 μm^2 at stage 45 (n = 8 animals)



3.3 The image forming properties of developing Xenopus eyes show a developmental improvement at the onset of vision

a) The diameters of the pupils of developing Xenopus tadpole eyes were measured in the temporal-nasal axis. **b)** The density of photoreceptors on the retina of tadpoles at different developmental stages was estimated from fixed sagittal sections of retina. The white square illustrates one 50 x 50 µm area used for counting the number of photoreceptors in a 2500 μm^2 area, and the white circle indicates one photoreceptor. **c)** The number of photoreceptors that a point source of light would activate at different distances from the eye was estimated for animals at stages 41–45, using the data for the development of focal length, pupil diameter, distance from the lens to the photoreceptors, and photoreceptor density. The image-forming abilities of tadpole eyes showed a developmental improvement. Notably, at hyperopic stages (41–43), there was no distance at which a point source could activate much less than 50 photoreceptors. At emmetropic stages (44–45), a point source of light would activate only a single photoreceptor at distances beyond several millimetres.

and 52 ± 4.6 photoreceptors/2500 μm^2 at stage 48 (n = 10 animals, r^2 = 0.08, p = 0.56).

With these values, equation 2.1 (see Methods) was used to calculate the size of the spot illuminated on the retina by light emanating from a single point at a given distance. This is a measure of how much the optics of the eye would blur a retinal image from an object in the environment. Because the resolving power of the retina is limited by the density of the photoreceptors, the spot size was expressed as the estimated number of photoreceptors within the spot. For stages 41-45 I inserted the values measured for pupil diameter, photoreceptor density, distance from lens to photoreceptors and lens focal length into equation 2.1 and calculated the number of photoreceptors in the retina that would be illuminated by a point source of light at a range of distances (Figure 3.3c). At early stages, but after innervation of the tectum by retinal ganglion cells, the eye was unable to focus a point source of light to anything less than a spot encompassing approximately 50 photoreceptors. Nevertheless, this represents only a small percentage of the total number of photoreceptors on the retina (about 5%, based on estimated photoreceptor density and eye size). This means that despite the significant blurring of the image, spatial information about the visual environment still reaches the retina, even from sources at short distances (on the order of millimetres). At stages 44-45 the eye performed considerably better, such that it was able to focus a point of light at distances of 7 mm or greater onto a single photoreceptor by stage 45. By these stages, therefore, the animal's visual system appears to be close to optimal in terms of its ability to form a sharp image that is matched to the resolution of the photoreceptor layer.

3.2 Visuospatial information is present in synaptic inputs to tectal neurons and can lead to spatially specific output at the onset of vision

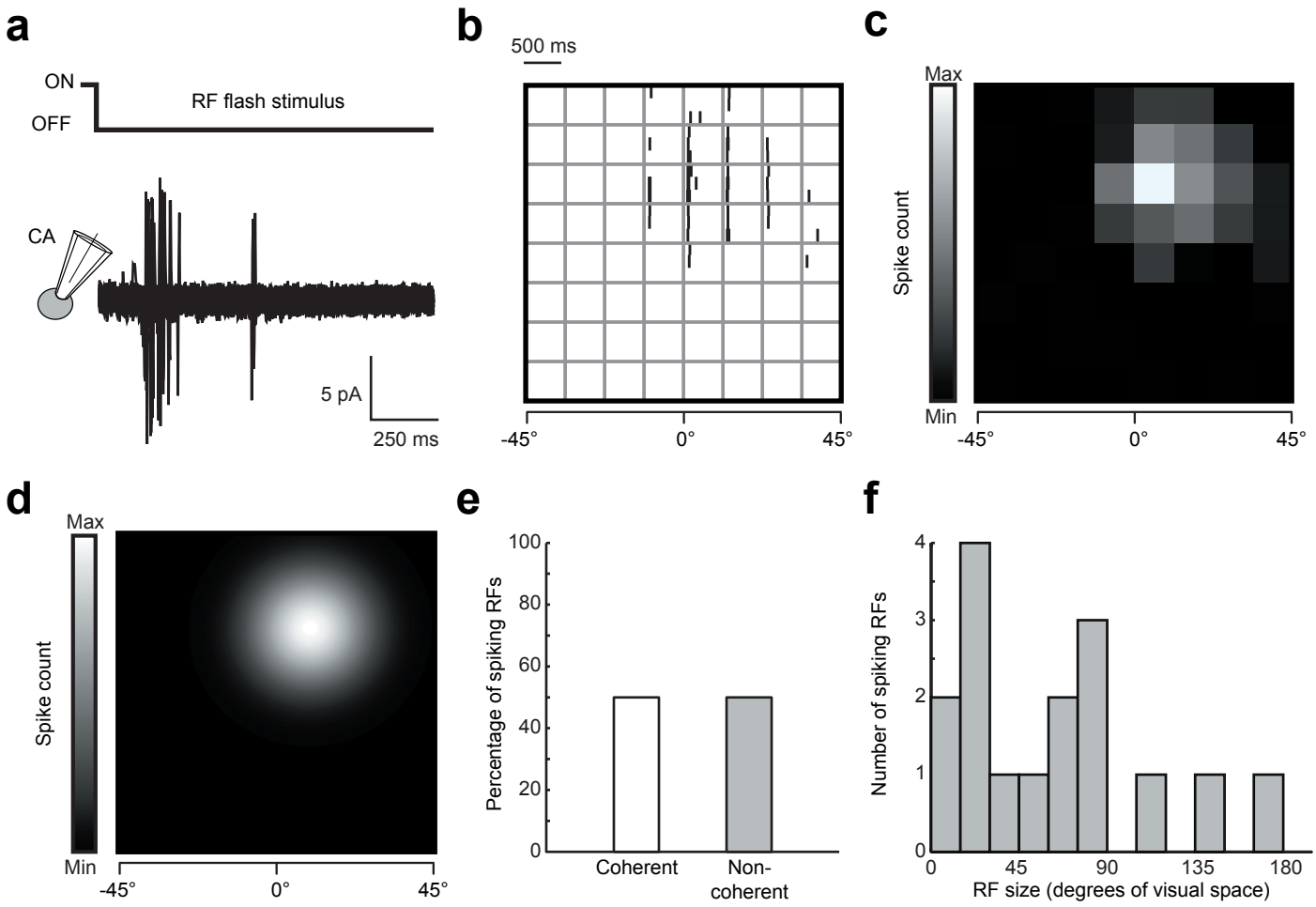
Since the optics of developing Xenopus eyes are able to project at least a blurred image onto the retina at the onset of vision, retinal inputs may be able to relay visuospatial information to the optic tectum. Indeed, multi-unit extracellular recordings indicate that spiking responses are broadly spatially tuned in the tectum shortly after innervation by retinal ganglion cell axons (Holt & Harris 1983). Here, I extend these observations by characterising not only the spatial tuning of the visually driven spiking output, but also that of the glutamatergic and GABAergic synaptic inputs to tectal neurons. To achieve this, *in vivo* patch-clamp recordings were conducted in embryos of stages 40-44 (4-6 days after fertilisation) (Nieuwkoop & Faber 1956) with intact

eyes, while presenting a set of visual RF mapping stimuli.

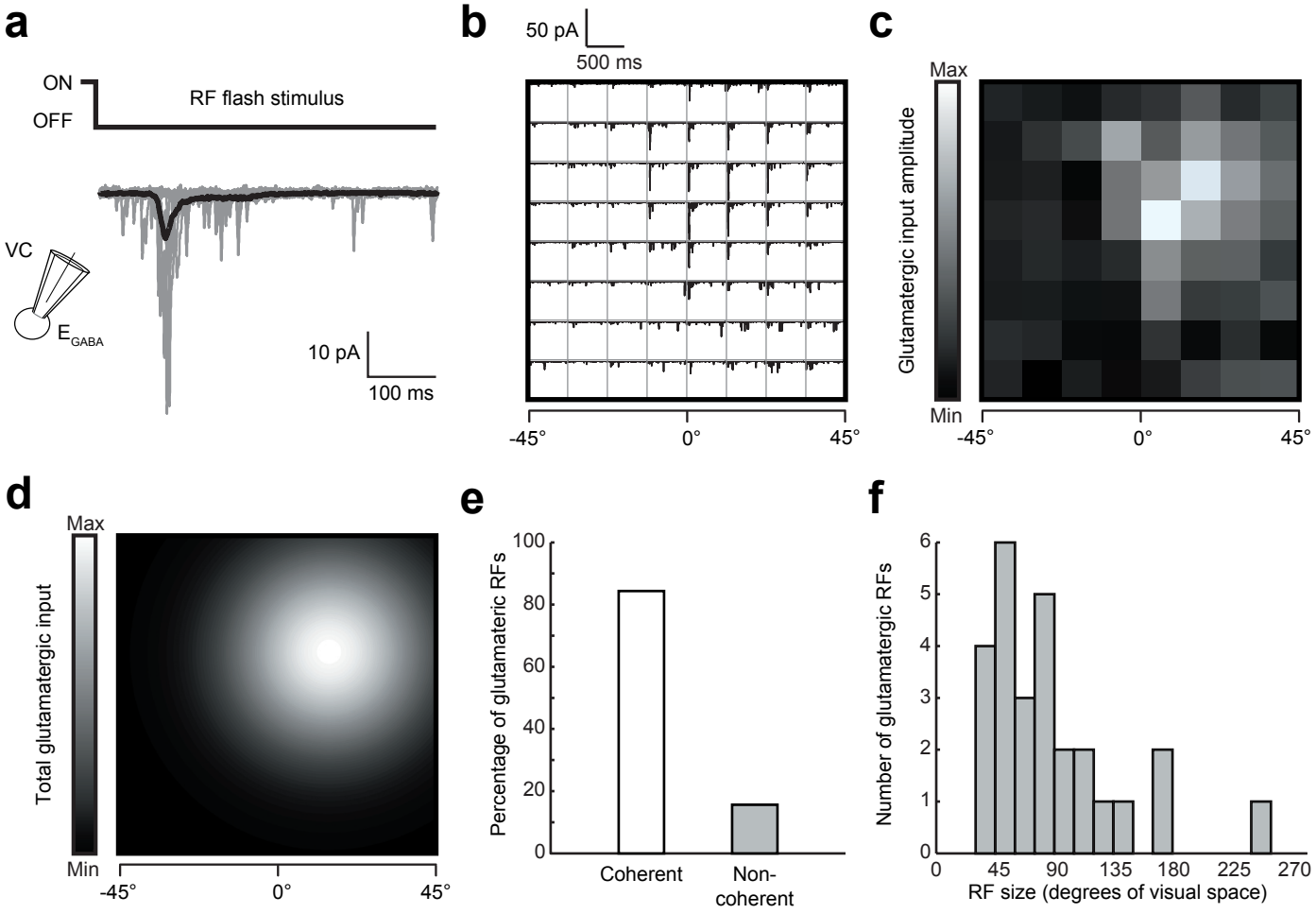
I developed a technique for conducting both extracellular and whole cell patch clamp recordings in the same neuron *in vivo*. Individual tectal neurons were targeted for recording and a gigaseal was established with the cell membrane using a glass recording pipette. Spiking responses of the neuron were recorded in this cell-attached gigaseal mode, which left the intracellular milieu undisturbed. After mapping the spiking RF, the recording configuration was changed to whole cell mode by breaking through the cell membrane. This allowed for the recording of glutamatergic visual inputs by holding the membrane potential at the reversal potential for GABAergic currents, and the recording of GABAergic inputs by holding the membrane potential at the reversal potential for glutamatergic currents (Tao & Poo 2005). I recorded visual responses of tectal neurons from across the caudal half of the tectum to sample a developmentally mixed population of neurons (Wu et al. 1996; Lázár 1973). The RF mapping protocol consisted of white squares flashed at 64 different visuospatial locations, created by dividing the screen (90x90 degrees of visual space) into an 8x8 grid. A RF map could then be created by quantifying the neuronal response to visual stimuli in each of the sampled locations (See Methods for a more detailed description of the experimental protocols for electrophysiology and RF mapping).

Many tectal neurons generated action potentials in response to the RF mapping protocol (Figure 3.4a). RF maps were constructed by quantifying the spike count in response to each of 3 repeats of the flash stimulus during the first 500 ms after OFF events and arranging the spiking responses according to the spatial location of the visual stimulus that evoked them (Figure 3.4b&c). The underlying RF could be approximated by a 2 dimensional Gaussian function (Figure 3.4d, see also Methods), which allowed for an estimation of the RF centre (the peak of the Gaussian function) and the RF size (defined as the minimum full width at half maximum). 50% of the spiking neurons (16/32) were found to have coherent RFs, defined as a statistically significant negative correlation ($p < 0.05$, bootstrap test, see Methods) between the response amplitude and distance from the RF centre as determined by the Gaussian function (Figure 3.4e). The mean RF size was 63.6 ± 12.2 degrees of visual space.

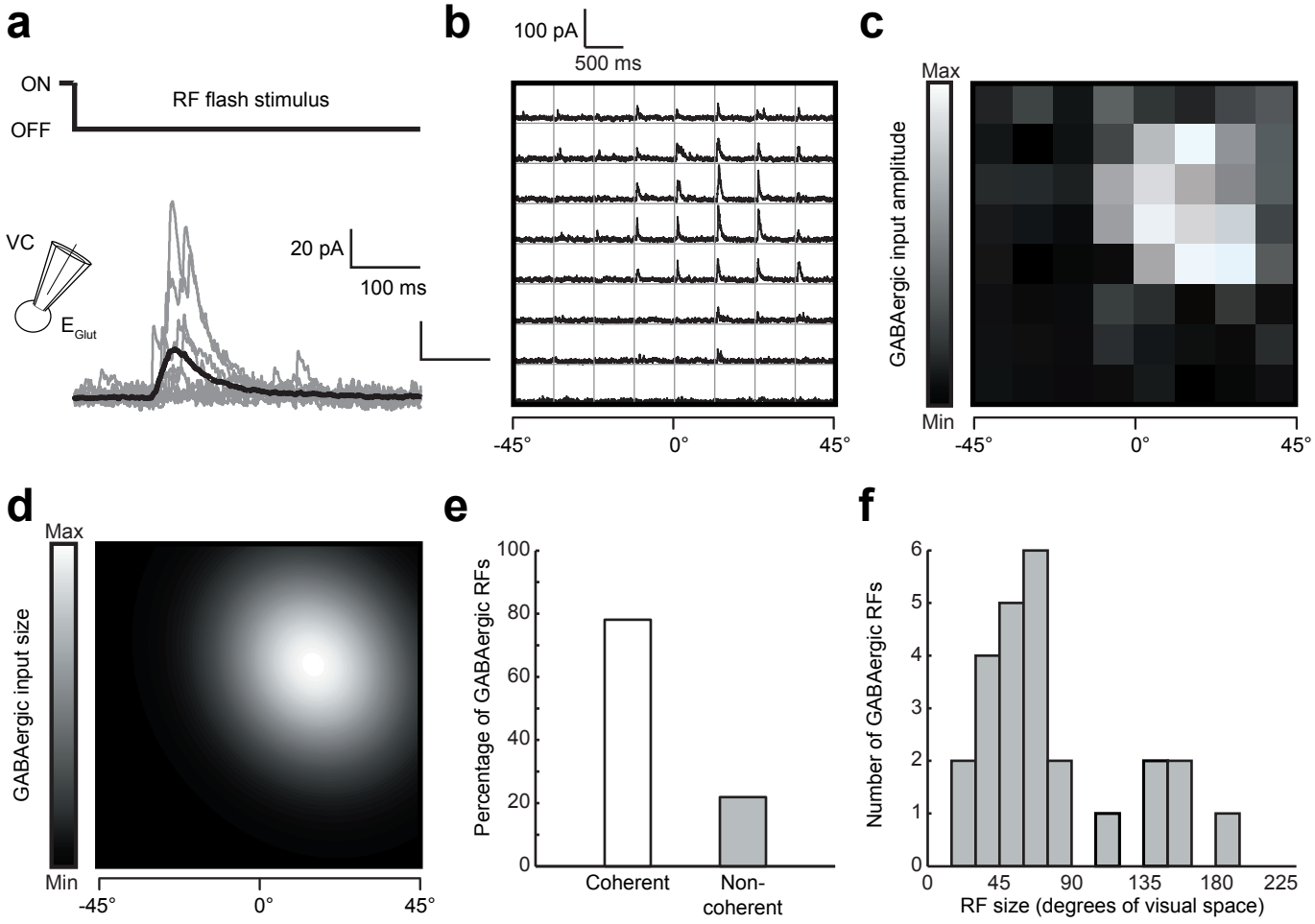
To examine the synaptic inputs to the same tectal neurons, the patch configuration was



3.4 Tectal neurons can exhibit spatially restricted spiking RFs at the onset of vision
a) Spiking responses recorded from a representative tectal neuron of a stage 43 animal. Spiking activity was recorded in cell-attached mode during presentation of a RF mapping protocol. Only responses to stimulus 'OFF' events are included and responses to 20 stimuli are superimposed. **b)** Spiking responses to 3 repeats of the RF mapping protocol for the tectal neuron shown in 'a', arranged by the location of the visual stimulus. White squares were flashed on a black background in each of the 64 locations in a pseudorandom order. This RF mapping protocol was repeated 3 times. Only responses observed within 500 ms after stimulus 'OFF' events are included. **c)** A RF map was created based on the number of spikes recorded in each location, as shown in 'b'. Brighter squares represent a greater number of spikes. **d)** A Gaussian function was used to estimate the spatial profile of the spiking RF of the neuron based on the RF map shown in 'c'. **e)** The percentage of visually responsive tectal neurons that exhibited a spatially coherent spiking RF, as determined from the fitting of a Gaussian function. 50% (16 / 32) of tectal neurons exhibited spatially coherent spiking RFs. **f)** The distribution of spiking RF sizes of tectal neurons with spatially coherent spiking RFs. RF size was defined as the minimum full width at half maximum of the Gaussian fit of the RF (mean RF size: 63.6 ± 12.2 degrees; n = 16).



3.5 Tectal neurons can exhibit spatially restricted glutamatergic RFs at the onset of vision
a) Glutamatergic compound postsynaptic currents (PSCs, grey lines) recorded in response to the RF mapping protocol, while holding a representative stage 43 tectal neuron at the reversal potential for GABAergic currents in whole-cell voltage clamp mode. Shown in black is the mean glutamatergic PSC. Only responses to stimulus 'OFF' events are included. **b)** A RF map showing the mean glutamatergic PSCs in response to 3 repeats of the RF mapping protocol for the same tectal neuron as in 'a', arranged according to the location of the visual stimulus. Responses are shown for the 500 ms following stimulus 'OFF' events. **c)** A RF map was created from the total integrated glutamatergic synaptic conductances. Brighter squares represent stronger glutamatergic input. **d)** A Gaussian function was used to estimate the spatial profile of the glutamatergic RF of the neuron shown in 'c'. **e)** The percentage of visually responsive tectal neurons that exhibited spatially coherent glutamatergic RFs, as determined from the fitting of a Gaussian function of the type shown in 'd'. 84.3% (27 / 32) of neurons exhibited spatially coherent glutamatergic RFs. **f)** The distribution of glutamatergic RF sizes of tectal neurons with spatially coherent glutamatergic RFs. RF size was defined as the minimum full width at half maximum of the Gaussian fit of the RF (mean RF size: 86.3 ± 9.6 degrees; n = 27).



3.6 Tectal neurons can exhibit spatially restricted GABAergic RFs at the onset of vision
a) GABAergic compound postsynaptic currents (PSCs, grey lines) recorded in response to the RF mapping protocol, while holding a representative stage 43 tectal neuron at the reversal potential for glutamatergic currents in whole-cell voltage clamp mode. Shown in black is the mean GABAergic PSC. Only responses to stimulus 'OFF' events are included. **b)** A RF map showing the mean GABAergic PSCs in response to 3 repeats of the RF mapping protocol for the same tectal neuron as in 'a', arranged according to the location of the visual stimulus. Responses are shown for the 500 ms following stimulus 'OFF' events. **c)** A RF map was created from the total integrated GABAergic synaptic conductances. Brighter squares represent stronger GABAergic input. **d)** A Gaussian function was used to estimate the spatial profile of the GABAergic RF of the neuron shown in 'c'. **e)** The percentage of visually responsive tectal neurons that exhibited spatially coherent GABAergic RFs, as determined from the fitting of a Gaussian function of the type shown in 'd'. 78.1% (25 / 32) of neurons exhibited spatially coherent GABAergic RFs. **f)** The distribution of GABAergic RF sizes of tectal neurons with spatially coherent glutamatergic RFs. RF size was defined as the minimum full width at half maximum of the Gaussian fit of the RF (mean RF size: 77.5 ± 9.1 degrees; n = 25).

converted from cell-attached mode to whole cell mode. Holding the neuron at the reversal potential for GABAergic currents allowed for the recording of glutamatergic postsynaptic currents (PSCs) in response to the RF mapping protocol. Figure 3.5a illustrates a set of visually evoked glutamatergic responses for the same tectal neuron as in Figure 3.4. The mean responses to the 3 repeats of the RF mapping protocol were again arranged according to the visual stimulus (Figure 3.5b), and the response was quantified as the total integrated conductance over the first 500 ms following stimulus OFF events (Figure 3.5c). A Gaussian fit to the glutamatergic RF maps allowed for determination of the RF centre and RF size (Figure 3.5d). The large majority of neurons (84%) had spatially coherent glutamatergic RFs (Figure 3.5e), with a mean RF size of 86.3 ± 9.6 degrees (Figure 3.5f). When the neurons were held at the glutamatergic reversal potential, GABAergic visually evoked PSCs could be detected. Figure 3.6a illustrates a set of visually evoked GABAergic responses for the same tectal neuron as in Figures 3.4 and 3.5. To create a RF map, the responses were again arranged according to the location of the visual stimulus (Figure 3.6b) and quantified as total integrated conductance during the first 500 ms following stimulus OFF events (Figure 3.6c). These RFs were fit with a Gaussian function (Figure 3.6d). 78% of neurons had spatially coherent GABAergic RFs (25/32, Figure 3.6e), with a mean RF size of 77.6 ± 9.2 degrees (Figure 3.6f). These findings illustrate that despite the animal's hyperopia, tectal neurons already receive spatially restricted visual input at developmental stages immediately after the onset of vision, and are able to translate these visually evoked synaptic inputs into spatially restricted spiking output.

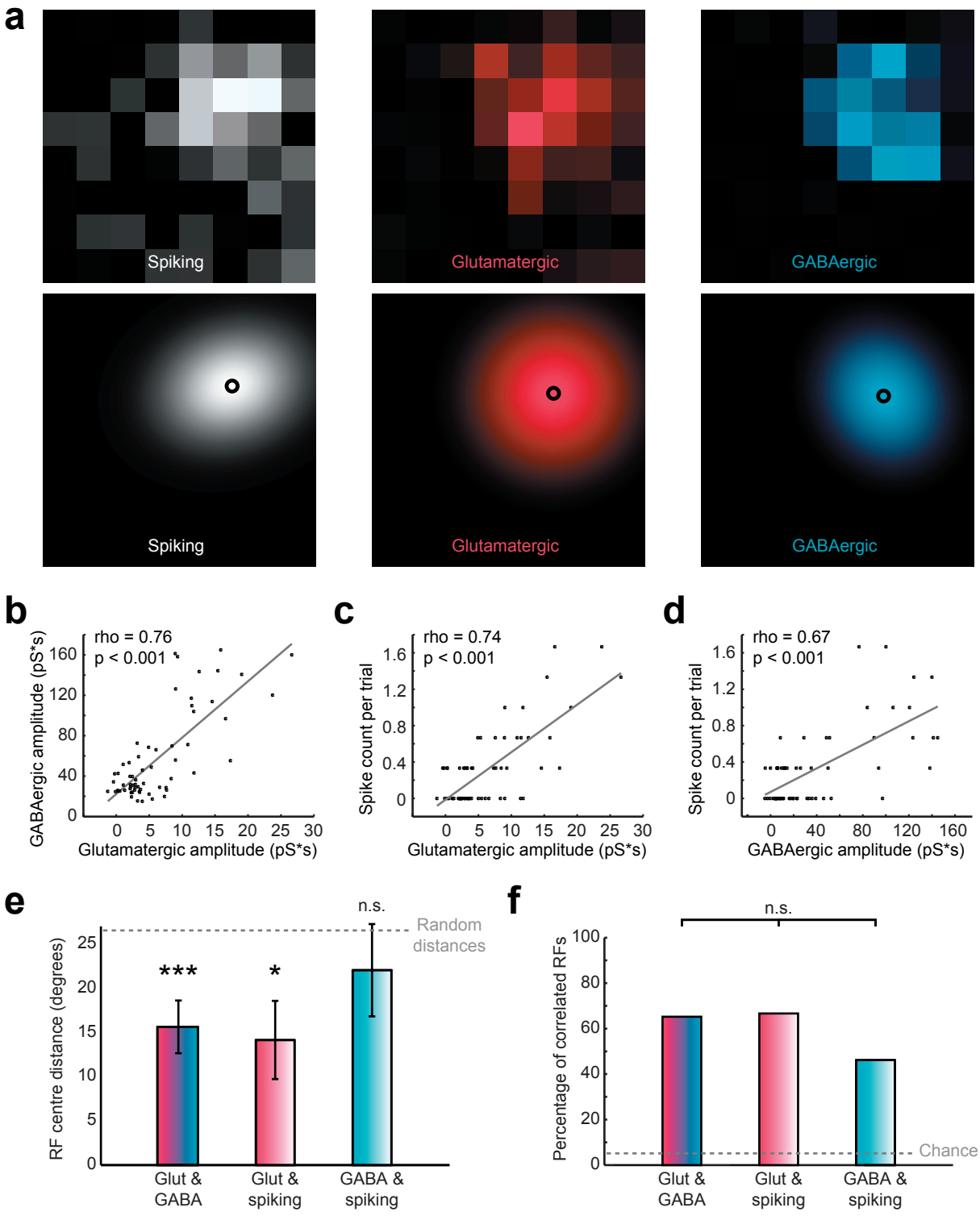
3.3 Glutamatergic inputs are the major driver of tectal neuron spiking activity at the onset of vision

In addition to excitatory glutamatergic inputs, GABAergic inputs could promote tectal neuron spiking activity due to their depolarising nature during early development (Akerman & Cline 2006). It is therefore not known whether glutamatergic or GABAergic inputs are the most important drivers of early tectal spiking output. In fact, the spatiotemporal relationship between glutamatergic and GABAergic inputs may be particularly important; depolarising GABAergic inputs that on their own would not be sufficient to generate an action potential could interact with glutamatergic inputs to generate spiking output (Gao et al. 1998; Gulledge & Stuart 2003). A previous study in the Xenopus retinotectal system by Tao and Poo (Tao & Poo 2005), found that glutamatergic and GABAergic inputs are initially not well matched in visual space,

but converge over time through an activity-dependent process that relies on GABAergic transmission. Recording both the spiking RF and the synaptic input RF from the same tectal neuron, I was able to investigate how tectal input and output relate to one another at the onset of vision.

The glutamatergic, GABAergic and spiking RFs of tectal neurons were often found to be spatially overlapping, with centres close together in visual space. To establish whether RF centres showed a significant tendency to be spatially matched at the earliest stages of visual responsiveness, distances between glutamatergic, GABAergic and spiking RF centres were compared to a distribution of distances obtained by randomly positioning points across the sampled area of visual space (Figure 3.7a&e). On average, glutamatergic and GABAergic RF centres were relatively close together in visual space, with a mean distance of 15.6 ± 3.0 degrees. This distance was significantly shorter than predicted by chance ($p < 0.001$). Glutamatergic and spiking RF centres were also found to be significantly spatially matched, with a mean centre-to-centre distance of 14.1 ± 4.4 degrees ($p = 0.011$). GABAergic and spiking RF centres, on the other hand, were not significantly spatially matched, with a mean distance of 22.0 ± 5.2 degrees ($p = 0.410$). These data reveal that glutamatergic and GABAergic inputs can show a significant degree of spatial matching at the onset of vision, and suggest that glutamatergic inputs are more important in determining spiking activity.

To further investigate the spatial relationships between the glutamatergic synaptic input, GABAergic synaptic input and spiking output of tectal neurons, I examined the correlation between their response amplitudes across visual space (Figure 3.7b-d & f). Consistent with the observations regarding the matching of RF centres, the majority of neurons showed a statistically significant correlation between glutamatergic RFs and both the GABAergic (65%, 15 / 23) and the spiking (67%, 10 / 15) RFs (Figure 3.7f). Meanwhile, just under half of neurons showed a significant correlation between GABAergic and spiking RFs (46%, 6 / 13). These percentages did not differ significantly from each other (glut & GABA vs. glut & spiking: $p = 1.000$, glut & GABA vs. GABA & spiking: $p = 0.310$, glut & spiking vs. GABA & spiking: $p = 0.445$, Fisher's exact test). However, in all cases the proportion of neurons with spatially correlated RFs was well above the number predicted by chance ($p < 0.001$). These results indicate that even at developmental stages shortly after the onset of vision, glutamatergic, GABAergic and



3.7 Spiking, glutamatergic and GABAergic RFs are spatially matched at the onset of vision

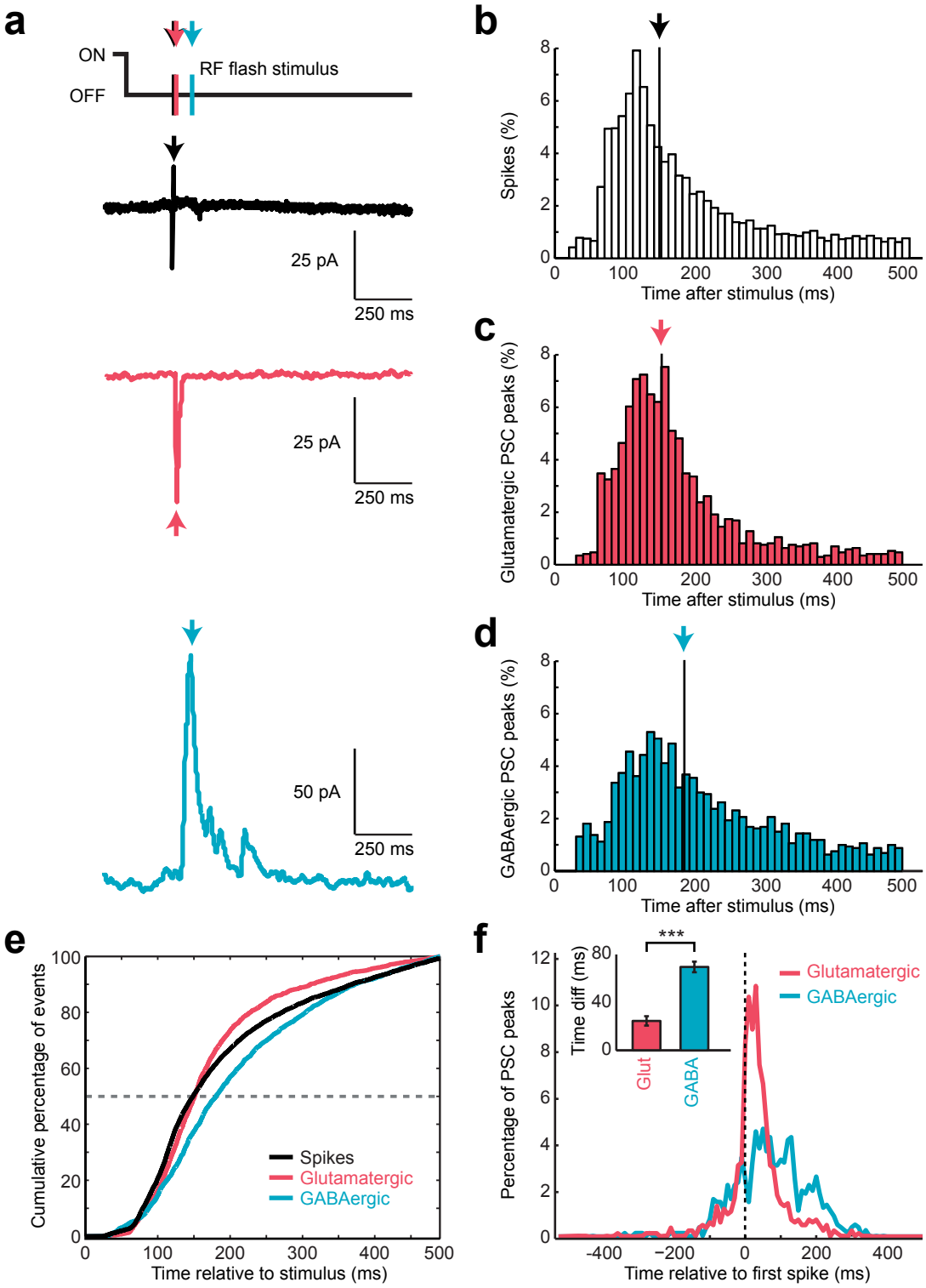
A legend is provided on the next page

Legend for Figure 3.7 (previous page)

3.7 Spiking, glutamatergic and GABAergic RFs are spatially matched at the onset of vision
a) Spiking (white), glutamatergic (red) and GABAergic (blue) RFs from a representative tectal neuron recorded in a stage 43 animal. Based on the raw RF maps (top row) a Gaussian fit to the RF map was used to estimate the RF centres (bottom row). **b)** A scatter plot illustrating the correlation between glutamatergic and GABAergic visual response amplitude for the RFs shown in 'a'. **c)** A scatter plot illustrating the correlation between glutamatergic response amplitude and spike count for the RFs shown in 'a'. **d)** A scatter plot illustrating the correlation between GABAergic response amplitude and spike count for the RFs shown in 'a'. **e)** A comparison of the mean distances between glutamatergic and GABAergic RF centres (15.6 ± 3.0 degrees; n = 23), glutamatergic and spiking RF centres (14.1 ± 4.4 degrees, n = 15), and GABAergic and spiking RF centres (22.0 ± 5.2 degrees, n = 13). Glutamatergic RF centres are closer to both GABAergic RF centres ($p < 0.001$) and spiking RF centres ($p = 0.011$) than would be predicted by chance, from a simulation of $1*10^6$ randomly distributed pairs of points (26.3 ± 0.0 degrees, n = $1*10^6$). Meanwhile, the distance between GABAergic and spiking RF centres is not significantly closer than chance ($p = 0.410$). **f)** The percentage of neurons with significantly correlated ($p < 0.05$) glutamatergic and GABAergic RF profiles (65.2%, 15 / 23), glutamatergic and spiking RF profiles (66.7%, 10 / 15), and GABAergic and spiking RF profiles (46.2 %, 6 / 13). All pairings display more correlated RFs than would be predicted by chance (5%, dotted line, $p < 0.001$ in all cases, binomial test). None of the RF pairings differed statistically in terms of their correlations (glut & GABA vs glut & spiking, $p = 1.000$; glut & GABA vs GABA & spiking: $p = 0.310$; glut & spiking vs. GABA & spiking: $p = 0.445$; Fisher's exact test).

Legend for Figure 3.8 (next page)

3.8 Glutamatergic inputs are the most important contributors to spike timing at the onset of vision
a) An example spiking (black), glutamatergic (red) and GABAergic response (blue) of a tectal neuron to the same visual RF stimulus. Arrows indicate spike time (spiking trace) or the time of the peak of the visually evoked synaptic conductance (glutamate and GABA). The glutamatergic peak and the spike are closely time-locked, followed by the GABAergic peak. The population data in the rest of the figure are from 32 tectal neurons from animals of stages 40-44. **b)** The distribution of spike times in relation to the RF flash stimuli, median (148.8 ms) indicated by arrow. **c)** The distribution of glutamatergic peak response times in relation to the RF flash stimuli, median (150.8 ms) indicated by arrow. **d)** The distribution of GABAergic peak response times in relation to the RF flash stimuli, median (180.3 ms) indicated by arrow. **e)** The cumulative distributions of spike times, glutamatergic peak times and GABAergic peak times. These three distributions were significantly different from one another ($p < 0.001$ in all cases, K-S test), although the distributions of glutamatergic peaks and spike times show considerable overlap in the early part of the stimulus window. **f)** A histogram of the glutamatergic (red) and GABAergic (blue) peak times in relation to the timing of first spikes in response to the same stimulus. The dashed line at 0 represents the point at which the peak of the PSC and the first spike occur simultaneously. The sides of the plot represent instances where the peak of the PSC preceded the first spike (left side), and where the first spike preceded the peak of the PSC (right side). The narrow distribution of glutamatergic peak responses indicates that these responses are especially time-locked with the first spike responses. Bar graph (inset) shows the difference between glutamatergic peak and first spike time (+24.6 ± 3.9 ms) compared to the difference between GABAergic peak and first spike time (+69.6 ± 4.4 ms, $p < 0.001$).



3.8 Glutamatergic inputs are the most important contributors to spike timing at the onset of vision

A legend is provided on the previous page

spiking RFs can be highly spatially correlated with one another.

The temporal precision of spiking is of crucial importance for sensory-driven synaptic plasticity in the tectum (Zhang et al. 1998; Mu & Poo 2006; Vislay-Meltzer et al. 2006; Richards, Aizenman, et al. 2010a). A previous study in the developing optic tectum found that the temporal profile of glutamatergic synaptic inputs and spiking output were very similar (Pratt et al. 2008). However, these experiments used electrical stimulation of the optic nerve rather than visual stimuli, and they were carried out under conditions of $GABA_AR$ blockade. I therefore sought to establish whether visually driven glutamatergic inputs are the major determinant of visual spike timing *in vivo*, and how GABAergic inputs relate to visually evoked spiking activity.

For each neuron, spike times for all spikes were derived from the spike detection algorithm (see Methods). To establish the timing of the synaptic inputs, I calculated the times of the peak of the glutamatergic and GABAergic PSCs across all RF locations (Figure 3.8a, see Methods). Spikes occurred at a median of 149 ms after stimulus events (Figure 3.8b), which was almost coincident with glutamatergic peak responses (151 ms, Figure 3.8c). Meanwhile, GABAergic peak responses occurred at a median time of 180.3 ms after the stimulus (Figure 3.8d), almost 30 ms after spike events. These distributions of response times were all significantly different from each other (Figure 3.8e, $p < 0.001$ in all cases, Kolmogorov-Smirnov test), indicating that, on average, glutamatergic PSC peaks occurred just before most spikes, and GABAergic PSC peaks occurred after both glutamatergic PSC peaks and most spikes. To further investigate the temporal relationship between spikes and synaptic inputs, I compared the timing of the PSCs relative to the median first spike time (over the 3 RF mapping repeats) for each visual location across all 32 neurons (Figure 3.8f). Glutamatergic PSC peaks were significantly more closely time-locked to the first spike events (+24.6 ± 3.9 ms) than GABAergic PSC peaks (+69.6 ± 4.4ms, $p < 0.001$). Taken together, these data suggest that, despite the potential for GABAergic inputs to depolarise tectal neurons at these stages of development, glutamatergic inputs are the most important drivers of spiking output at the onset of vision.

3.4 Discussion

In this chapter I investigated the availability of visuospatial information to the developing optic tectum at the onset of vision and its potential to underlie sensory-driven plasticity processes. I

first examined the limitations of the optics of the developing eye and its ability to form a sharp image on the retina. Next, I investigated the spatial and temporal profile of the visually driven synaptic inputs to tectal neurons shortly after the onset of vision and related this to their spiking output.

Anatomical and optical measurements revealed that, in agreement with findings in other species (Easter & Nicola 1996; Wallman et al. 1981), Xenopus tadpoles are hyperopic at early developmental stages. Notably, this is the case during a developmental period when retinal ganglion cells have innervated the tectum and the system is responsive to visual stimuli (Holt & Harris 1983). However, this initial hyperopia is quickly corrected over subsequent stages of development in a process of emmetropisation, which relies chiefly on a developmental shortening of the focal distance of the lens, resulting in correct vision at stages 44-45. At this point, the lens shows a trend towards increasing focal length, in a manner that tracks the developmental increase in eye size. This process of emmetropisation is consistent with a study of developing zebrafish eyes (Easter & Nicola 1996). However, previous work from a number of laboratories has shown that spatially structured visual stimuli can drive activity-dependent processes in the Xenopus optic tectum at stages before emmetropic vision is established (Richards, Voss, et al. 2010b; Engert et al. 2002; Vislay-Meltzer et al. 2006). This suggests that even at these stages, the system can extract some degree of spatially organised information. Consistent with this, an investigation into the expected amount of blurring of an image on the retina revealed that even at hyperopic stages, a point source of light would activate a spatially restricted subset of photoreceptors.

To investigate the extent of visuospatial information available to tectal neurons, I characterised the spatiotemporal properties of their synaptic inputs that can be driven by visual stimulation through the intact eye at hyperopic stages (40-44). Most visually responsive neurons had spatially coherent glutamatergic and GABAergic RFs. This led to spatially coherent spiking output in about half of the visually spiking neurons. RFs could be approximated by a Gaussian function and were often large, covering most of the 90 degrees of visual space that were sampled in the RF mapping protocol. The large RF sizes reported in this chapter are in accordance with the results of other studies in developing Xenopus embryos at stages shortly after the onset of vision (Gaze et al. 1974; Holt & Harris 1983). These large RF sizes may partly

be explained by blurring of the visual scene created by the hyperopic eye. However, it should be noted that Tao & Poo (Tao & Poo 2005) observed large RF sizes in developing Xenopus at similar stages using animals in which the lens had been removed from the eye and images were formed directly onto the retina with a microscope objective. A more direct comparison with Tao & Poo (Tao & Poo 2005) is difficult, due to differences in experimental setup as well as data analysis. First, because Tao & Poo projected images directly onto the excised retina, it is hard to make a precise statement about the extent of visual field that was covered by their stimulus. Second, their definition of receptive field did not incorporate an element of spatial structure such as the Gaussian fits performed in this chapter. Instead, they considered any consistently responsive RF location to be part of a neuron's RF. Nevertheless, their finding of relatively large RFs in young animals illustrates that while hyperopia may have an effect on RF size in young Xenopus larvae, diffuse synaptic connectivity is likely to be the principal determinant of the large RF size in these animals.

This chapter also included an investigation into the relationship between the synaptic input RFs and spiking output RFs of tectal neurons at stages immediately after the onset of vision. This part of the study revealed that glutamatergic and GABAergic visual inputs are spatially organised with respect to one another, such that their RF centres tend to be close to one another and responses across visual space are correlated. This extends the findings of Tao and Poo (Tao & Poo 2005), who reported that the spatial matching of glutamatergic and GABAergic RFs becomes more precise over the course of development through an activity-dependent process. Moreover, this work reveals that glutamatergic RF centres and spiking RFs centres are more closely matched in visual space than GABAergic RF centres and spiking RF centres. This suggests that the spatial distribution of glutamatergic input is most predictive of spiking activity. A characterisation of the temporal relationship between synaptic inputs and spiking output revealed that spikes were most closely time-locked with the peak of glutamatergic inputs, rather than GABAergic inputs. Therefore, despite the depolarising nature of GABAergic inputs to tectal neurons at early stages of development (Akerman & Cline 2006), glutamatergic inputs appear to be the most important source of excitation for spike generation in developing tectal neurons, closely correlating with both the spatial and temporal distribution of spiking activity.

The availability of visuospatial information to the optic tectum supports the idea that visually

driven activity can provide informative correlations for the refinement of the retinotectal system, almost immediately after the onset of vision. This may be of particular importance for Xenopus larvae, as they lack the spontaneous retinal waves of patterned activity (Demas et al. 2012) that instruct visual system development in other species (Meister et al. 1991; Penn et al. 1998; Wong et al. 1993; Sernagor & Grzywacz 1996; Ackman et al. 2012; Galli & Maffei 1988). More generally, such a formative role for the earliest visual experience in visual system development parallels observations in other species (Akerman et al. 2002; Tian & Copenhagen 2003; Lu & Constantine-Paton 2004). The findings in this chapter therefore further validate the use of developing Xenopus as a suitable model system for the investigation of sensory-driven development, while acknowledging that the spatial information available to the tectum may not be optimal at the onset of vision.

In summary, Xenopus eyes are hyperopic at the onset of vision (stages 39-40) but undergo a rapid process of emmetropisation that results in correct vision around stage 45. Even at hyperopic stages, however, the optics of the eye allow for the projection of blurred images that already contain visuospatial information and have the potential to drive local correlated activity on the retina. Recordings of the synaptic inputs and spiking output of tectal neurons revealed that visuospatial information reaches the tectum and leads to spatially tuned spiking activity. Emerging glutamatergic and GABAergic RFs are already correlated with one another, and despite the depolarising nature of GABAergic inputs to developing tectal neurons, glutamatergic inputs appear to be the strongest driver of spiking activity. These observations confirm that, from the onset of vision, the development of the retinotectal system has the potential to be guided by neuronal activity driven by the visual environment.

Chapter 4

A population of non-spiking neurons in the developing optic tectum

In the previous chapter I established that visual stimuli drive patterned neuronal activity in the developing optic tectum of Xenopus laevis from the onset of vision. In the retinotectal system, these patterns of activity can influence aspects of neuronal morphology such as dendritic arborisation (Haas et al. 2006; Sin et al. 2002) and axonal branching (Ruthazer et al. 2003; O'Rourke et al. 1994), as well as the maturation of synaptic transmission and the refinement of visual receptive fields (RFs) (Pratt et al. 2008; Tao & Poo 2005). Such activity-dependent processes are often dependent on postsynaptic depolarisation paired with incoming synaptic inputs (Sastry et al. 1986; Gustafsson et al. 1987; Gustafsson & Wigström 1988), which are thought to rely on correlated spiking activity in the presynaptic and postsynaptic neurons (Markram et al. 1997; Magee & Johnston 1997). In the retinotectal system of Xenopus in particular, the critical relationship between pre- and postsynaptic spiking activity and synaptic plasticity has been well characterised. Spike timing dependent plasticity (STDP) was first demonstrated *in vivo* in the optic tectum (Zhang et al. 1998), and has been shown to lead to input-specific plasticity from early developmental stages (Tao et al. 2001) and to be capable of driving changes to the RFs of tectal neurons (Vislay-Meltzer et al. 2006; Mu & Poo 2006). The control of spike generation and timing has also been implicated in the maturation of visual response properties in the tectum (Richards et al. 2010; Tao & Poo 2005).

The ability to spike in response to incoming synaptic excitation is therefore important to a developing neuron, not only because it allows the neuron to contribute to information processing, but also because the ability to spike seems to be a prerequisite for many of the mechanisms that govern a neuron's activity-dependent development. Indeed, a study interfering with the spiking output of tectal neurons found that neurons with impaired spiking output failed to develop mature RFs (Dong & Aizenman 2012). There are two basic requirements

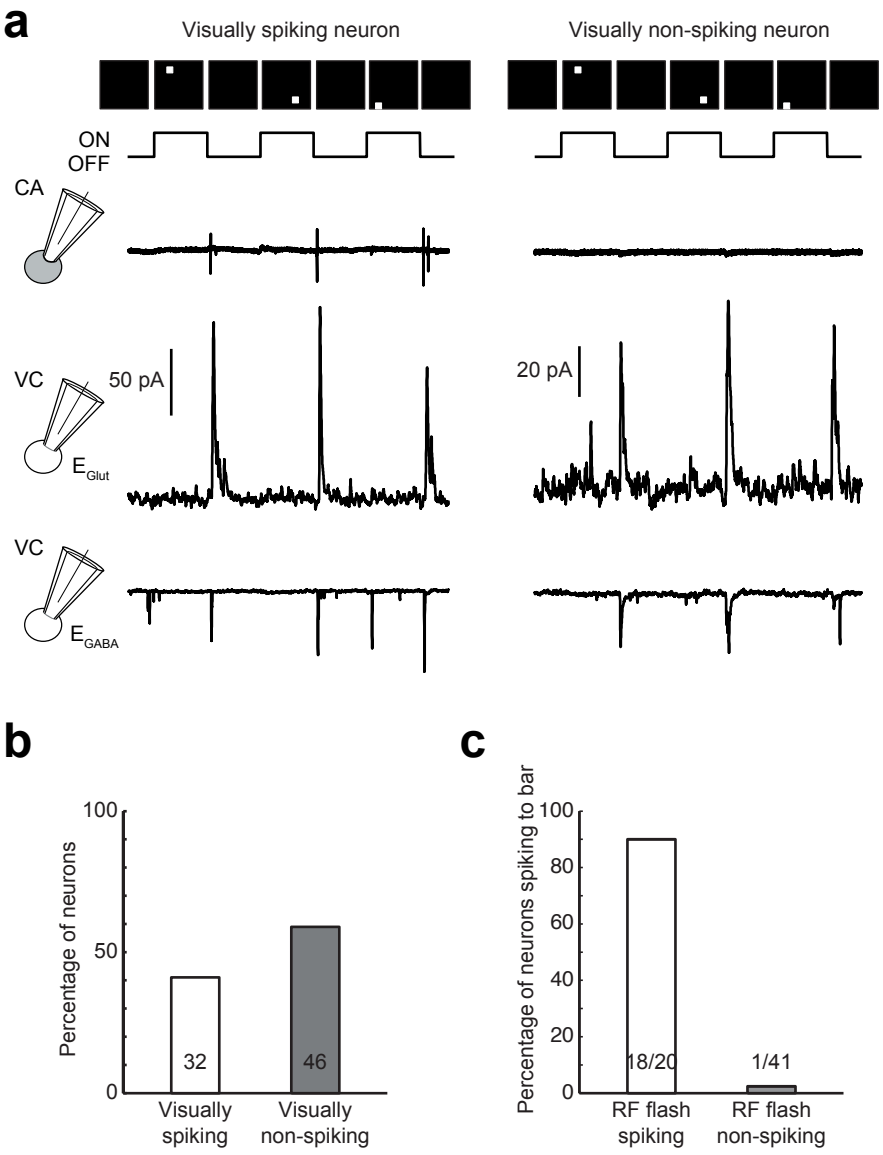
for synaptically driven spiking. First, a neuron needs to be electrically excitable, through the appropriate expression of voltage-gated ion channels that provide the active mechanism for spike generation (Hodgkin & Huxley 1952; Hille 2001). Second, a neuron needs a synaptic source of membrane depolarisation that will raise the membrane voltage to the spike threshold - the voltage at which voltage-gated sodium (Na^+) channels activate rapidly to generate a spike (Katz 1959; Eccles 1961). This requires presynaptic release of excitatory neurotransmitters, as well as the expression of the appropriate postsynaptic receptors (Monaghan & Bridges 1989; Dingledine et al. 1999).

Visually driven spiking activity is evident in the optic tectum as soon as retinal ganglion cell axons begin innervating this structure (Holt & Harris 1983), and it has been observed that the majority of developing neurons in Xenopus develop the necessary intrinsic properties for spike generation before this time (Spitzer & Lamborghini 1976; Spitzer & Ribera 1998). In this chapter, however, I describe a large population of developing tectal neurons that does not exhibit visually driven spiking activity, even though these neurons receive visually evoked glutamatergic and GABAergic synaptic inputs. The experiments described in the next section therefore set out to establish:

1) Whether there are any neurons in the developing tectum that do not generate a spiking output.
2) The likely cause for a lack of visually evoked spiking activity.
3) Whether neurons that lack spiking activity exhibit differences in the spatiotemporal properties of their synaptic inputs.

4.1 A population of visually non-spiking neurons in the developing optic tectum

In chapter 3, I characterised the visually evoked spiking output of developing tectal neurons by combining *in vivo* patch-clamp recordings with an RF mapping protocol (e.g. Figure 3.4). In addition to the neurons that exhibited clear stimulus-dependent spiking activity, I observed a separate population of neurons that failed to exhibit action potentials to visual stimuli when recorded in cell-attached configuration. After having recorded spiking activity (or lack of spiking activity) in cell-attached mode, the recording configuration was changed to whole-cell mode in order to record glutamatergic and GABAergic visual synaptic inputs. Interestingly, many of the visually non-spiking neurons were found to receive robust visually evoked synaptic input



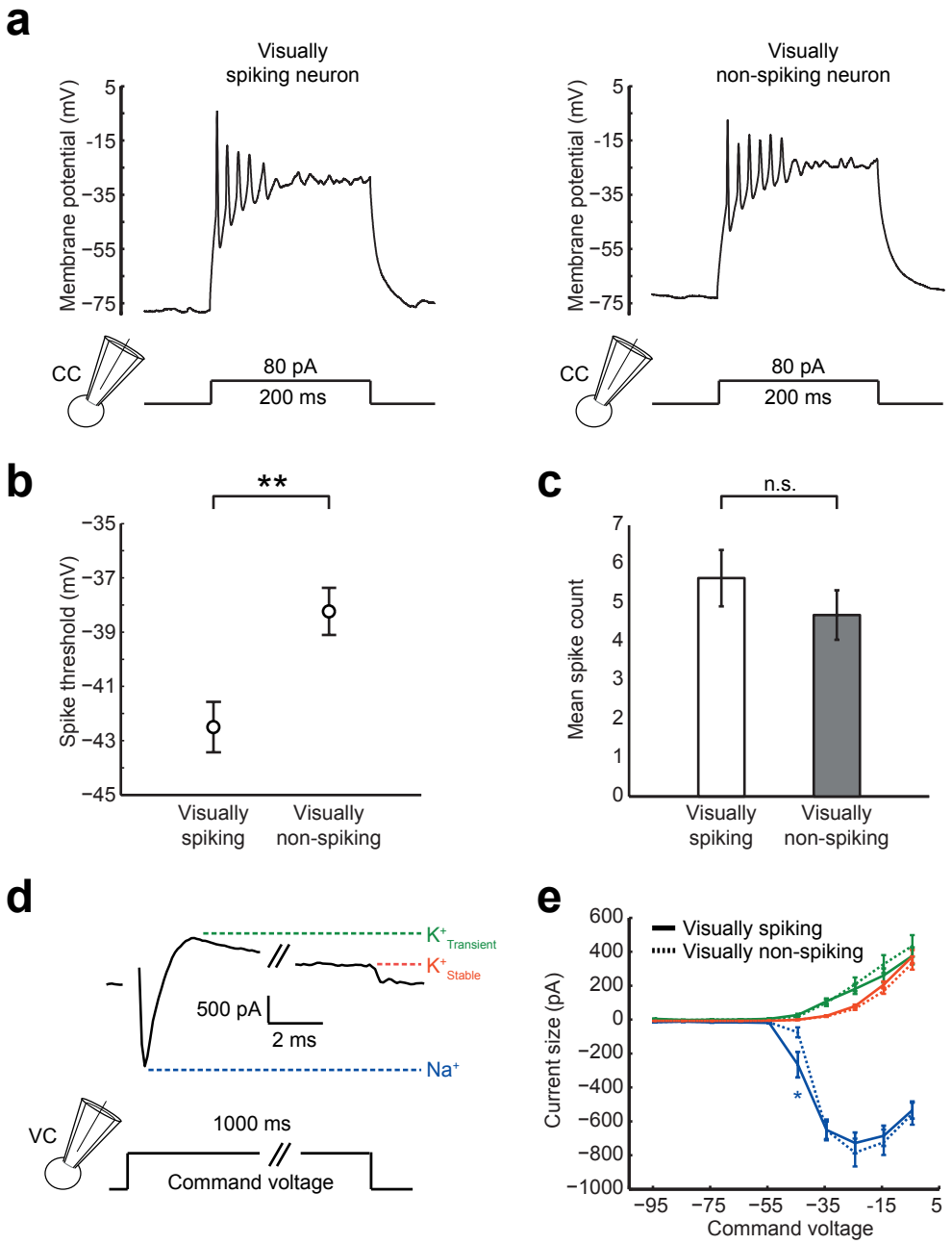
4.1 A large proportion of developing tectal neurons receives visually evoked synaptic input but does not generate visually evoked spikes

a) Example cell-attached and whole cell voltage clamp recordings from a visually spiking (left) and a visually non-spiking (right) tectal neuron in response to the same stimulus sequence (top). The spiking activity of each neuron was first recorded in cell-attached mode (CA). The recording configuration was then converted to whole cell voltage clamp (VC). GABAergic inputs were recorded at the reversal potential for glutamatergic currents (E_{glut}) and glutamatergic inputs were recorded at the reversal potential for GABAergic inputs (E_{GABA}). Note that clear visually evoked glutamatergic and GABAergic synaptic conductances can be observed for both neurons. **b)** The percentage of visually spiking and visually non-spiking neurons. 59.0% of neurons (46 / 78) did not spike in response to the RF mapping protocol. **c)** The lack of visual spiking activity is not stimulus-specific. 97.6 % of neurons (40 / 41) that did not spike in response to the RF flash stimulus also did not spike in response to a drifting bar stimulus. Conversely, 90.0% of neurons (18 / 20) that exhibited spikes in response to the RF flash stimulus also exhibited spikes in response to the drifting bar stimulus.

(Figure 4.1a). Out of all neurons for which clear visually evoked glutamatergic and GABAergic synaptic inputs could be recorded, 59% did not spike in response to the visual stimulation protocol (46/78, Figure 4.1b). In a separate experiment, I confirmed that the lack of spiking behaviour was not limited to the RF mapping protocol – all but one of 41 visually non-spiking neurons recorded in loose patch configuration also did not spike in response to a high contrast moving bar stimulus (2.4%, n = 41; Figure 4.1c). Conversely, 90% (18/20) of neurons that spiked in response to the RF mapping protocol also spiked in response to the moving bar stimulus. Therefore, the lack of visual spiking output was not stimulus-specific, but rather a general feature of these neurons. Given that the ability to spike is crucial for a neuron, both in terms of its contribution to neural processing and its ability to participate in activity-dependent plasticity processes, the presence of such a large population of visually non-spiking neurons merited further investigation. I therefore proceeded to determine the most likely cause of the lack of visual spiking activity.

4.2 Visually non-spiking tectal neurons have weak glutamatergic synaptic drive

In order to spike, a neuron needs to have developed the appropriate set of voltage-gated currents that underlie the action potential (Hodgkin & Huxley 1952; Hille 2001). One potential explanation for the lack of visually evoked action potentials in non-spiking neurons is that such neurons might have poorly developed intrinsic excitability. In order to test this, I used whole cell current clamp to investigate whether visually non-spiking neurons were able to spike in response to somatic injection of depolarising currents. Having first established in cell-attached configuration whether the neuron exhibited spikes in response to visual stimuli, I moved to whole cell configuration and recorded the membrane potential response to a series of current injection steps (Figure 4.2a; see Methods). Without exception, visually non-spiking neurons were able to generate spikes in response to somatic current injection (n = 22). The spike threshold of the neurons was determined from the point of inflection of the membrane potential response, where the active membrane properties took over from the passive membrane currents to generate the action potential. I found that non-spiking neurons tended to have a slightly higher spike threshold (Figure 4.2b; Spiking neurons: -42.5 ± 0.9 mV, n = 18; non-spiking neurons: -38.2 ± 0.9mV, n = 22; p = 0.0019), indicating that they were somewhat less excitable. However, spiking and non-spiking neurons were able to support similar numbers of spikes in response to a current injection (Figure 4.2c; spiking neurons: 5.6 ± 0.7 spikes, n

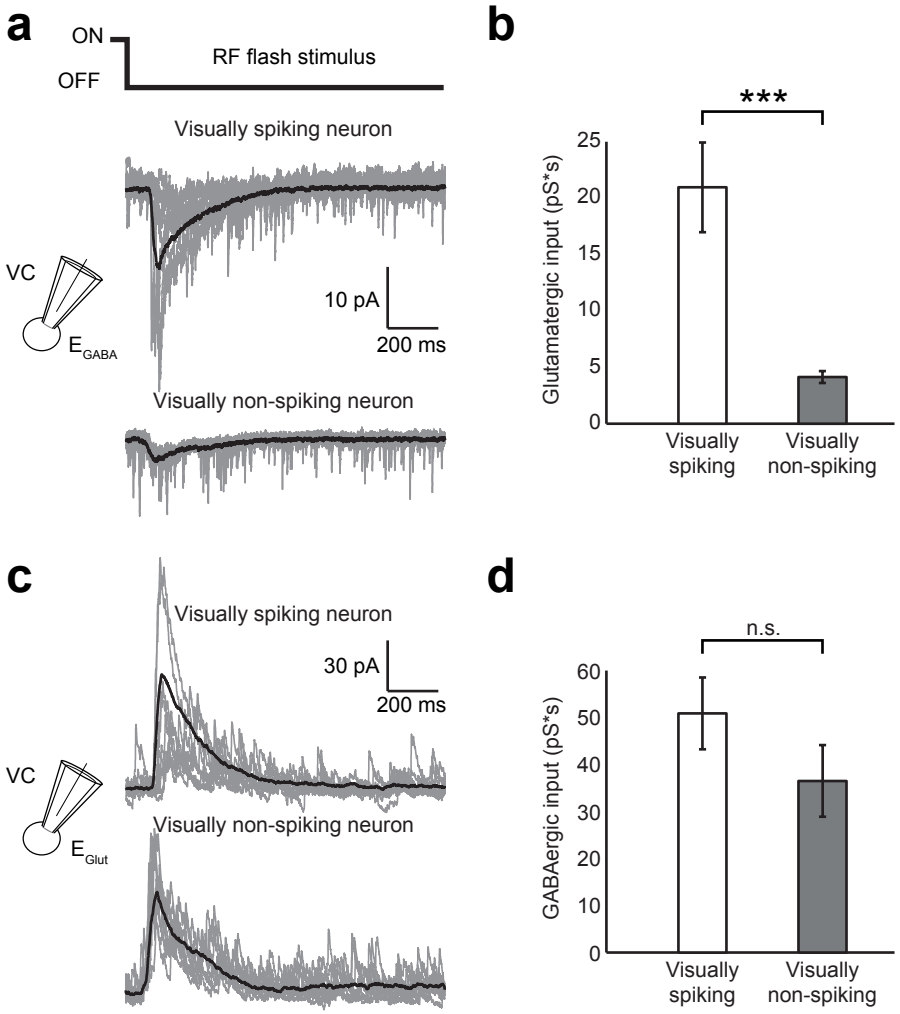


4.2: Non-spiking tectal neurons are excitable and have voltage-gated currents similar to those of spiking neurons

a) Current clamp recordings of a visually spiking tectal neuron (left) and a visually non-spiking tectal neuron (right) subjected to an 80 pA current injection for 200 ms. Both visually spiking and visually non-spiking neurons are able to generate action potentials in response to current injection. **b)** The spike threshold of a neuron was defined as the point of inflection in the membrane potential response to current injection, indicating the transition from passive membrane depolarization to active spike generation. The mean spike threshold for visually spiking neurons (-42.5 ± 0.9 mV, n = 18) was significantly lower than the spike threshold for visually non-spiking neurons (-38.2 ± 0.9 mV, n = 22, p = 0.002). **c)** Visually spiking and non-spiking neurons were able to support similar numbers of spikes in response to an 80 pA current injection step (visually spiking: 5.63 ± 0.73 spikes, n = 18; visually non-spiking 4.68 ± 0.59 spikes; p = 0.31, n = 22). **d)** A representative tectal neuron current response to a voltage step protocol. The holding potential was stepped from -75 mV to -25 mV. A fast inward Na^+ current plus a transient and stable outward K^+ current could be identified. **e)** Visually spiking and visually non-spiking neurons have similar voltage-gated currents. The current sizes are not significantly different at any command voltage ($p > 0.05$) apart from -30 mV, where the mean sodium current is larger for the visually spiking neurons ($p = 0.017$), consistent with a lower spike threshold for visually spiking neurons as observed in 'b'.

= 18; non-spiking neurons: 4.7 ± 0.6 spikes, n = 22; p = 0.31). To further assess the intrinsic excitability of visually spiking and non-spiking neurons I conducted a series of voltage-clamp recordings in which I measured voltage-gated currents. Having first established whether a neuron was visually spiking or non-spiking in cell-attached mode, I changed the configuration to whole cell voltage clamp and investigated the different components of the voltage-gated conductances by stepping the neuron to different holding potentials. A fast Na^+ current, plus transient and stable potassium (K^+) currents, could be reliably observed in all neurons when the membrane was sufficiently depolarised (Figure 4.2d). Consistent with the observed difference in spike threshold, visually spiking neurons exhibited stronger Na^+ currents at the membrane potential approaching the spike threshold (-45 mV) than the visually non-spiking neurons. The mean Na^+ current at this voltage was -67 ± 29 pA for visually non-spiking neurons, whereas it was -258 ± 75 pA for the visually spiking neurons (p = 0.017). The peak amplitudes of the Na^+ current were not different at any other membrane potential (p > 0.05), and neither the transient nor the stable K^+ current was different between visually spiking and non-spiking neurons at any membrane potential (p > 0.05; Figure 4.2e). This indicates that visually non-spiking neurons do possess the machinery to support the generation of action potentials, although a small difference in spike threshold was observed.

An alternative explanation for the difference between visually spiking and non-spiking tectal neurons is that they could differ in their visually evoked synaptic inputs. To determine whether a lack of synaptic excitation or an excess of synaptic inhibition could provide an explanation for an absence of visually evoked action potentials in non-spiking neurons, I compared the visually evoked synaptic inputs of spiking and non-spiking neurons. Having first classified the neuron as visually spiking or non-spiking in cell-attached mode, I broke through the cell membrane into whole cell mode to be able to record glutamatergic and GABAergic PSCs (see Methods). For each neuron, the mean integrated synaptic conductance was calculated for the first 0.5 s after stimulus onset for all the RF stimulus locations to which a significant visually evoked synaptic conductance was observed. While both spiking and non-spiking neurons received visually evoked glutamatergic and GABAergic synaptic inputs, the glutamatergic conductances of the non-spiking neurons were five times smaller than those of the spiking neurons (Figure 4.3a&b; spiking neurons: 21.0 ± 4.0 pS*s, n = 32; non-spiking neurons: 4.1 ± 0.5 pS*s, n = 46; p < 0.001). This strongly suggests that a lack of synaptic excitation contributes to the lack of



4.3: Visually non-spiking neurons receive weaker glutamatergic synaptic input, but similar GABAergic synaptic input

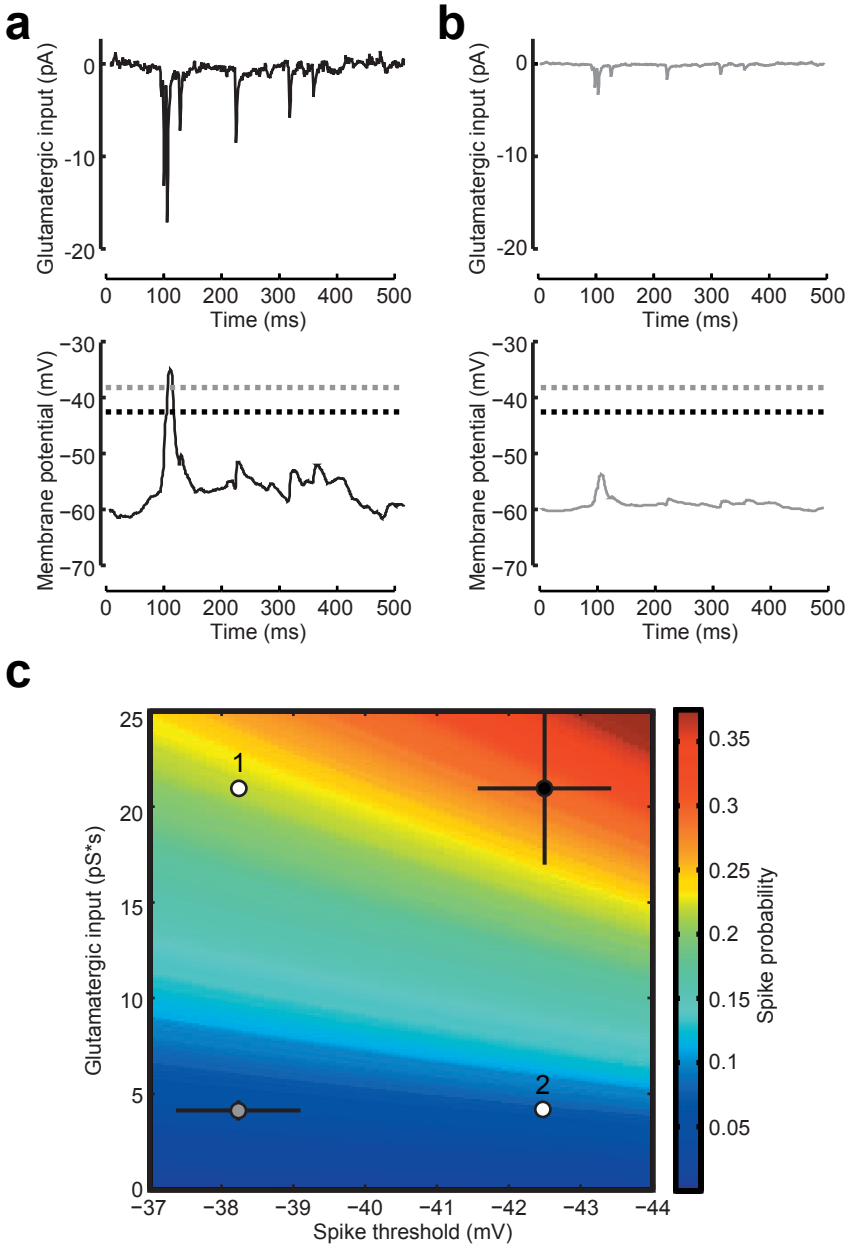
a) Examples of visually evoked glutamatergic synaptic currents for a spiking (top) and a non-spiking (bottom) tectal neuron. The black lines represent the mean visually evoked glutamatergic current for the neurons; the grey lines are 10 superimposed representative example responses to individual visual stimuli. **b)** Bar graph comparing the mean visually evoked glutamatergic synaptic conductances for visually spiking and visually non-spiking neurons. Non-spiking neurons receive significantly weaker glutamatergic synaptic input (4.1 ± 0.5 pS*s, n = 46) compared to spiking neurons (21.0 ± 4.0 pS*s, n = 32, $p < 0.001$). **c)** Examples of visually evoked GABAergic synaptic currents for a spiking (top) and a non-spiking (bottom) tectal neuron. The black lines represent the mean visually evoked GABAergic current for the neurons; the grey lines are 10 superimposed representative example responses to individual visual stimuli. **d)** Bar graph comparing the mean visually evoked GABAergic synaptic conductances for visually spiking and visually non-spiking neurons. The two groups of neurons receive similar GABAergic input (visually spiking: 50.9 ± 7.7 pS*s, n = 32; visually non-spiking: 36.5 ± 7.6 pS*s, n = 46, $p = 0.20$).

visually evoked spiking activity. In contrast, there was no significant difference in the size of visually evoked GABAergic conductances (Figure 4.3c&d; spiking neurons: 50.9 ± 7.7 pS*s, n = 32; non-spiking: 36.5 ± 7.6 pS*s, n = 46; p = 0.20).

To summarise, visually non-spiking neurons have a somewhat higher spike threshold (~3mV) and a fivefold smaller amount of glutamatergic input. Both of these would be predicted to make the neurons less likely to fire action potentials in response to visual stimuli. In order to explore which parameter is likely to be most important, I used a computer simulation of a single tectal neuron in order to explore how changes in intrinsic excitability and synaptic excitation might influence spiking activity (see Methods). This allowed for an estimate of how spike probability varied as a function of glutamatergic synaptic conductance and spike threshold in the range that I had observed experimentally. For each trial, passive cell membrane properties and recordings of glutamatergic and GABAergic PSCs were sampled randomly from the experimental data set. The synaptic responses were scaled up or down to achieve the desired glutamatergic conductance, while GABAergic conductances were scaled to the observed mean. Using these parameters as inputs to the model, the membrane potential response of the model neuron was calculated (Figure 4.4a&b). If the membrane potential of the simulated tectal neuron crossed the spike threshold, this was registered as a 'spike' event. The spike probability for a given combination of glutamatergic synaptic conductance and spike threshold was estimated from 500 trials. Importantly, the model neuron generated realistic numbers of spike events, with a very low spike probability when the mean synaptic conductance and excitability values were taken from the non-spiking population (~4.4%), and a high probability of spike events when values were taken from the spiking population (~29%; Figure 4.4c).

The model then offered the opportunity to explore what happens to spiking probability when either the intrinsic excitability or the synaptic excitation is altered. Increasing the glutamatergic drive from the mean of the non-spiking neurons to the mean of the spiking neurons (point 1 on Figure 4.4c) made a sizeable and significant difference in spike probability (4.4% to 21.6%, p < 0.001, chi-squared test). In contrast, keeping the glutamatergic drive constant, but shifting the spike threshold (point 2 on Figure 4.4c) did not lead to a significant difference in spike probability (4.4% to 6.4%, p = 0.1618, chi-squared test). Shifting the spike threshold could affect the spike probability, but this effect was only evident if a sufficient level of glutamatergic

4.4: Weak glutamatergic synaptic input accounts for the absence of visual spiking



A computer simulation of a developing tectal neuron was used to examine the contribution of spike threshold and synaptic input strength in controlling visually evoked spiking. **a)** A visually evoked glutamatergic synaptic current (top) was randomly selected from the experimental data set and scaled to correspond to the mean glutamatergic amplitude of a visually spiking neuron. Similarly, a visually evoked GABAergic synaptic current was randomly selected and scaled to correspond to the mean GABAergic amplitude. The computer model was used to simulate the effect of these inputs on the membrane potential of a tectal neuron (bottom). The dashed lines represent the mean spike threshold for visually spiking (black) and visually non-spiking (grey) neurons. Note that the membrane potential crosses both spike thresholds in response to the 'visually spiking' glutamatergic input. **b)** The same visually evoked glutamatergic synaptic current as in 'a', scaled to correspond to the mean synaptic conductance of a visually non-spiking neuron (top). As in 'a', this scaled glutamatergic input was paired with a visually evoked GABAergic synaptic current that was scaled to correspond to the mean GABAergic amplitude. The computer model was used to simulate the effect of these inputs on the membrane potential of a tectal neuron (bottom). The dashed lines represent the mean spike threshold for visually spiking (black) and visually non-spiking (grey) neurons. Note that the membrane potential crosses neither spike threshold in response to the 'visually non-spiking' glutamatergic input. **c)** Spike probability plotted as a function of spike threshold and glutamatergic input size, as determined from simulated membrane responses such as those shown in 'a' and 'b'. Each data point represents 500 simulations. The grey dot represents the mean glutamatergic input and spike threshold observed experimentally for visually non-spiking neurons, the black dot represents the same for visually spiking neurons. The error bars represent standard errors of the mean. Point 1 represents a hypothetical neuron that has the same mean glutamatergic input as a visually spiking neuron but the spike threshold of a visually non-spiking neuron. This hypothetical neuron has a significantly higher spike probability than the experimentally observed visually non-spiking neurons (4.4% vs. 21.6%, $p < 0.001$, chi-squared test). Point 2 represents a hypothetical neuron that has the same mean glutamatergic input as a visually non-spiking neuron, but the spike threshold of a visually spiking neuron. The spike probability of this hypothetical neuron is not significantly different from the spike probability of experimentally observed visually non-spiking neurons (4.4% vs. 6.4%, $p = 0.1618$, chi-squared test).

excitation was present. This argues that it is the lack of visually evoked glutamatergic drive, and not the difference in spike threshold, that prevents visually non-spiking neurons from spiking.

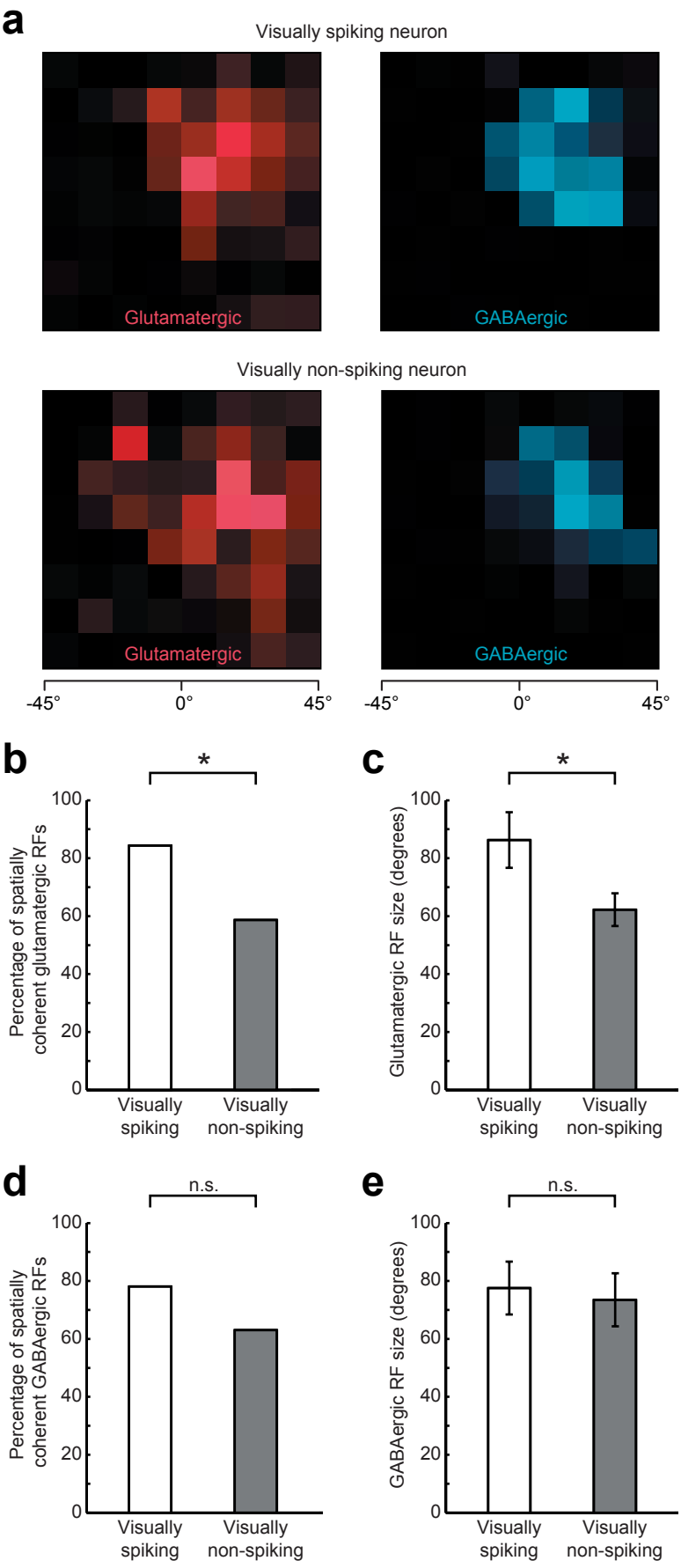
4.3 Spatiotemporal organisation of synaptic inputs to non-spiking neurons

Having established that the synaptic inputs are most likely to underlie whether a developing neuron exhibits visually evoked spiking activity, I set out to more carefully compare the spatiotemporal organisation of synaptic inputs to spiking and non-spiking neurons. To compare the RF properties of visually spiking and visually non-spiking tectal neurons, I first established whether a tectal neuron exhibited visual spikes in cell-attached mode, and then broke through into whole cell mode to map the glutamatergic and GABAergic RFs (Figure 4.5a). It became clear that the synaptic inputs could be spatially organised for both spiking and non-spiking neurons. Making a RF map of the synaptic conductances and fitting a Gaussian function to approximate the RF centre and profile (as illustrated in Chapter 3, Figures 3.5 and 3.6), I found that the majority of non-spiking neurons also exhibited spatially coherent glutamatergic and GABAergic RFs. Nevertheless, visually spiking neurons had a larger percentage of spatially coherent glutamatergic RFs (84%, 27/32) than the visually non-spiking neurons (59%, 27/46; $p = 0.014$, Fisher's exact test). Interestingly, the average size of the spatially coherent glutamatergic RFs of non-spiking neurons was, in fact, significantly smaller than that of the spiking neurons (Figure 4.5c, spiking neurons: 86.3 ± 9.6 degrees, $n = 27$; non-spiking neurons: 62.2 ± 5.7 degrees, $n = 27$; $p = 0.036$), suggesting that a lack of visual spiking does not predict larger RF size. A comparison of the spatial organisation of the GABAergic inputs of visually spiking and non-spiking neurons (Figure 4.5d), on the other hand, revealed that the proportion of coherent GABAergic RFs was not significantly different between the two groups (spiking neurons: 78% (25/32), non-spiking neurons: 63% (29/46); $p = 0.12$, Fisher's exact test). Moreover, the sizes of GABAergic RFs were similar for non-spiking and spiking neurons (Figure 4.5e, spiking neurons: 77.55 ± 9.15 degrees, $n = 25$; non-spiking neurons: 73.50 ± 9.18 degrees, $n = 29$; $p = 0.75$). Hence, spatially coherent glutamatergic and GABAergic RFs are present even in most tectal neurons that do not exhibit visual spiking activity.

Tectal neurons receive both monosynaptic excitatory input from the retina and polysynaptic input generated by the recurrent excitatory circuitry of the tectum (Pratt et al. 2008). Visual inputs can also drive a feedforward GABAergic circuit that generates $GABA_AR$ conductances

4.5: Visually non-spiking neurons can have spatially restricted RFs

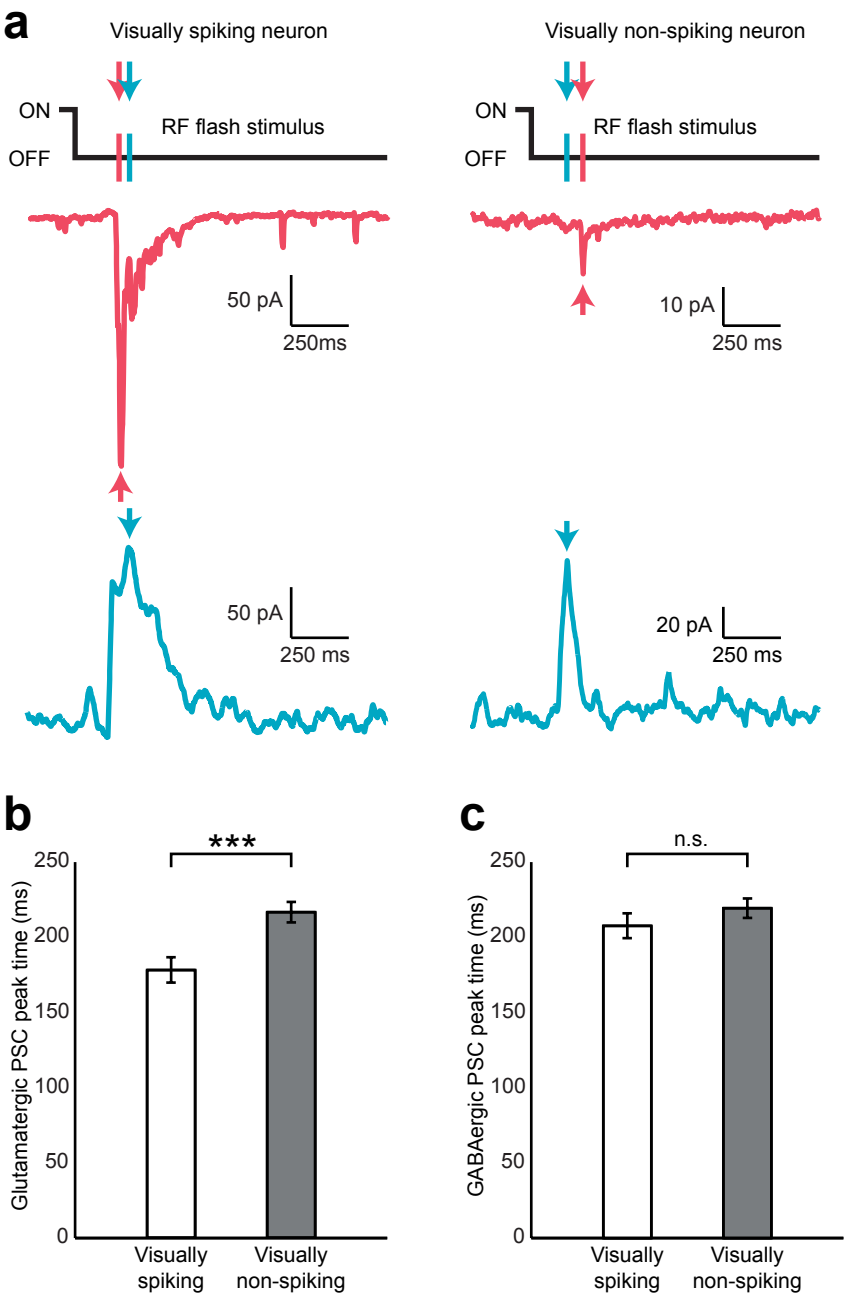
a) Glutamatergic (left) and GABAergic (right) RF maps for a visually spiking (top) and a visually non-spiking neuron (bottom). Responses are arranged according to the spatial location of the visual stimulus, and brighter colours represent stronger responses. **b)** The percentage of neurons with spatially coherent glutamatergic RFs. RFs were fitted with a Gaussian function to provide an estimate of RF centre, and were deemed spatially coherent if there was a significant negative correlation between distance from the RF centre and response size. Visually spiking neurons have a larger percentage of coherent glutamatergic RFs than non-spiking neurons (visually spiking: 84% (27 / 32), visually non-spiking: 59 % (27 / 46); p = 0.014, Fisher's exact test). **c)** Comparison of glutamatergic RF sizes between visually spiking and non-spiking neurons. RF size was defined as the minimum full width at half maximum (FWHM) of the Gaussian fit. Non-spiking neurons with coherent glutamatergic RFs have smaller RFs than visually spiking neurons (visually spiking: 86.3 ± 9.6 degrees, n = 27; visually non-spiking: 62.2 ± 5.7 degrees, n = 27; p = 0.036). **d)** The percentage of neurons with spatially coherent GABAergic RFs. Visually spiking neurons and visually non-spiking neurons have a similar percentage of coherent GABAergic RFs (visually spiking: 78% (25 / 32); visually non-spiking: 63%, (29 / 46); p = 0.12, Fisher's exact test). **e)** A comparison of GABAergic RF sizes between visually spiking and visually non-spiking neurons. Visually spiking neurons and visually non-spiking neurons with coherent GABAergic RFs have similar RF sizes (visually spiking: 77.6 ± 9.2 degrees, n = 25, visually non-spiking 73.5 ± 9.2 degrees, n = 29; p = 0.76).



in tectal neurons, which have a short latency with respect to glutamatergic input from the retina (Akerman & Cline 2006). Because the temporal relationship of excitatory and inhibitory inputs is an important determinant of spiking activity, I investigated whether the timing of synaptic inputs was different between visually spiking and non-spiking neurons. Input time was defined as the time of the peak of the visually evoked PSCs recorded during the RF mapping protocol (Figure 4.6a). A comparison of the timing of glutamatergic synaptic inputs between visually spiking and visually non-spiking neurons revealed that glutamatergic inputs to non-spiking neurons arrive significantly later, by approximately 40 ms (Figure 4.6b; spiking neurons: 176 ± 8.3 ms; non-spiking neurons: 218 ± 6.2 ms, $p < 0.001$). GABAergic currents, on the other hand, arrived at comparable times for spiking and non-spiking neurons (Figure 4.6c; spiking neurons: 206 ± 7.3 ms; non-spiking neurons: 216 ± 6.5 ms; $p = 0.33$). To explore the temporal relationship between glutamatergic and GABAergic inputs in more detail, I explicitly investigated the temporal sequence of glutamatergic and GABAergic PSCs for each visual location across RFs. In visually spiking neurons, the peak of the glutamatergic PSC preceded the peak of the GABAergic PSC by 32 ± 8 ms, while in visually non-spiking neurons the peak of the glutamatergic PSC followed the peak of the GABAergic PSC by 4 ± 6 ms ($p < 0.001$). Hence, glutamatergic input to visually non-spiking neurons is not only much smaller, but also delayed with respect to that of spiking neurons. The result is that in visually non-spiking neurons, the peak of the GABAergic input tends to coincide with that of the glutamatergic input.

4.4 Discussion

In this chapter, I have made the observation that a large proportion of developing tectal neurons does not fire action potentials in response to visual stimuli, despite receiving visually evoked glutamatergic and GABAergic synaptic inputs. I demonstrated that these non-spiking neurons are nevertheless electrically excitable and possess the appropriate voltage-gated currents to support spike generation. An investigation of the synaptic inputs to these neurons revealed that the amplitude of the glutamatergic synaptic input to non-spiking neurons is much smaller than that to spiking neurons. Meanwhile, the amplitude of their GABAergic synaptic inputs was found to be similar. A computer simulation of a developing tectal neuron revealed that the most likely reason for the lack of visually evoked action potentials in visually non-spiking neurons is that their glutamatergic inputs are not yet sufficient to drive the cell membrane to the spike threshold. An investigation of the spatiotemporal properties of the synaptic inputs to



4.6: Visually evoked glutamatergic synaptic input arrives later to visually non-spiking neurons
a) Glutamatergic (red) and GABAergic (blue) synaptic currents in response to a single RF flash for a visually spiking (left) and a visually non-spiking neuron (right). The peak time of the PSCs is indicated with an arrow. **b)** A comparison of the mean glutamatergic peak response time for visually spiking and visually non-spiking neurons. Glutamatergic input to visually non-spiking neurons arrives later than glutamatergic input to visually spiking neurons (visually spiking: 176 ± 8.3 ms, n = 32; visually non-spiking: 218 ± 6.2 ms, n = 46; $p < 0.001$). **c)** A comparison of the mean GABAergic peak response time for visually spiking and visually non-spiking neurons. There was no difference between the mean GABAergic PSC peak time for visually spiking and visually non-spiking neurons (spiking: 206 ± 7.3 ms, non-spiking: 216 ± 6.5 ms; $p = 0.33$).

non-spiking neurons revealed further differences in the glutamatergic and GABAergic synaptic inputs. Whereas the spatiotemporal properties of GABAergic inputs were indistinguishable between spiking and non-spiking neurons, the glutamatergic inputs to non-spiking neurons were less often spatially coherent, and tended to peak later than glutamatergic inputs to spiking neurons. This suggests that the excitation of non-spiking neurons may rely more on recurrent excitatory circuitry within the tectum and less on direct monosynaptic input from the retina.

Very little is known about neurons that do not generate action potentials in response to experimental protocols, even though they are likely to form a large part of any neuronal population (Shoham et al. 2006). They are a relatively understudied population by virtue of their silence, and it is often assumed that such neurons are simply not tuned to the experimental stimulus. However, the observation that the lack of spiking output of these tectal neurons is not stimulus specific, and the finding that visually non-spiking neurons have spatially coherent glutamatergic and GABAergic RFs with RF centres that fall within the sampled area of visual space, suggests that this is not the case for the population of silent neurons described here. Moreover, the fact that I observed a clear difference between spiking and non-spiking neurons in terms of glutamatergic input argues that the presence or absence of visual spiking activity represents a real difference between these groups. It seems likely that the visually non-spiking neurons represent a population that will begin to generate spiking activity at later stages of development, but still need to acquire sufficient glutamatergic drive. This is supported by calcium imaging studies at later stages of Xenopus development (48-52, i.e. 16-64 days after fertilisation) conducted in the Akerman lab, which reveal that the vast majority of mature tectal neurons generates visual spikes (Muldal, Lillicrap & Brodersen, personal communication).

The finding that the visually non-spiking neurons in the immature optic tectum already have voltage-gated currents, and can generate action potentials in response to somatic current injection, is consistent with previous work. Spitzer and colleagues (Spitzer & Ribera 1998; Spitzer & Lamborghini 1976) reported that the action potential mechanism in cultured Xenopus neurons develops before the developmental stages under investigation in this chapter. Therefore, in the retinotectal system, the ability of neurons to support spikes develops before the maturation of synaptic transmission and is consistent with the idea that the emergence of stimulus-driven spiking is governed principally by the development of the appropriate synaptic

connectivity. In support of this, it was found that the lack of spiking output of visually non-spiking neurons was largely attributable to weak glutamatergic synaptic input, suggesting that the acquisition of more glutamatergic input is key to how a developing tectal neuron becomes a visually spiking neuron.

The observation that visually non-spiking neurons are less likely to have spatially coherent glutamatergic RFs could reflect the less mature state of the glutamatergic system, and may be partially explained by a lower signal-to-noise ratio in response sizes. However, the coherent glutamatergic RFs of non-spiking neurons tended to be smaller than those of the spiking neurons. This is not likely to be explained by the smaller size of the glutamatergic responses of non-spiking neurons, as a reduction in response size would in fact be more likely to yield a wider Gaussian fit and an *increased* RF size. The presence of spatially coherent synaptic RFs in neurons that do not generate visual spiking output suggests that the initial emergence of spatially organised RFs is not dependent on spiking output. This stands in contrast to the evidence that spiking activity is required for subsequent refinement of the structure of tectal RFs (Tao & Poo 2005). Moreover, the fact that GABAergic inputs to visually spiking and non-spiking neurons were found to be statistically indistinguishable indicates that both neuron types are likely to be embedded in similar inhibitory synaptic circuitry. This focuses further attention onto why these neurons lack sufficient synaptic excitation to spike and how this might change as the neuron matures.

It was observed that glutamatergic inputs tend to arrive later in non-spiking neurons than in spiking neurons. Because the peak response was used to quantify the timing of responses (rather than, for instance, response onset time), this represents a temporal difference in the point of maximum glutamatergic drive. This measure also avoided effects of absolute response size on timing (as larger responses would be more likely to cross a threshold earlier). These findings therefore strongly suggest that the major glutamatergic drive of spiking and non-spiking neurons have different presynaptic origins. One possibility is that faster, direct monosynaptic input from the retina provides more synaptic excitation for spiking neurons, while non-spiking neurons rely more on indirect excitation via recurrent circuitry that is present in the tectum, particularly at earlier developmental stages (Pratt et al. 2008). Conversely, the similarity in the spatiotemporal properties of GABAergic synaptic inputs suggests that they have a similar

synaptic origin in both spiking and non-spiking neurons. The temporal delay in the arrival of glutamatergic inputs to visually non-spiking neurons resulted in glutamatergic and GABAergic inputs being nearly coincident. It seems likely that this could also contribute to the lack of spiking output in these neurons.

The weak glutamatergic drive may reflect an immature state of glutamatergic synaptic contacts. This is plausible, as developing glutamatergic synapses in the optic tectum have been shown to have a very low AMPA/NMDA ratio, making them weak or even silent at the resting membrane potential (Wu et al. 1996). Subsequent maturation of these synapses, which would involve an increase in their AMPAR content (Wu et al. 1996), could then provide the increase in synaptic drive that would enable a previously silent neuron to start generating spikes. The different stages of maturation of GABAergic and glutamatergic transmission parallel observations made in other studies of developing systems (Hennou et al. 2002; Tyzio et al. 1999) and suggest that in the optic tectum, too, GABA is a pioneer transmitter. Indeed, the presence of established GABAergic inputs to non-spiking neurons raises the possibility that GABAergic inputs could play a role in the maturation of glutamatergic synapses, as has been hypothesised in other systems (Ben-Ari et al. 1997; Ben-Ari 2002).

In summary, shortly after the onset of vision there is a large proportion of non-spiking neurons in the developing optic tectum that nevertheless receives organised visual synaptic input. These non-spiking neurons are electrically excitable and embedded into tectal inhibitory circuitry, but lack strong glutamatergic drive. The majority of the visually non-spiking tectal neurons receives structured glutamatergic and GABAergic input, although glutamatergic input seems to be mediated more by polysynaptic recurrent excitation rather than the shorter latency inputs received by the visually spiking neurons. The picture emerging from these findings is that GABAergic connectivity of the non-spiking neurons is already established in terms of strength, RF properties and timing, whereas the glutamatergic inputs are relatively immature. This supports the role of GABA as a pioneer neurotransmitter system and raises the possibility that GABAergic transmission is involved in the maturation of silent tectal neurons. This idea is a focus of Chapter 5.

Chapter 5

Visually driven unsilencing of non-spiking tectal neurons

In the previous Chapter I established that there is a significant proportion of neurons in the developing optic tectum that does not fire action potentials in response to visual stimulation. However, these 'silent' tectal neurons were shown to receive visuospatially organised synaptic inputs. Silent neurons differed from visually spiking neurons in terms of their intrinsic excitability as well as the strength of the glutamatergic synaptic input that they receive. Given the observation that most tectal neurons appear to generate spikes in response to visual stimulation at later stages of development (Muldal, Brodersen and Lillicrap, personal communication), a logical hypothesis is that the more immature non-spiking neurons may still be in the process of acquiring sufficient synaptic excitation or intrinsic excitability.

The process by which individual neurons first start firing action potentials in relation to sensory input has not been studied *in vivo*. In developing the ability to spike, a neuron must balance the voltage-gated currents that govern its excitability with the excitatory and inhibitory synaptic inputs that it receives. Not developing the ability to spike will limit a neuron's contribution to network computations and is likely to impair its ability to establish appropriate connectivity (Linden 1999). Meanwhile, excessive levels of excitation are associated with over-exuberant formation of synapses and ultimately, excitotoxicity (Meldrum & Garthwaite 1990). There is evidence that the intrinsic excitability of tectal neurons can change in response to visual stimulation (Aizenman et al. 2003; Pratt & Aizenman 2007). Such change in intrinsic excitability could underlie the development of spiking output in developing neurons. However, the results in Chapter 4 revealed that the difference in excitability between visually non-spiking and spiking neurons is relatively small and that the most effective way to become a visually spiking neuron is to enhance the strength of glutamatergic excitatory input. What kind of process could bring about the recruitment of more glutamatergic synaptic excitation? One possibility is that

the tectal neurons still need to physically integrate into the tectal circuitry by extending their dendritic arbour and forming new synaptic contacts (Cohen-Cory 2002). However, the finding that GABAergic responses of spiking neurons and non-spiking neurons are indistinguishable suggests that the non-spiking neurons are already physically integrated into the tectal circuit.

Another option is that non-spiking neurons have already established excitatory synapses, but that these are not yet capable of producing strong postsynaptic excitation. Such 'silent synapses' have been reported previously (Isaac et al. 1995; Liao et al. 1995; Durand et al. 1996; Nusser et al. 1998), particularly during development (Petralia et al. 1999; Liao et al. 1999). Silent synapses can be either presynaptically or postsynaptically silent. Presynaptically, they can exhibit a low probability, or limited quantity, of glutamate release (Voronin & Cherubini 2004). A postsynaptically silent synapse, meanwhile, is characterised by a lack of postsynaptic AMPA receptors (AMPARs) (Kerchner & Nicoll 2008). Importantly, such postsynaptically silent synapses can be 'unsilenced' in an activity-dependent manner (Isaac et al. 1995; Liao et al. 1995; Durand et al. 1996). A study of the maturation of glutamatergic synapses in Xenopus embryos found that postsynaptically silent synapses, lacking in AMPARs but containing NMDA receptors (NMDARs), are common in developing tectal neurons (Wu et al. 1996). Over time, these synapses appear to increase their AMPAR content and glutamatergic synaptic function becomes dominated by AMPAR-mediated currents (Wu et al. 1996). In Xenopus as well as in other developing systems, this process of 'AMPAfication' is thought to be activity-dependent, requiring Ca^{2+} entry into the postsynaptic neuron through either voltage-gated calcium channels or NMDARs, either of which require membrane depolarisation (Wu et al. 1996). Considering that AMPAR-mediated glutamatergic synaptic inputs are the main source of neuronal excitation in the CNS, this presents a conundrum: if there are very few functional AMPAR-containing glutamatergic synapses, how can a neuron be sufficiently depolarised for NMDAR-mediated Ca^{2+} entry or voltage-gated Ca^{2+} channel activation? This question becomes more relevant when one considers that the best characterised activity-dependent process in the retinotectal system is spike time dependent plasticity (STDP), which is able to enhance glutamatergic transmission, but is critically dependent on spiking activity in the postsynaptic neuron (Richards, Aizenman, et al. 2010a; Zhang et al. 1998).

An early property of GABAergic synaptic transmission may play an important role in the process

of strengthening excitatory synapses. It has been demonstrated in a variety of species and brain regions that GABAergic inputs to developing neurons can actually have a depolarising effect on the postsynaptic neuron (Mueller et al. 1984; Ben-Ari et al. 1989; Owens et al. 1996). This is the result of high intracellular Cl^- levels, which mean that $GABA_AR$ activation is more likely to lead to Cl^- efflux and therefore a depolarising effect on the postsynaptic neuron. These high levels of intracellular Cl^- are established by the Cl^- transporter NKCC1, which moves Cl^- into neurons, plus low expression levels of the KCC2 transporter that transports Cl^- out of mature neurons (Delpire 2000; Fiumelli & Woodin 2007).

In the Xenopus retinotectal system GABAergic inputs have been found to be able to exert a depolarising effect during early development (Akerman & Cline 2006) and it has been proposed that such depolarising GABAergic inputs are well placed to provide a source of membrane depolarisation that would facilitate Ca^{2+} entry through NMDARs (Akerman & Cline 2006; Akerman & Cline 2007). A number of recent studies also point to a role for GABAergic transmission in the maturation of glutamatergic synapses (Ge et al. 2005; He et al. 2010; Wang & Kriegstein 2011; Chancey et al. 2013). Indeed, making GABA prematurely hyperpolarising by early expression of KCC2 in developing tectal neurons can prevent the maturation of glutamatergic synapses (Akerman & Cline 2006). Therefore, considering that visually non-spiking neurons already have well-established GABAergic inputs, and at least a small amount of glutamatergic input, I hypothesised that GABAergic and glutamatergic inputs could cooperate in order to increase AMPAR-mediated glutamatergic input and thereby convert a silent neuron into a neuron that generates a spiking output.

An advantage of using the retinotectal system to investigate such a process of synapse maturation is that the appropriate selection of visual stimuli affords experimental control of the activity patterns in the developing tectum. This makes it possible to investigate whether the activity-dependent maturation of glutamatergic synapses is permissive or instructive (Crair 1999), which previous work has been unable to address (Wang & Kriegstein 2008; Wang & Kriegstein 2011; Chancey et al. 2013; He et al. 2010; Ge et al. 2005). A number of studies in the optic tectum have demonstrated that the visual environment can instruct the development of neuronal response properties, but the effects that were observed in these studies all required postsynaptic spiking (Richards, Voss, et al. 2010b; Richards, Aizenman, et

al. 2010a; Vislay-Meltzer et al. 2006; Engert et al. 2002; Pratt et al. 2008). Moreover, using an *in vivo* experimental protocol that makes it possible to investigate the responses of the same neuron before and after a period of enhanced visual stimulation will enable me to characterise the functional consequences for the output of the neuron.

In this chapter I investigate whether visually non-spiking neurons can be driven to start spiking by visual stimulation and set out to establish:

1) Whether such a process is permissive or instructive.
2) Whether changes in intrinsic excitability or synaptic inputs underlie the activity-dependent emergence of spiking output.
3) Whether there is a role for depolarising GABAergic inputs in recruiting more glutamatergic excitation to developing neurons.

5.1 Visually non-spiking neurons can be rapidly converted into spiking neurons

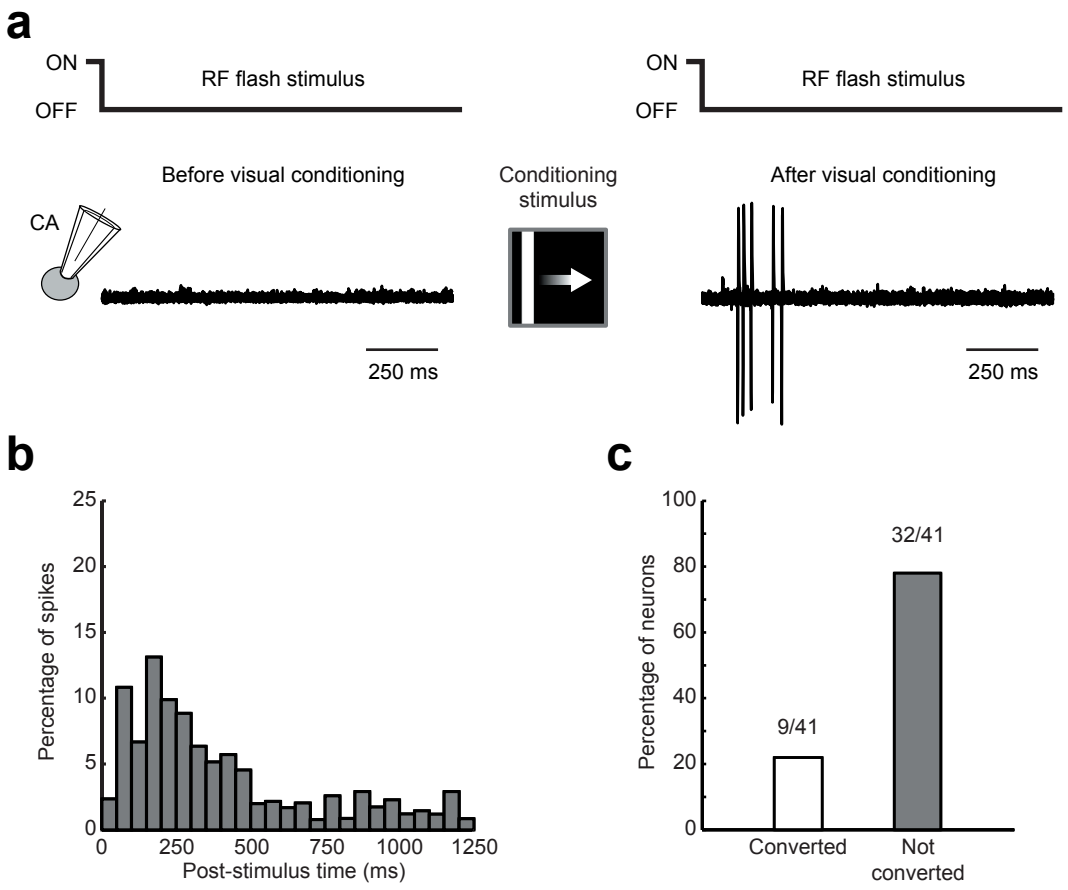
In the previous chapter I characterised a large population of tectal neurons that does not generate spikes in response to visual stimulation, even though these neurons already receive visually driven synaptic inputs. These silent neurons were found to have weak glutamatergic inputs, as well as a slightly higher spike threshold, compared to visually spiking neurons. It has been reported that both glutamatergic synaptic strength (Zhang et al. 2000; Engert et al. 2002; Mu & Poo 2006) and the intrinsic excitability (Aizenman et al. 2003; Pratt & Aizenman 2007) of tectal neurons can be modulated by visual experience. However, it has never been determined whether these can occur in a neuron that is unable to generate action potentials. I therefore investigated whether visually driven activity in the tectum could have an impact on silent neurons, such that they could be converted from non-spiking to spiking and become active contributors to sensory processing in the tectum.

To test this I performed cell-attached recordings from tectal neurons in the caudal half of the Xenopus optic tectum at stages 40-44 - immediately after the onset of vision. If the neuron did not spike in response to the RF mapping protocol, the animal was exposed to 15 minutes of a visual conditioning stimulus. The conditioning stimulus was a drifting white bar moving on a black background in one of the cardinal directions. The bar moved at a speed of 90 degrees

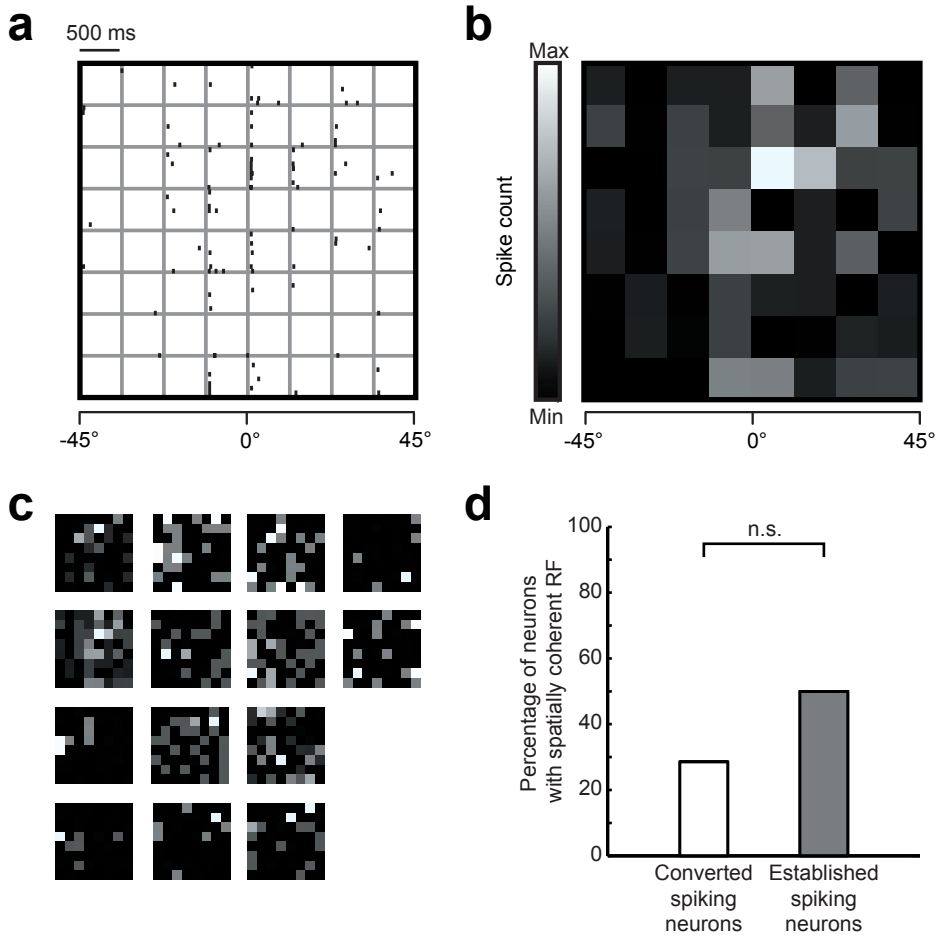
of visual space per second, and was repeated at a frequency of 0.2-0.4 Hz. This moving bar stimulus has previously been used to drive activity-dependent changes in the responses of spiking tectal neurons (Richards, Voss, et al. 2010b). After the conditioning protocol, I once again performed the original RF mapping protocol and recorded the responses of the same tectal neuron (Figure 5.1a). Interestingly, a subset of neurons that previously did not spike in response to the RF mapping protocol now started to generate spikes that were time-locked with the visual stimulus. I refer to these as 'converted' neurons to reflect the fact that they had converted from visually non-spiking to visually spiking.

To confirm that spikes in converted neurons were visually evoked and not spontaneous, I constructed a post-stimulus time histogram of the spiking responses and compared the peak of this histogram to a probability distribution generated from spike times that were randomly distributed with respect to the visual stimulus (see Methods). All of the converted neurons had spiking responses that were significantly more time-locked to the visual stimulus than the random distributions ($p < 0.05$, bootstrap test, Figure 5.1b). Out of 41 visually non-spiking neurons that were recorded in loose patch configuration and exposed to the conditioning stimulus, 9 neurons were converted into visually spiking neurons. This equates to a conversion rate of 22% (Figure 5.1c) and represents the first experimental observation of neurons making the transition from silence to stimulus-driven spiking. Moreover, these findings show that this conversion can be a rapid, stimulus driven, activity-dependent process.

I next characterised the output of these converted neurons to see whether the first spiking responses of a neuron already convey visuospatial information. To estimate the spatial coherence of RFs of converted neurons, their spiking responses were arranged according to the location of the stimulus (Figure 5.2a) and RF maps were constructed from the number of spikes observed at each location (Figure 5.2b). As in previous chapters, the RF centre was estimated by means of a Gaussian fit, and a neuron was considered to have a spatially coherent RF if there was a significant negative correlation between the distance from the RF centre and the spike count (see Methods). In 4 out of 14 converted neurons (29%), the RF maps had significantly spatially coherent responses (Figure 5.2d), which is a lower proportion than was observed amongst visually spiking neurons (Chapter 3, Figure 3.4; 50%), although this difference was not significant ($p = 0.16$, Fisher's exact test). This illustrates that although



5.1: Visual conditioning can convert visually non-spiking neurons into visually spiking neurons
a) Cell-attached recordings from a tectal neuron in a stage 44 animal, showing responses to the standard RF mapping protocol. This neuron was converted from visually non-spiking (left) to visually spiking (right) by exposing the animal to a conditioning stimulus (centre). Cell-attached recordings show 30 superimposed responses. The conditioning stimulus consisted of a moving bar drifting repeatedly in one of four cardinal directions for 15 minutes. Note the emergence of visual spikes in the neuron. **b)** A post-stimulus time histogram of spike events for 'converted neurons', which had started spiking after visual conditioning. Stimulus offset occurred at 0 ms. Spike times are time-locked to the visual stimulus, clustering at a short latency after visual stimulus offset (n = 14 converted neurons). **c)** The percentage of visually non-spiking neurons that could be converted into visually spiking neurons (22.0%, 9 / 41).

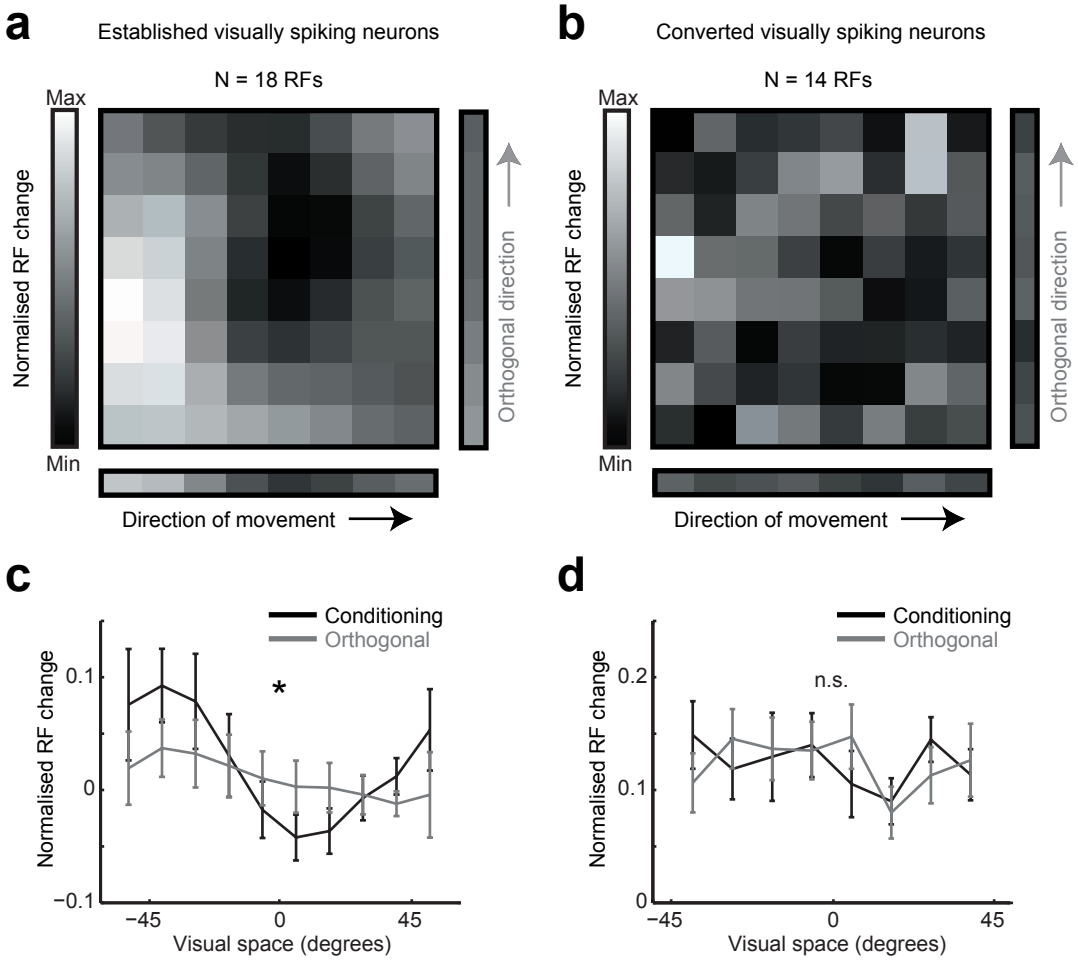


5.2: Emergent spiking RFs of converted neurons can be spatially coherent
a) Spiking responses for a tectal neuron that was converted from visually non-spiking to visually spiking, arranged according to the spatial location of the visual stimulus. Spike events are indicated by vertical lines. Note the spatial clustering of responsive regions of visual space. **b)** A RF map constructed from the responses in 'a'. Brighter squares indicate more spike events. **c)** Spike count RF maps for all 14 converted neurons. **d)** Comparison of the spatial coherence of RFs of converted neurons and established visually spiking neurons. For the converted neurons, 28.6% of the RF maps (4 / 14) show significantly spatially coherent visual responses. This is a smaller percentage of RF maps than that for the established visually spiking neurons (50%, 16 / 32) although this was not statistically significant ($p = 0.16$, Fisher's exact test).

their spiking responses are just emerging, a proportion of converted neurons already have spatially coherent RFs. This is consistent with observations made in Chapter 4, where it was reported that the majority of non-spiking neurons already have spatially coherent subthreshold RFs.

Having established that visually driven activity can convert tectal neurons from visually non-spiking to visually spiking, I investigated whether this represented a form of *instructive* or *permissive* plasticity. To address this question, I determined whether the outcome of the conditioning protocol was related to the spatiotemporal properties of the visual stimulus; in this case, the direction of the moving bar. A previous study demonstrated that visual stimuli can be instructive in inducing RF changes in the developing retinotectal system (Richards, Voss, et al. 2010b). Using the same moving bar stimulus as the one used in the current conditioning protocol, Richards and colleagues found that RFs of spiking tectal neurons showed asymmetric potentiation along the direction of movement of the moving bar stimulus, but not along the orthogonal direction. This is consistent with the idea that spiking neurons can extract spatiotemporal information about sensory input and use this to guide RF changes. I therefore used a similar approach to establish whether the conditioning stimulus played an instructive role in the process of unsilencing tectal neurons.

In the study by Richards and colleagues (Richards, Voss, et al. 2010b), visual conditioning with the moving bar stimulus led to an asymmetric change in the RFs of spiking tectal neurons along the direction of movement of the moving bar (Figure 5.3a). The RFs showed potentiation on the side of the RF that was exposed to the drifting bar earliest and no potentiation on the side of the RF that was exposed later (Figure 5.3c). To investigate whether this structure to the RF change was statistically significant, I used the data from Richards and colleagues (Richards, Voss, et al. 2010b) and calculated to what extent the RF position along the direction of movement could account for the total variance in RF change. This calculation produced an r^2-value, which was compared to a distribution of r^2-values obtained from a bootstrap procedure that repeated the same procedure on 10,000 shuffled RFs (see Methods). The RF position along the direction of movement of the conditioning stimulus was able to explain a significant amount of the variance ($r^2 = 0.15$, n = 18 RFs, $p = 0.001$), whereas this was not the case for the orthogonal direction ($r^2 = 0.03$, n = 18 RFs, $p = 0.81$). This confirmed that the moving bar stimulus was instructive



5.3: The conversion from visually non-spiking to visually spiking does not reflect the spatial properties of the conditioning stimulus

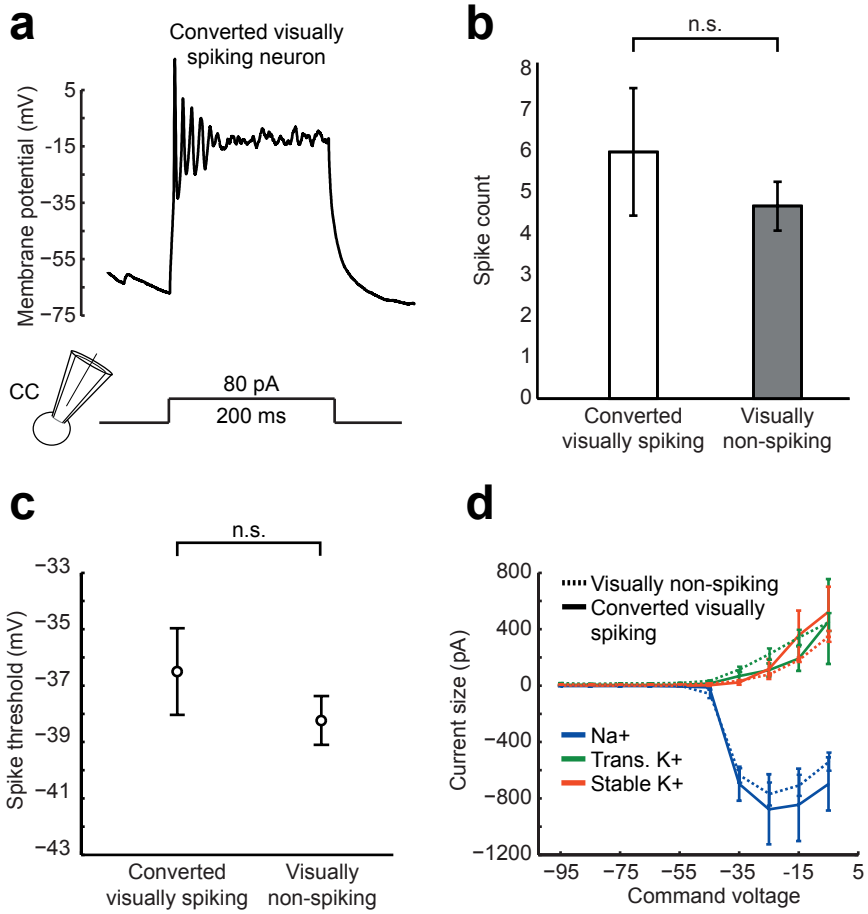
To investigate whether the spatiotemporal properties of the conditioning stimulus had an influence on the spatial structure of the RFs, all RFs were aligned according to the direction of movement of the drifting bar stimulus used for visual conditioning. **a)** The mean RF change of visually spiking neurons. Data are from Richards et al., 2010b. **b)** The mean RF change of converted neurons. **c)** The mean RF change along the direction of movement of the conditioning stimulus (black) as well as along the orthogonal direction (grey) for established visually spiking neurons. There was a significant spatial structure to the RF change along the direction of movement of the conditioning stimulus ($p = 0.001$, bootstrap test, see main text), but not along the orthogonal direction ($p = 0.81$, bootstrap test). **d)** The mean RF change along the direction of movement of the conditioning stimulus (black) as well as along the orthogonal direction (grey) for converted visually spiking neurons. There was no structure to the RF change along either the direction of movement of the conditioning stimulus or the orthogonal direction (conditioning direction: $p = 0.80$, orthogonal direction: $p = 0.65$; bootstrap test, see text).

with respect to driving RF potentiation in the spiking tectal neurons (Richards, Voss, et al. 2010b). Applying the same approach to investigate the emerging RFs of converted neurons revealed no such structure in RF change (Figure 5.3b). For converted neurons, there was no systematic change along either the direction of movement of the conditioning stimulus (r^2 = 0.04, n = 14 RFs, p = 0.80) or the direction orthogonal to it (r^2 = 0.05, n = 14 RFs, p = 0.65; Figure 5.3d). This observation is inconsistent with instructive plasticity and instead suggests that the conversion of visually non-spiking neurons into spiking neurons represents a form of permissive plasticity. Thus, whereas visually spiking neurons appear to undergo instructive plasticity in the developing tectum (Richards, Voss, et al. 2010b; Richards, Aizenman, et al. 2010a), the activity-dependent emergence of visual spiking activity in previously silent neurons is not related to the statistics of the stimulus-driven activity.

5.2 Increased glutamatergic input underlies tectal neuron unsilencing

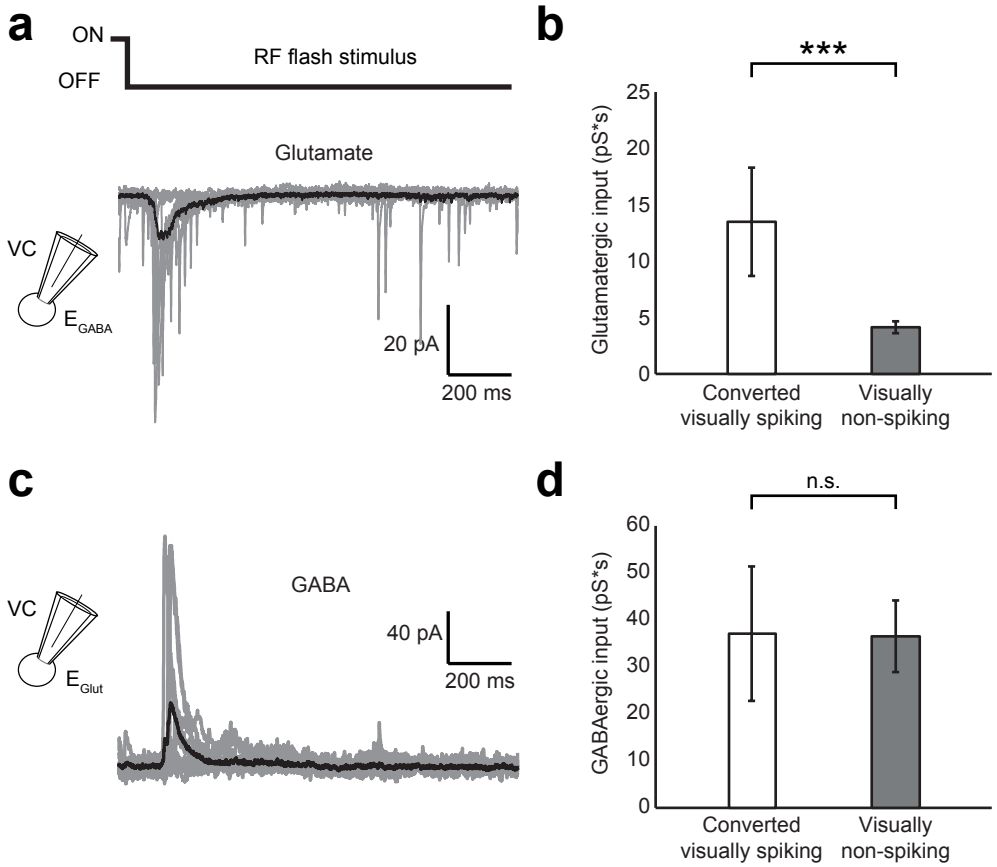
The visually driven conversion of non-spiking neurons into spiking neurons could be mediated by a net increase in excitatory synaptic drive and/or by an increase in intrinsic excitability. Both visual synaptic inputs (Zhang et al. 2000; Engert et al. 2002; Mu & Poo 2006) and intrinsic excitability (Aizenman et al. 2003) of tectal neurons have been shown to be affected by visual stimulation. To investigate which of these factors had changed, I performed whole cell patch clamp recordings on tectal neurons that had been converted in the gigaseal patch configuration (see Methods).

I first tested for evidence of any changes in intrinsic excitability. Current clamp recordings of the membrane potential response to a series of current injection steps (Figure 5.4a) allowed for estimation of a neuron's spike threshold and its ability to sustain action potential firing. The mean spike threshold for converted neurons was -36.5 ± 0.9 mV (n = 5), which was not significantly different from that of visually non-spiking neurons (-38.2 ± 0.9 mV, n = 22; p = 0.39; Figure 5.3b). Converted neurons were also able to fire a similar number of spikes in response to a 200 ms, 80 pA current injection (converted neurons: 6.00 ± 1.6 spikes, n = 5; non-spiking neurons: 4.68 ± 0.6 spikes, n = 22; p = 0.37). Moreover, voltage clamp recordings showed that the voltage-gated currents of converted neurons and visually non-spiking neurons were not significantly different at any membrane potential (Figure 5.4d; p > 0.05 in all cases). Therefore, the emergence of spiking output does not seem to rely on changes in intrinsic excitability. This



5.4 The conversion from visually non-spiking to visually spiking does not involve changes in intrinsic excitability

a) Whole cell current clamp recording of a converted tectal neuron, subjected to an 80 pA current injection for 200 ms. **b)** The mean spike threshold for converted neurons (-36.5 ± 0.9 mV, n = 5) was not significantly different from that of the visually non-spiking neurons (-38.2 ± 0.9 mV, n = 22; p = 0.39). **c)** The mean number of spikes generated by converted neurons in response to an 80 pA current injection step (6.0 ± 1.6 spikes, n = 5) was not different from that of the visually non-spiking neurons (4.7 ± 0.6 spikes, n = 22; p = 0.37). **d)** To investigate voltage-gated currents, the holding potential was stepped from -75 mV to a range of voltages (-95 to -5 mV). Converted neurons and visually non-spiking neurons exhibited similar voltage-gated currents, as none of the currents were significantly different at any command voltage (p > 0.05).



5.5 The conversion from visually non-spiking to visually spiking involves the recruitment of stronger glutamatergic input

a) Examples of visually evoked glutamatergic synaptic currents for a converted tectal neuron. The black line represents the mean visually evoked glutamatergic current for the neuron; the grey lines are 10 superimposed representative example responses to individual visual stimuli. **b)** Bar graph comparing the mean glutamatergic visually evoked conductances for converted and visually non-spiking neurons. Converted neurons receive significantly stronger glutamatergic synaptic input (13.5 ± 4.8 pS*s, n = 5) compared to visually non-spiking neurons (4.1 ± 0.5 pS*s, n = 46; $p < 0.001$). **c)** Examples of visually evoked GABAergic synaptic conductances for a converted neuron. The black line represents the mean visually evoked GABAergic current for the neuron; the grey lines are 10 superimposed representative example responses to individual visual stimuli. **d)** Bar graph comparing the mean GABAergic visually evoked conductances of converted (37.0 ± 14.3 pS*s, n = 5) and visually non-spiking (36.5 ± 7.6 pS*s, n = 46) neurons. Non-spiking and converted neurons receive similar GABAergic input ($p = 0.98$).

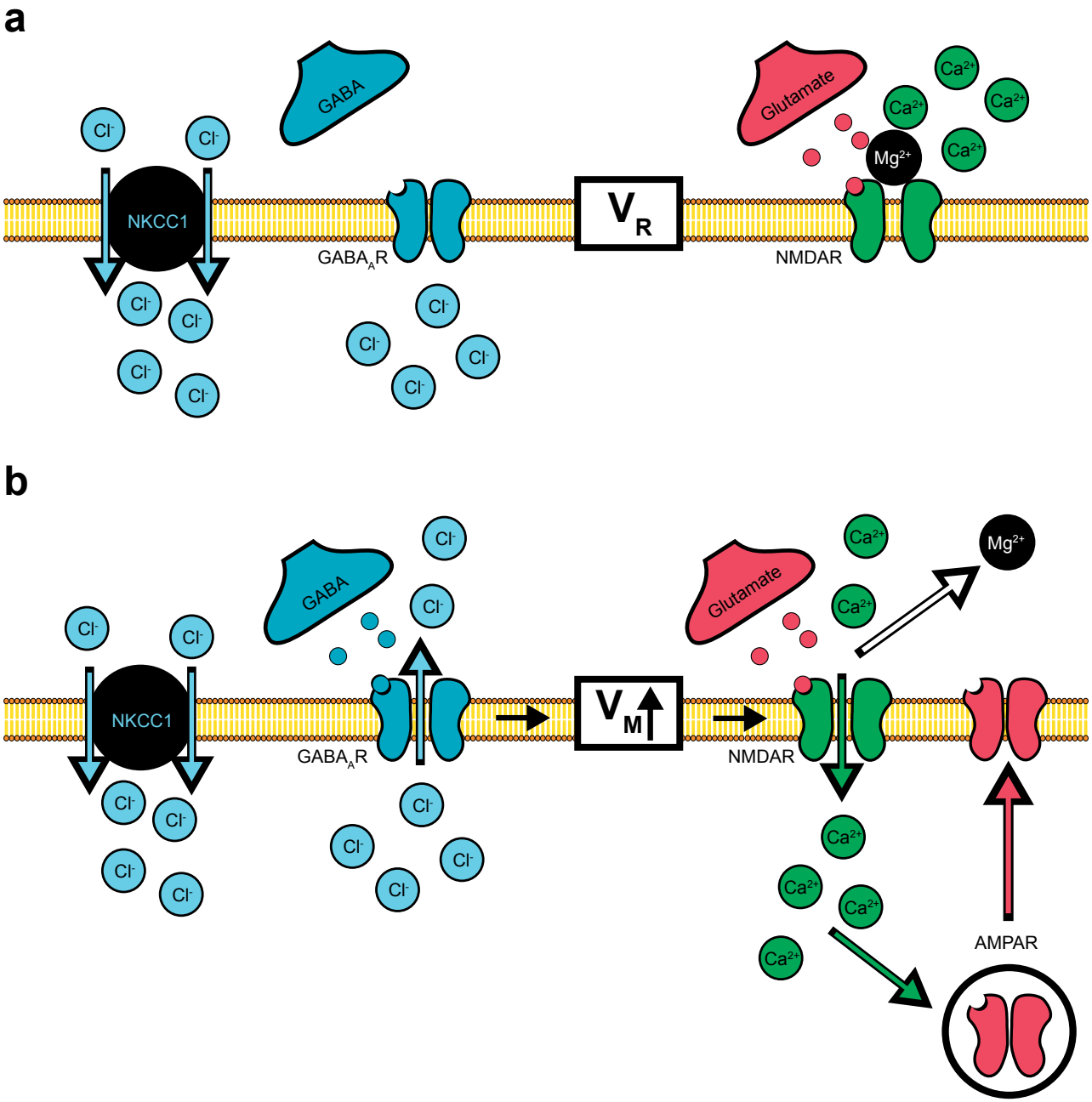
is consistent with the predictions of the computer simulation in Chapter 4, which showed that increased excitability would be unlikely to lead to a significant change in spiking output for non-spiking neurons (Figure 4.4). A change in synaptic excitation, however, was predicted to generate a significant increase in spike probability.

To establish whether converted neurons had acquired increased synaptic excitation, I measured the size of visually evoked glutamatergic and GABAergic synaptic inputs during the RF mapping protocol. Visually evoked glutamatergic inputs were found to be much larger in converted neurons than in non-spiking neurons (Figure 5.5a&b; converted neurons: 13.5 ± 4.8 pS*s, n = 5; visually non-spiking neurons: 4.1 ± 0.5 pS*s, n = 46; $p < 0.001$). This threefold difference in glutamatergic synaptic input is consistent with the prediction that increased synaptic excitation is the principal difference between spiking and non-spiking neurons. Meanwhile, visually evoked GABAergic currents in the converted neurons were indistinguishable from those in non-spiking neurons (Figure 5.5c&d; converted neurons: 37.0 ± 14.3 pS*s, n = 5; visually non-spiking neurons: 36.5 ± 7.6 pS*s, n = 46; $p = 0.98$). This shows that the effect of the conditioning stimulus is specific to the glutamatergic inputs that converge on non-spiking neurons.

Hence, the activity-dependent conversion of visually non-spiking neurons into visually spiking neurons relies on a selective increase in glutamatergic synaptic excitation. Whilst visually driven potentiation of glutamatergic inputs has been reported previously in the tectum (Engert et al. 2002; Mu & Poo 2006), these changes have all been dependent upon postsynaptic spiking activity. A non-spiking neuron must therefore use an alternative activity-dependent mechanism, which does not rely upon postsynaptic spiking and yet can lead to the recruitment of more glutamatergic synaptic input.

5.3 The unsilencing of tectal neurons requires depolarising GABAergic inputs and NMDA receptor activation

In the developing retinotectal system, as in other developing systems (Ben-Ari 2002), GABAergic synaptic inputs can depolarise the postsynaptic neuron (Akerman & Cline 2006). Moreover, it has been postulated that such depolarising GABAergic inputs in young neurons are well placed to relieve the Mg^{2+} block of NMDARs (Akerman & Cline 2006). Ca^{2+} influx through

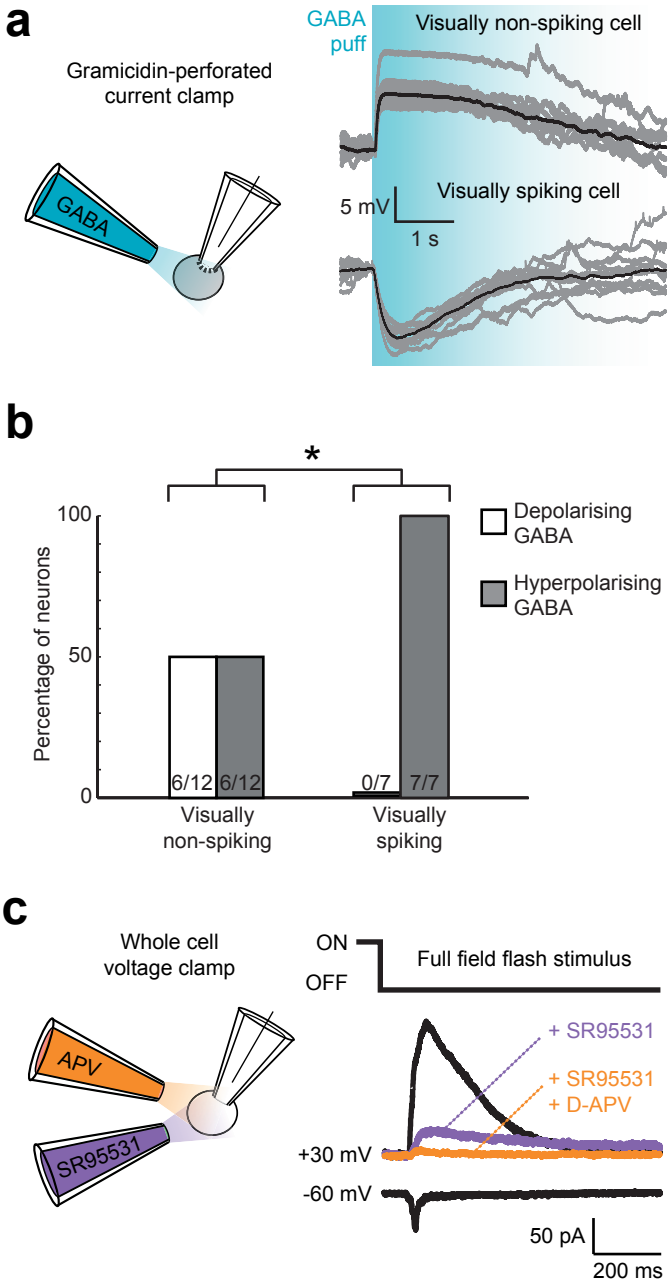


5.6 A proposed mechanism for the recruitment of AMPAR-mediated glutamatergic input in visually non-spiking neurons.
a) Glutamate release at a silent synapse that expresses NMDARs but no AMPARs. Without simultaneous activation of $GABA_A$Rs, no current is generated through the NMDARs due to the Mg^{2+}-dependent block of the NMDAR at the resting membrane potential (V_R). **b)** Cooperative effects of $GABA_A$R-mediated depolarisation and glutamate release result in AMPAfication at a silent synapse. Activity of the Cl^- transporter NKCC1 in immature neurons results in elevated intracellular Cl^- levels, such that activation of the $GABA_A$R results in a Cl^- efflux and a depolarization of the membrane potential (V_M). This removes the Mg^{2+}-dependent block of nearby NMDARs, which if activated by glutamate, permit the influx of Ca^{2+}. This Ca^{2+} influx can trigger intracellular mechanisms that lead to the insertion of AMPARs into the postsynaptic membrane.

NMDARs, in turn, is implicated in plasticity processes that lead to an increase in the AMPAR content at glutamatergic synapses (Lu et al. 2001). Theoretically, this means that visually evoked depolarising GABAergic inputs could facilitate the activity-dependent recruitment of glutamatergic input to developing tectal neurons (Figure 5.6).

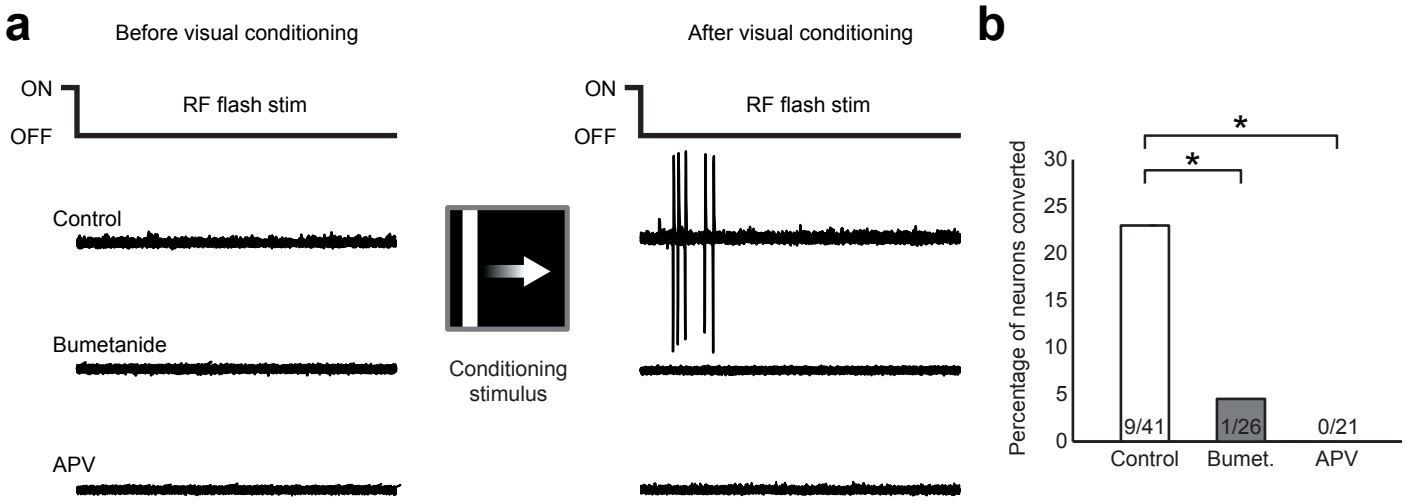
To examine this possibility it was first necessary to investigate whether non-spiking neurons exhibit depolarising GABAergic inputs. To do this, I performed *in vivo* gramicidin-perforated patch clamp recordings of tectal neurons and activated $GABA_A$Rs by delivering focal puffs of GABA to the soma. This enabled me to assess the effect of $GABA_A$R activation on the membrane potential of non-spiking neurons, without disrupting intracellular Cl^- levels (Ebihara et al. 1995; Kyrozis & Reichling 1995). After establishing a gigaseal, but before significant membrane perforation had occurred (i.e. in cell-attached mode), I was able to record the spiking behaviour of the neuron in response to the RF mapping protocol and thereby classify the neuron as either visually spiking or visually non-spiking. I then proceeded to characterise the neuron's membrane potential response to $GABA_A$R activation. These recordings revealed that a large proportion of visually non-spiking neurons exhibited depolarising GABAergic responses. In contrast, visually spiking neurons recorded in the same animals only ever exhibited hyperpolarising responses to $GABA_A$R activation (Figure 5.7a&b; 6/13 non-spiking neurons vs. 0/7 spiking neurons, $p = 0.034$, Fisher's exact test).

Next, to examine whether non-spiking neurons exhibit visually evoked NMDAR currents, I identified non-spiking neurons in gigaseal mode and characterised their visually evoked synaptic currents after breaking through into whole cell mode. By controlling the holding potential in voltage clamp, and combining this with local application of receptor blockers, I was able to isolate different components of the visually evoked postsynaptic response (Figure 5.7c). First, a small AMPAR-mediated current was observed while holding the neuron at the reversal potential for GABAergic currents (-60 mV). At +30 mV, a large outward current was observed, the main component of which was blocked by local application of the selective $GABA_A$R antagonist SR95531 (50 μM). Under conditions of $GABA_A$R blockade, a current with the characteristic slower dynamics of NMDARs was evident, and this current could be blocked by local application of the selective NMDAR-antagonist D-APV (1 mM). Therefore, non-spiking tectal neurons have depolarising GABAergic inputs as well as NMDAR-containing



5.7 Visually non-spiking neurons exhibit depolarising GABAergic responses and NMDAR currents

a) Membrane potential responses of a visually spiking (bottom) and a visually non-spiking (top) neuron exposed to a GABA puff during a gramicidin perforated current clamp recording. Note that in the visually spiking neuron, the GABA puff had a hyperpolarising effect on the membrane potential, while the visually non-spiking neuron exhibited depolarising responses to $GABA_A$R activation. **b)** The percentage of visually spiking and visually non-spiking neurons with depolarising GABAergic responses. Visually non-spiking neurons were more likely to exhibit depolarising GABAergic responses (Fisher's exact test, p = 0.034). **c)** Visually non-spiking neurons exhibit visually evoked NMDAR-dependent synaptic currents. A small, AMPAR-mediated current was observed in response to a full-field flash stimulus while holding a tectal neuron at the reversal potential for GABAergic currents (-60 mV, bottom trace). At +30mV, a large combined current can be observed (top trace). When the $GABA_A$-receptor mediated component of this current is blocked with SR95531, a current with the characteristic slower dynamics of the NMDAR remains. This component of the current could be blocked with the NMDAR-antagonist D-APV, showing that visually non-spiking neurons have NMDAR-mediated visually evoked glutamatergic inputs.



5.8 Conversion of non-spiking neurons into visually spiking neurons is dependent on depolarising GABAergic responses and NMDAR activation

a) Example cell-attached responses to visual stimuli before (left) and after (right) exposing the animal to a visual conditioning stimulus. Representative traces are shown for a control neuron (top), as well as for neurons that were conditioned in the presence of bumetanide (middle) or APV (bottom) to block NKCC1 and NMDARs, respectively. Both disrupting depolarising $GABA_AR$-mediated transmission with bumetanide and blocking NMDARs with APV abolished the conversion of visually non-spiking neurons into visually spiking neurons. **b)** The percentage of converted neurons in control (22%, 9 / 41), bumetanide (4%, 1 / 26) and APV (0%, 0 / 21) conditions (bumetanide vs. control, p = 0.041, APV vs. control, p = 0.017, Fisher's exact test).

glutamatergic synapses that are activated by visual stimulation. These observations confirm that non-spiking neurons could utilise a combination of depolarising $GABA_AR$ responses and NMDAR activation to recruit more glutamatergic synaptic input. If this is the case, one would predict that interfering with either of these aspects (depolarising GABA or NMDARs) would prevent the conversion of visually non-spiking neurons into visually spiking neurons.

To determine whether the activity-dependent conversion of visually non-spiking tectal neurons requires GABAergic inputs to be depolarising, I interfered with the chloride transporter NKCC1 by bath application of bumetanide (100 μM). This has the effect of lowering the concentration of Cl^- ions within the neuron, thereby ensuring that GABAergic inputs become prematurely hyperpolarising (Wang & Kriegstein 2011). Preventing depolarising effects of GABA with bumetanide greatly reduced the number of neurons that became visually responsive (control: 9/41, bumetanide: 1/26, $p = 0.043$; Figure 5.8a, top two traces, and Figure 5.8b), indicating that the depolarising action of GABA is required for, or at least facilitates, the conversion of non-spiking neurons into spiking neurons.

I next investigated whether the conversion of non-spiking neurons into spiking neurons requires NMDAR activation. Application of the NMDAR blocker D-APV (100 μM) to the bath solution once again abolished the conversion of non-spiking neurons into spiking neurons (Figure 5.7a, bottom trace, and Figure 5.7b; APV: 0/21, $p = 0.020$), indicating that this conversion is also dependent on NMDAR activation. This supports the model illustrated in Figure 5.6, in which depolarising GABAergic inputs and NMDARs can act in synergy to recruit more AMPAR-mediated glutamatergic synaptic input to a non-spiking neuron. This provides a mechanism for the unsilencing of previously silent neurons.

5.4 Discussion

In this chapter I have observed that non-spiking tectal neurons can be converted into visually spiking neurons in an activity-dependent manner *in vivo*. As a result of visual stimulation, a subset of previously silent tectal neurons acquired stronger glutamatergic input through a mechanism that was independent of postsynaptic spiking, but dependent upon depolarising GABAergic inputs and NMDAR activation. This is the first description of an activity-dependent mechanism that can guide a neuron through the transition from non-spiking to spiking, and the

first time that the emergence of stimulus driven spiking has been observed *in vivo*.

The observation that non-spiking tectal neurons can be converted into spiking neurons in an activity-dependent, stimulus driven manner illustrates the important role of the environment in the development of neuronal circuitry. The principal change that underlies the activity-dependent switch to spiking is the recruitment of more excitatory synaptic input. This is consistent with a central role for visual activity in driving the maturation of glutamatergic synapses in the retinotectal system, as proposed by Wu and colleagues (Wu et al. 1996). However, the fact that this process does not require postsynaptic spiking sets it apart from the spike-dependent plasticity processes that have previously been described in the tectum (Zhang et al. 1998; Tao et al. 2001; Engert et al. 2002; Vislay-Meltzer et al. 2006; Mu & Poo 2006; Richards, Aizenman, et al. 2010a). Instead, the findings in this chapter require a mechanism by which subthreshold visually evoked synaptic inputs can promote the recruitment of more excitatory input.

I have illustrated that this mechanism requires both a depolarising reversal for the $GABA_AR$ and NMDAR activity. It is therefore consistent with a model in which these receptor systems work in synergy to recruit more glutamatergic excitation. Non-spiking neurons receive visually evoked NMDAR-mediated glutamatergic inputs and a significant proportion also receives depolarising GABAergic inputs. Moreover, either disrupting the depolarising effects of GABAergic inputs by blocking the NKCC1 chloride transporter with bumetanide or blocking NMDARs with APV abolished the visually driven unsilencing of previously silent neurons. Depolarising GABA is well placed to provide tectal neurons with a network-driven source of depolarisation that could facilitate postsynaptic Ca^{2+}-influx via the NMDAR (Akerman & Cline 2006). NMDAR-mediated Ca^{2+}-entry into the neuron, in turn, is well-established as the trigger for long term potentiation of glutamatergic inputs that generates larger AMPAR-mediated currents (Malenka 1999).

A role for depolarising GABAergic inputs in the maturation of glutamatergic synapses is consistent with predictions made by Ben-Ari and colleagues (Ben-Ari et al. 1997). It has been argued that such a mechanism would allow for the maturation of glutamatergic synapses without the risk of recruiting excitation at cytotoxic levels (Ben-Ari 2002). The current work confirms such predictions and extends their scope by indicating a direct role for the sensory environment in driving the GABAergic and glutamatergic signals that are necessary for this

process. This possibility has already been raised by Akerman and Cline (Akerman & Cline 2006; Akerman & Cline 2007) but has never been directly demonstrated. While other studies have indicated a crucial role for depolarising GABA in the maturation of glutamatergic synaptic transmission (Ge et al. 2005; He et al. 2010; Wang & Kriegstein 2011; Chancey et al. 2013), these studies had no control over the sensory environment and have not established a direct link with environmental stimulation. The current work represents the first demonstration of such a process being directly driven by visual stimuli *in vivo*, and the first demonstration of its important functional consequences for a developing neuron. Furthermore, the fact that it can be induced on an experimentally viable timescale, on the lab bench and *in vivo,* opens up possibilities to further dissect its mechanisms.

My observation that depolarising GABAergic inputs can act as a stimulus-driven promoter of glutamatergic excitation raised the possibility that early GABAergic activity could exercise an *instructive* role in establishing neuronal circuitry (Crair 1999). Because GABAergic inputs convey visuospatial information to both visually non-spiking neurons and spiking neurons (Chapter 4), GABAergic neurons could play an instructive role in how glutamatergic synaptic excitation is recruited to a non-spiking neuron. However, an analysis of the structure of the RFs of converted neurons revealed no relationship to the spatiotemporal properties of the visual conditioning protocol. This suggests that GABAergic transmission plays a more *permissive* role in the conversion of non-spiking neurons. When viewed in the context of previous work, this observation argues for a model in which neurons are first concerned with developing the ability to spike in response to their inputs. Only after they have developed the capacity to spike do they have the ability to adjust their inputs to reflect the statistics of the visual environment. A series of studies in the optic tectum indicate that plasticity mechanisms that are dependent on postsynaptic spiking are especially suited for changing RF properties in response to sensory input (Engert et al. 2002; Vislay-Meltzer et al. 2006; Mu & Poo 2006; Richards, Aizenman, et al. 2010a). The conversion of non-spiking neurons into spiking neurons could therefore mark a transition from a permissive phase of recruiting excitatory synaptic input, to an instructive, postsynaptic spike-dependent phase, which is well placed to refine RF structure in a manner that reflects the spatiotemporal properties of the visually driven activity (Engert et al. 2002; Vislay-Meltzer et al. 2006; Mu & Poo 2006; Richards, Aizenman, et al. 2010a).

The retinotectal system may be particularly suited to the plasticity mechanism described in this chapter. Tectal neurons receive structured stimulus-driven input at the same time that the earliest synaptic contacts between retinal ganglion cells and tectal neurons are forming (Chapter 3). However, the most important conditions for this plasticity process – synapses with a low AMPAR/NMDAR ratio, depolarising GABAergic inputs and the presence of patterned GABAergic and glutamatergic synaptic activity – are present throughout the developing nervous system (Ben-Ari 2002). Therefore, the emergence of spiking activity through an activity-dependent process that is governed by depolarising GABAergic inputs may be a common feature of the developing brain.

Chapter 6

General discussion

6.1 Experimental findings

In this thesis, my principal aims were to characterise the potential for visual information to guide neuronal circuit development in the retinotectal system of Xenopus laevis; to investigate a population of developing tectal neurons that receives visually evoked synaptic inputs, yet does not spike; and to investigate how such visually non-spiking tectal neurons may become 'unsilenced' during development. In this section, I will review how these aims have been achieved.

In Chapter 3, I investigated the availability of visuospatial information to the tectum at the onset of vision. I conducted anatomical and optical measurements of the eyes of developing Xenopus larvae, as well as *in vivo* patch clamp recordings of the visually evoked synaptic inputs and spiking output of developing tectal neurons. The anatomical measurements revealed that at the onset of vision (stages 39-40), the lens of the developing Xenopus eye is not able to project a focused image onto the retina. Instead, the animal's lens projects the image of the visual environment beyond the retina, making the animal hyperopic. This initial hyperopia is quickly corrected over the next stages of development, a process that was found to be principally driven by a shortening of the focal length of the lens. This leads to emmetropic vision by stage 45, after which the focal length of the lens appears to track the developmental increase in eye size and thus maintain emmetropia. A calculation of the resolving power of developing Xenopus eyes before the development of emmetropic vision revealed that despite their initial hyperopia, spatially localised stimuli would be expected to activate a restricted area of the retina. In principle, this would allow for the visual environment to drive spatially patterned activity, which could guide circuit formation in the tectum even at developmental stages when the animal is hyperopic.

I next investigated whether visuospatial information was indeed present in the tectum at developmental stages immediately after the onset of vision. Using a protocol for first mapping the spiking receptive fields (RFs) of tectal neurons in cell-attached mode, and then mapping their glutamatergic and GABAergic RFs in whole cell mode, I was able to show that tectal neurons receive visual inputs that are localised in visual space. Moreover, tectal neurons already exhibit spatially coherent spiking RFs in response to these visual synaptic inputs. An investigation of the spatial properties of glutamatergic, GABAergic and spiking RFs illustrated that emerging glutamatergic and GABAergic RFs were already matched in visual space. Glutamatergic inputs were most closely spatially matched with spiking output and an examination of the timing of synaptic inputs revealed that glutamatergic synaptic inputs are time-locked to spiking output. This suggests that, despite the potential for GABAergic inputs to depolarise developing tectal neurons (Akerman & Cline 2006), glutamatergic inputs are the most important drivers of tectal spiking activity.

In Chapter 4, I identified a population of tectal neurons that did not fire action potentials in response to visual stimuli, despite receiving visually evoked glutamatergic and GABAergic synaptic inputs. Compared to visually spiking neurons, the non-spiking neurons were found to exhibit similar levels of intrinsic excitability, although they did exhibit a slightly higher spike threshold. However, an investigation of the synaptic inputs to the two groups of neurons revealed marked differences. Whereas their GABAergic synaptic conductances were of similar amplitude, the visually non-spiking neurons had substantially less excitatory glutamatergic input. Computer simulations of developing tectal neurons supported the conclusion that the paucity of glutamatergic excitation, and not the difference in spike threshold, was the most likely explanation for the lack of spiking output. Investigating the spatiotemporal properties of synaptic inputs to the different groups of neurons, it was found that visually non-spiking neurons can still exhibit spatially coherent synaptic RFs, which are comparable to those observed in visually spiking neurons. This indicates that the development of spatially coherent glutamatergic and GABAergic RFs may be independent of postsynaptic spiking. Interestingly, it was also found that the glutamatergic inputs to visually non-spiking neurons reach their peak later than the glutamatergic inputs to visually spiking neurons. This observation is consistent with the idea that visually non-spiking neurons receive relatively more glutamatergic input through recurrent

excitatory circuitry within the optic tectum, and less from monosynaptic inputs from retinal ganglion cells (Pratt et al. 2008).

In Chapter 5, I demonstrated that visually non-spiking tectal neurons, such as those I had characterised in Chapter 4, can be converted into visually spiking neurons by subjecting the animal to a brief period of visual conditioning. This represents the first demonstration of the emergence of stimulus-driven spiking in developing neurons *in vivo*. Furthermore, it was shown that the first visual spiking output of converted tectal neurons could already be spatially coherent. However, an examination of how the converted RFs relate to the spatiotemporal properties of the conditioning stimulus suggested that this activity-dependent process is distinct from the effects that can be achieved through spike-dependent plasticity processes. Whereas STDP processes can mediate *instructive* changes to RFs that reflect the statistical properties of the stimulus-driven activity (Richards et al. 2010), the conversion to a spiking neuron does not reflect the input statistics and is more consistent with a *permissive* form of plasticity (Crair 1999).

In order to understand the changes that underlie this activity-dependent process, I performed a series of whole cell recordings in neurons that I had first converted into spiking neurons in cell-attached mode. These experiments revealed that the intrinsic excitability of converted spiking neurons was not different from visually non-spiking neurons. However, recordings of the synaptic inputs demonstrated that converted neurons had significantly increased glutamatergic inputs compared to visually non-spiking neurons, while the amplitude of their GABAergic inputs was similar. This is consistent with a mechanism in which the activity-dependent unsilencing of spiking activity in developing tectal neurons is mediated by the recruitment of more glutamatergic synaptic excitation. To investigate the possibility that this recruitment of glutamatergic input could be mediated by depolarising GABAergic inputs acting in synergy with the NMDA receptor (NMDAR), I first performed *in vivo* gramicidin perforated patch clamp recordings and observed that depolarising GABAergic responses were exclusively found in visually non-spiking neurons. Having confirmed that non-spiking neurons exhibit NMDAR-mediated synaptic currents, I then used pharmacological techniques to investigate the requirement for both depolarising GABAergic inputs and NMDAR activation for the activity-dependent unsilencing of tectal neurons. Either reducing the depolarising action of $GABA_A$

receptor ($GABA_AR$) signalling by blocking the NKCC1 chloride (Cl^-) transporter, or blocking NMDAR-mediated transmission, abolished the conversion of visually non-spiking neurons into visually spiking neurons. Taken together, these data support a model in which the activity-dependent unsilencing of tectal neurons relies on depolarising GABAergic inputs acting in synergy with the NMDAR in order to recruit more glutamatergic excitation.

Having reviewed the central observations of this thesis, I will use the remainder of this chapter to relate these findings to previous work, to consider potential caveats and unresolved questions, and to discuss the wider implications for understanding circuit development.

6.2 The development of emmetropic vision

The finding that developing Xenopus eyes are initially hyperopic but undergo a developmental emmetropisation is consistent with findings in other species (Wallman et al. 1981; Easter & Nicola 1996). As in zebrafish (Easter & Nicola 1996), the process of emmetropisation in Xenopus at the onset of vision seems to be driven mainly by two changes in the lens. First, embryonic lenses become progressively larger over development. Second, the refractive characteristics of the lens change, which leads to a shortening of their focal length. This change in refractive index suggests that there are interesting developmental changes to the material composition of the lens. Easter and Nicola (Easter & Nicola 1996) reported a change in the 'core' region of the lens, which is its most refractive element (Fernald & Wright 1983). While it was not quantitatively addressed in this thesis, I did observe that the Xenopus lens also appears to acquire a more distinct core region over the course of development. What material changes underlie this change in the optical characteristics of the lens, and particularly its core region, will require further research.

Changes in the ratio of focal length to lens diameter may only occur in the earliest phase of Xenopus development, as it has been shown that the ratio of focal length to lens diameter remains constant at later stages (Land & Stirling 1975). Interestingly, a study of the optical properties of Xenopus eyes from stage 46 through metamorphosis and into adulthood found that, as the eyes of developing Xenopus larvae continue to grow, they become mildly hyperopic in water (Land & Stirling 1975). This slight hyperopia in water reduces their myopia in air, and may represent an adaptive 'trade-off' for an amphibian that must use its visual system both on

land and in water. It also implies that even during later stages of life, Xenopus laevis may not experience a perfect image of the world, such that their visual acuity remains limited by the optics of their eyes.

How does the eye of the animal 'know' whether it has reached a sufficiently emmetropic state? There is evidence from other species that the development of emmetropic vision may be dependent on visual experience (Troilo 1992), which implicates some form of feedback mechanism. For instance, disrupting visual input through lid suturing or translucent occlusion of the eyes can produce myopia in the monkey, the cat and the chicken (Wiesel & Raviola 1977; Gollender et al. 1979; Troilo & Wallman 1991). As visual experience regulates emmetropia even when the optic nerve is severed (Troilo & Wallman 1991), this is likely to be an eye-autonomous process. These comparative studies suggest that the development and / or maintenance of emmetropia in Xenopus may also depend on visual experience. However, it is worth noting that the initial emmetropisation of developing zebrafish eyes, which parallels that of Xenopus larvae at the onset of vision, does not depend on visual experience (Easter & Nicola 1996). One explanation for this may be that the experience-dependent regulation of emmetropia reported in other species is thought to depend on changes in eye size (Wiesel & Raviola 1977; Gollender et al. 1979; Troilo & Wallman 1991), whereas the process of emmetropisation reported in larval zebrafish (Easter & Nicola 1996) and now here in Xenopus, appears to be primarily driven by changes in the refractive index of the lens. Therefore, the emmetropisation of the eyes of developing Xenopus larvae observed in Chapter 3 may involve different mechanisms to those involved in the experience-dependent regulation described in other species.

6.3 The availability of visuospatial information to the optic tectum

In Chapter 3, I showed that in spite of their initial hyperopia, the optics of the eye in developing Xenopus larvae are adequate to allow stimuli in the environment to drive patterned activity on a spatially restricted area of the retina. I confirmed that such visuospatial information was available to developing tectal neurons at stages immediately after the onset of vision, showing that tectal neurons can respond only to a restricted area of visual space. These findings extend previous observations of the extent of spatial information present in the spiking output of tectal neurons through intact eyes (Gaze et al. 1974; Holt & Harris 1983). In agreement with these earlier findings, tectal neurons were typically found to have large RFs. While the imperfect

optics of the developing eye and the resultant blurring of the visual image on the retina are likely to contribute to the large size of RFs of tectal neurons, large RFs were also observed in a study in which visual images were projected directly onto the excised retina (Tao & Poo 2005). This suggests that large RFs at these earliest stages of vision are an intrinsic feature of the developing retinotectal circuitry.

Despite the relatively large size of RFs in the optic tectum, the observation that the visual environment can drive patterned activity immediately after the onset of vision has important implications for visually guided development of the Xenopus retinotectal system. It was noted earlier that the developing Xenopus retina does not exhibit the spontaneous waves of correlated activity that have been found to instruct visual system development in other species (Demas et al. 2012). The observation that, in Xenopus, visual stimuli can evoke spatially patterned activity from the time that retinal ganglion cell axons first arrive in the tectum suggests that correlations driven by the environment may fulfill the role that retinal waves play in the mammalian visual system (Meister et al. 1991; Penn et al. 1998; Sernagor & Grzywacz 1996; Stellwagen & Shatz 2002; Wong et al. 1993; Ackman et al. 2012). From an evolutionary perspective, the situation in Xenopus may represent a more ancient mechanism for driving correlated activity, which can propagate through the visual system to guide circuit formation. Xenopus embryos, like other anamniotes, develop *ex utero* and *ex ovo*, and are freely navigating a visual environment that is able to drive patterned activity on spatially restricted areas of the retina. Amniotes, on the other hand, develop within opaque enclosures (i.e. eggs or uteri), which prevent visual stimuli from driving retinal activity until after the time of hatching or birth. Retinal waves may therefore be an evolutionary adaptation to this developmental 'dark' period, allowing the animal's visual system to refine synaptic connectivity even before visual experience. This hypothesis would predict that visual experience is the principal regulator of activity-dependent development in the visual system of all anamniotes, and that retinal waves are only to be found in the retinae of amniotes (Demas et al. 2012).

6.4 Silent neurons in the developing tectum

A major aim of this thesis was to understand the regulation of early spiking activity in the developing optic tectum. One of the most significant observations was that the immature tectum contains a substantial population of visually non-spiking neurons. The detection of

these neurons was possible because of the particular recording techniques that were used. By performing visually guided patch clamp recordings, I was able to ensure that neurons were not selected as a function of their responsiveness to stimuli. This is in contrast to other *in vivo* methods that use blind extracellular recordings, which are likely to be biased towards responsive neurons (Shoham et al. 2006). Furthermore, by recording spiking activity in cell-attached mode, I ensured that the intrinsic properties and ionic gradients of the neurons remained undisturbed.

I hypothesised that visually non-spiking neurons were a feature of early tectal development, and that these neurons acquire the ability to generate spikes as the system matures. One important question, of course, is whether these neurons are a genuine non-spiking population, or whether they were simply not stimulated appropriately by the experimental protocol. For instance, these neurons may be selective to other visual stimuli. This did not appear to be the case however, as it was confirmed that the lack of spiking output was not stimulus-specific; neurons that did not spike to the RF mapping protocol also did not spike in response to a moving bar stimulus. Moreover, the observation that the majority of visually non-spiking neurons had spatially coherent synaptic inputs, with RF centres that lay within the area of visual stimulation, suggests that these neurons were tuned to the RF mapping stimuli. Also, calcium (Ca^{2+})-imaging experiments conducted in tadpoles of stages 48-52 (16-64 days post fertilisation; Muldal, Lillicrap and Brodersen, personal communication) reveal that the vast majority of mature tectal neurons exhibits visual spiking responses to the same stimuli that were used in this thesis. This supports the conclusion that the population of visually non-spiking neurons is indeed a developmental property of the optic tectum. The fact that I was able to convert these visually non-spiking neurons into spiking neurons by means of a relatively brief period of visual stimulation is consistent with this idea.

6.5 The relationship between spiking output and synaptic input in the developing optic tectum

In this thesis I set out to relate spiking activity to the properties of excitatory and inhibitory synaptic inputs in developing tectal neurons. In order to achieve this, it was necessary to develop a method for recording extracellular spiking activity and then synaptic input activity within the same neuron *in vivo*. This technique enabled me to examine the relationship between

spiking behaviour, glutamatergic inputs and GABAergic inputs.

A first question was whether the depolarising actions of GABA that have been reported in the developing optic tectum (Akerman & Cline 2006), mean that the GABAergic system drives tectal spiking activity. In support of this idea, depolarising GABAergic inputs have been shown to elicit spikes in other developing systems (Chen et al. 1996). However, a series of observations described in this thesis support the conclusion that despite the potential for GABA to be depolarising (Akerman & Cline 2006), glutamatergic inputs are the principal driver of spiking activity in developing tectal neurons. In Chapter 3, I reported that glutamatergic inputs correlate best with tectal spiking output, both in terms of spatial arrangement and temporal distribution. Moreover, in Chapter 4 it was shown that neurons that do not elicit spikes in response to visual stimuli have significantly smaller glutamatergic synaptic conductances, but their GABAergic synaptic conductances are comparable to those in visually spiking neurons. Finally, in Chapter 5, the emergence of spiking activity was accompanied by a selective increase in glutamatergic synaptic input. These observations suggest that GABA does not have a direct excitatory effect on tectal neurons, and support the conclusion that although the reversal potential for $GABA_A$Rs may lie above the membrane potential (Akerman & Cline 2006), the reversal potential lies below the spike threshold. This is consistent with the findings of Richards and colleagues, who found that blocking GABAergic neurotransmission in the developing tectum at stages 40-44 does not alter the overall levels of tectal spiking (Richards et al. 2010). The absence of a simple excitatory or inhibitory role for $GABA_A$Rs does not mean that GABAergic inputs are unimportant for tectal development. In fact, GABAergic inputs have been shown to enable instructive changes to the RFs of tectal neurons (Richards et al. 2010; Tao & Poo 2005) by preventing spurious correlations in tectal spiking activity (Richards et al. 2010). Therefore, depolarising GABAergic inputs seem to exert more subtle effects upon spiking activity in the tectum, presumably through a combination of shunting inhibition and the facilitation of spiking activity, and in a manner that depends upon the temporal relationship of glutamatergic and GABAergic inputs (Gao et al. 1998; Gulledge & Stuart 2003; Staley & Mody 1992; Richards et al. 2010).

The developmental changes in GABA's effect upon developing neurons also mean that this neurotransmitter plays a constantly changing role. In fact, the observation in Chapter 5 that

spiking and non-spiking tectal neurons exhibit opposing responses to $GABA_AR$ activation (Figure 5.7) suggests that GABAergic transmission has multiple roles at any particular stage. This could reflect cell-type specific differences in Cl^- gradients, which have been reported in the mature brain (Martina et al. 2001). However, it seems more likely to reflect developmental differences between tectal neurons (Wu et al. 1996). Such a situation would not be unique to the tectum; in the most extreme case of a developmental heterogeneity amongst neurons, newborn granule cells in the mature dentate gyrus have been shown to exhibit depolarising GABAergic inputs, whilst the mature neurons that surround them experience hyperpolarising GABA (Chancey et al. 2013; Ge et al. 2005).

It was noted above that in addition to the strength of glutamatergic and GABAergic synaptic inputs, their relative timing is also an important determinant of spiking output (Gao et al. 1998; Gulledge & Stuart 2003; Staley & Mody 1992). In investigating the temporal properties of visually driven synaptic inputs in the developing tectum, it is important to realise that the timing of responses is heavily influenced by phototransduction kinetics in the retina, which introduce a delay of at least 100 ms and are also likely to generate significant variability (Akerman & Cline 2006; Aizenman et al. 2003). It is therefore difficult to clearly distinguish visually evoked monosynaptic retinal input from polysynaptic tectal input, or feedforward inhibition from feedback inhibition. Nevertheless, it was evident that the strongest glutamatergic input tends to arrive later in non-spiking neurons than in spiking neurons, by tens of milliseconds. While it may seem surprising to find differences on the order of tens of milliseconds in the timing of stimulus-evoked synaptic input, this is likely to be explained by the fact that measurements were made from the peak rather than the onset of compound synaptic currents and it is known that recurrent tectal circuitry can drive tectal activity for up to hundreds of milliseconds after a stimulus (Pratt et al. 2008). Indeed, this suggests that the reason glutamatergic drive to visually non-spiking neurons occurs much later than to spiking neurons is due to a relatively larger contribution of recurrent excitatory circuitry in the tectum (Pratt et al. 2008) and a relatively small contribution of direct, monosynaptic input from the retina. It remains to be tested whether a greater reliance on recurrent excitatory inputs in non-spiking neurons could be a cause, or effect, of their lack of spiking activity. However, it is worth noting that Pratt and colleagues have previously reported that the maturation of excitatory synaptic transmission in the tectum involves a gradual reduction of recurrent excitation, in a process that relies on spike timing

dependent plasticity processes (Pratt et al. 2008).

6.6 The emergence of visual spiking activity in tectal neurons

Having identified a large population of visually non-spiking neurons in the developing tectum, a major focus of this thesis was to explore how neurons might become able to generate visual spikes and thereby take part in sensory processing. There are a number of conceivable ways in which a neuron could accomplish this. First, through morphological growth processes a neuron could elaborate its dendrites and thereby form more excitatory synaptic contacts (Cohen-Cory 2002; Cline 2001). Second, the neuron could increase its intrinsic excitability (Aizenman et al. 2003). Third, the neuron could increase the efficacy of existing excitatory synaptic contacts (Wu et al. 1996).

I focused on the novel question of whether a non-spiking neuron can be rapidly converted into a spiking neuron in an activity-dependent manner. This question is particularly relevant for non-spiking tectal neurons, as all previously described activity-dependent processes that modify synaptic strength in the tectum rely upon postsynaptic spiking activity (Richards et al. 2010; L. I. Zhang et al. 1998; L. I. Zhang et al. 2000). I found that a brief period of enhanced visual stimulation was able to convert non-spiking neurons into spiking neurons. Investigating what activity-dependent changes enabled these neurons to start spiking, it was observed that the activity-dependent unsilencing of non-spiking tectal neurons relied on an increase in glutamatergic synaptic input. While this could represent a presynaptic change (Voronin & Cherubini 2004), previous work most strongly supports a postsynaptic locus (Isaac 2003). Many developing systems are characterised by glutamatergic synapses that are rich in NMDARs but lack AMPA receptors (AMPARs) (Liao et al. 1995; Durand et al. 1996; Isaac et al. 1995; Petralia et al. 1999; Liao et al. 1999) and there is evidence that this also holds true for the first glutamatergic synapses onto tectal neurons (Wu et al. 1996). Such ‘silent synapses’ can be ‘unsilenced’ through neuronal activity (Durand et al. 1996; Isaac et al. 1995; Petralia et al. 1999; Liao et al. 1995; Liao et al. 1999), in a manner that is dependent upon postsynaptic NMDAR activation and the insertion of AMPARs into the postsynaptic membrane (Liao et al. 2001). The rapid dynamics of AMPAR-delivery to postsynaptic membranes would enable this process to occur on a time scale similar to that of the experiments described in this thesis (Shi et al. 1999). Such a process is consistent with my observations that the neurons that had

converted to spiking had acquired stronger AMPAR-mediated excitation and that blockade of NMDARs prevented the conversion of non-spiking neurons. Future work could explicitly test whether the locus of plasticity is pre- or postsynaptic, for instance by selectively interfering with postsynaptic AMPAR-insertion mechanisms (Takahashi et al. 2003).

6.7 A postsynaptic mechanism for activity-dependent unsilencing of silent neurons

In Chapter 5, I proposed and tested a mechanism by which depolarising GABAergic currents and NMDAR-activation can act in synergy to trigger the recruitment of AMPAR-mediated glutamatergic excitation to visually non-spiking tectal neurons (Figure 5.6). This model is in line with predictions by Ben-Ari and colleagues (Ben-Ari et al. 1997; Ben-Ari 2002), who proposed that the large GABAergic depolarisations observed in developing hippocampus could play a role in the recruitment of AMPAR-mediated excitation. The findings in Chapter 5 confirm such predictions, and extend them by showing that this process can be directly linked to activity driven by the visual environment. Moreover, it was shown that this process could convert previously silent neurons into neurons that are able to generate visually driven spikes - the first time that any activity-dependent process has been shown to mediate such a transition.

The proposed model represents a cell-autonomous mechanism, in the sense that an individual neuron has the properties (i.e. depolarising GABAergic inputs and NMDAR-containing glutamatergic synapses) that it requires to integrate into the circuit, and the changes that mediate this are changes to the neuron itself. However, the possibility remains that there are upstream effects resulting in increased excitation of tectal neurons. It is conceivable that the emergence of spiking did not represent a change in the neuron that I recorded from, but rather a change in retinal output or recurrent excitation within the tectum. Excitatory synapses within the retina can be potentiated following periods of enhanced visual stimulation (Wei et al. 2012), which could contribute to an increase in spiking activity in the tectum and the ‘unsilencing’ of tectal neurons described in Chapter 5. However, an increase in visually evoked retinal output would be predicted to not only increase the level of glutamatergic excitation in the tectum, but also the strength of GABAergic inputs to tectal neurons. The observation that glutamatergic inputs are selectively strengthened in converted tectal neurons suggests that any changes in the retina do not lead to a general increase in tectal spiking. Alternatively, visual stimulation could enhance recurrent excitation within the tectum through driving (spike-dependent) plasticity

processes in visually spiking tectal neurons (Engert et al. 2002; Mu & Poo 2006; L. I. Zhang et al. 2000; Richards et al. 2010). However, to account for the data reported here, such changes in recurrent excitatory circuits would have to involve depolarising GABAergic transmission, for which there is currently no evidence.

To fully rule out that changes upstream of visually non-spiking tectal neurons could underlie their activity-dependent unsilencing, a manipulation at the level of the postsynaptic neuron would be required. One possibility would be to use premature expression of the KCC2 Cl^- transporter in tectal neurons, which has been shown to lower the reversal potential for $GABA_A$Rs and force GABAergic inputs to be prematurely hyperpolarising (Akerman & Cline 2006). Selective interference with postsynaptic NMDARs could be used to similar effect, and has already been shown to impact glutamatergic synapse maturation in other systems (Z.-W. Zhang et al. 2013). It should be noted, however, that given the relatively low success rate of conversion to visual spiking (22%) and the duration of the experiments (holding the neuron in cell-attached mode for over 25 minutes, followed by at least 15 minutes of whole cell recording), it would be a technical challenge to carry out such experiments *in vivo*.

Further support for the postsynaptic mechanism comes from earlier work in Xenopus, where it was shown that visually driven depolarising GABAergic inputs to the developing retinotectal system are well placed to relieve the magnesium (Mg^{2+})-block of the NMDAR, and that interfering with GABAergic depolarisation by premature expression of the KCC2 Cl^--transporter has a detrimental effect on the maturation of glutamatergic inputs to tectal neurons (Akerman & Cline 2006; Akerman & Cline 2007). This is complemented by work in the developing mammalian cortex, where it was shown that interference with GABAergic depolarisation disrupts the maturation of excitatory synapses, and that this can be rescued by the postsynaptic expression of a voltage-independent form of the NMDAR (Wang & Kriegstein 2011; Wang & Kriegstein 2008). Indeed, a recent paper by Chancey and colleagues has pointed towards a role for the environment and the GABAergic system in regulating glutamatergic synapse maturation in newly born neurons of the adult dentate gyrus (Chancey et al. 2013). This is in line with earlier findings that an enriched environment during early postnatal life affects the maturation of glutamatergic and GABAergic neurotransmission (He et al. 2010). The findings in Chapter 5 extend these observations by showing for the first time that such a process can be driven

by direct sensory input and also provide the first study of its functional consequences for developing neurons (i.e. altered spiking output). Moreover, I have shown that this process can take place on a rapid time scale (i.e. ~15 minutes), *in vivo*, and on the lab bench.

An open question is whether this mechanism is available to all, or just a subset, of developing tectal neurons. Although the sampling of tectal neurons in this study is not biased in terms of responsiveness of the neurons, the recordings are conducted without knowledge of tectal neuronal subtype. While a diversity of tectal neurons has been characterised in the mature tectum (Lázár 1973), cell identity is much less clearly defined at the stages of development that were investigated in this thesis. Nevertheless, there are a number of observations from this thesis that suggest that the population of neurons in the developing optic tectum may be heterogeneous. First, not all non-spiking neurons showed an activity-dependent conversion to spiking. Second, not all non-spiking neurons were found to have depolarising GABAergic inputs. While this could represent differences in the maturational state or history of the neurons (Chancey et al. 2013; Ge et al. 2005), another possibility is that this is due to differences in Cl^- homeostasis associated with different cell types (Martina et al. 2001). This raises the possibility that the unsilencing mechanism described in this thesis is only available to a subset of neurons. A particularly relevant distinction would be that between excitatory and inhibitory subtypes of neurons, especially considering that inhibitory tectal circuits appear to develop first. Future work could address this question by fixing experimental tissue after the *in vivo* recordings, to relate the functional data to immunohistochemical markers of excitatory and inhibitory neurons.

6.8 Implications for activity-dependent development in the optic tectum

The data presented is therefore compatible with a model in which the first glutamatergic synapses onto developing tectal neurons are characterised by a low AMPAR and high NMDAR content (Wu et al. 1996), and are therefore silent at the resting membrane potential (Figure 5.6). However, when glutamatergic inputs are coincident with GABAergic inputs that depolarise the neuron, the voltage-dependent Mg^{2+} block of NMDARs is removed, leading to Ca^{2+} entry into the neuron (Leinekugel et al. 1995; Leinekugel et al. 1997). This triggers intracellular mechanisms that lead to the addition of AMPARs to the postsynaptic membrane, thereby ‘unsilencing’ these silent synapses (Liao et al. 1995; Liao et al. 1999; Petralia et al.

1999; Durand et al. 1996; Isaac et al. 1995), in a process that is likely to rely on postsynaptic activation of Ca^{2+}-calmodulin dependent protein kinase II (CaMKII) (Wu et al. 1996; Liao et al. 2001). This places depolarising GABAergic inputs at the centre of a spiking-independent plasticity process that is available to neurons that have weak glutamatergic input and cannot generate spikes in response to sensory stimulation.

The developmental transition in GABA's effect upon the postsynaptic neuron, from depolarising to hyperpolarising, may ensure that there is a restricted time window for this type of plasticity to occur. In fact, the recruitment of AMPAR-mediated excitation by depolarising GABAergic inputs may be self-limiting. In Chapter 5 (Figure 5.7), I made the observation that spiking neurons, which have presumably already acquired sufficient glutamatergic input, do not exhibit depolarising $GABA_AR$ responses. This implies that there could be a feedback mechanism in operation to reduce GABAergic depolarisation once sufficient AMPAR-mediated glutamatergic excitation has been recruited and / or reliable postsynaptic spiking occurs. There is evidence for activity-dependent regulation of Cl^- transporters (Fiumelli & Woodin 2007), including effects mediated by spiking activity (Brumback & Staley 2008). It would be interesting to specifically test this idea by exploring what happens to the reversal potential for $GABA_ARs$ in a converted neuron.

If it were found that the conversion of a non-spiking neuron into a spiking neuron affects the reversal potential for $GABA_ARs$, this would lead to the question of whether it is the emergence of postsynaptic spiking or the recruitment of AMPARs that is responsible. In other words, how do spiking activity and / or AMPAR-mediated transmission relate to mechanisms of Cl^- homeostasis? To test whether an increase in spiking behaviour affects a neuron's $GABA_AR$ reversal potential, one approach could be to use optogenetic tools to increase the spiking activity of tectal neurons, for instance by expression of channelrhodopsin-2 (Boyden et al. 2005). It is possible to use electroporation to deliver channelrhodopsin-2 expressing constructs in a mosaic fashion to the tectum of Xenopus (Falk et al. 2007). A light source could then be used to enhance activity in tectal neurons to test whether a period of enhanced spiking activity is sufficient to drive a change in the reversal potential for $GABA_ARs$. Alternatively, to test if a change in $GABA_AR$ reversal potential results from increased AMPAR-mediated transmission, AMPAR-insertion could be experimentally induced by expressing a constitutively active form of

CaMKII (Wu et al. 1996). The effects of AMPAR-insertion could be dissociated from effects of spiking activity by using optogenetic tools such as archaerhodopsin to dampen spiking activity (Chow et al. 2010).

A related question is whether this mechanism is a one-way developmental progression for the neuron, or whether it represents a bidirectional process. It has already been shown that the AMPAfication of silent synapses can be reversed in some conditions (Xiao et al. 2004). If this occurs, and a neuron loses its ability to spike in response to visual stimuli, could a neuron alter its reversal potential for $GABA_A$Rs and use this as a homeostatic mechanism to re-establish its spiking output? As alluded to above, Cl^- transporter function and expression have been shown to be sensitive to neuronal activity (Fiumelli & Woodin 2007), which enables a neuron to dynamically adjust its reversal potential for $GABA_A$Rs. This raises the possibility that the relationship between depolarising GABA and spiking output is a fundamental homeostatic process that serves to keep neurons within a functional input-output range. The most appropriate way to test such a mechanism would be to experimentally induce changes in spiking output and investigate their impact on the reversal potential for $GABA_A$Rs. Long term manipulation of spiking activity could be achieved by, for instance, altering neuronal excitability in a subset of neurons (Dong & Aizenman 2012). Manipulations of spiking activity on a more rapid timescale could be achieved using pharmacological blockade of activity, or in a cell-specific manner using eletroporation of optogenetic constructs for increasing or decreasing neuronal activity (Boyden et al. 2005; Chow et al. 2010). Finally, in order to homeostatically adjust the reversal potential for $GABA_A$Rs in response to activity, a neuron must have a mechanism to detect intracellular Cl^- levels. It has recently been demonstrated that it is possible to manipulate Cl^- levels in neurons using halorhodopsin, traditionally viewed as an optogenetic silencing tool (Raimondo et al. 2012). This approach would enable an exploration of the neuronal response to changes in the reversal potential of $GABA_A$Rs.

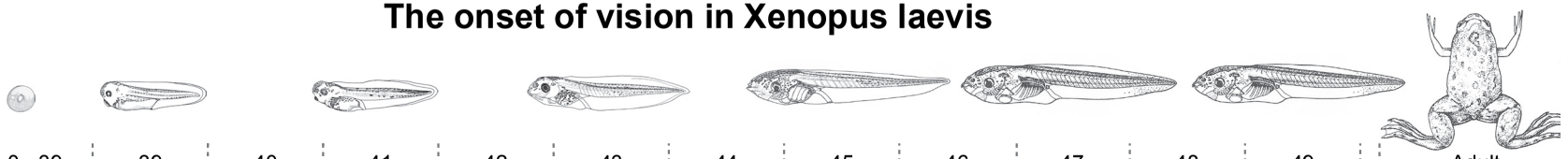
The fact that the activity-dependent conversion from non-spiking to spiking is dependent on depolarising GABAergic inputs suggests that this form of plasticity will be most prevalent during early stages of neuronal development. Indeed, the developmental period in which GABAergic inputs to tectal neurons are depolarising may represent the first stage in a two-tier model for synaptic circuit development: First, visually evoked depolarising GABAergic inputs

may enable tectal neurons to recruit AMPAR-mediated glutamatergic input. According to the data reported in Chapter 5, this recruitment is likely to be a permissive process that simply drives the potentiation of AMPAR-mediated input by unsilencing NMDAR-rich, AMPAR-poor synapses. As glutamatergic input increases, the neuron begins to exhibit consistent, stimulus-driven spiking output. This ability to generate spikes marks a transition to a second stage of plasticity for the developing neuron, allowing it to take part in spike time dependent, instructive plasticity processes that can lead to both synaptic potentiation and synaptic depression. These plasticity processes enable the precise sculpting of synaptic connections and neuronal response properties. At the same time, GABAergic inputs are becoming more hyperpolarising, perhaps maintaining the balance of excitation and inhibition, and closing the time window for GABA-mediated potentiation of glutamatergic inputs. It would be interesting to address this possibility by means of an experiment designed to take an individual neuron through both of these stages of plasticity. This could be accomplished by first employing a conditioning stimulus to convert a non-spiking neuron into a spiking neuron. Once this has been accomplished, a second conditioning protocol could be used to investigate whether the neuron undergoes instructive RF changes that are dependent upon the neuron's ability to spike.

6.9 Concluding remarks

In this thesis I have investigated the emergence of visual responses in the developing retinotectal system of Xenopus laevis *in vivo*. I have proposed a model in which visually driven, depolarising GABAergic inputs act in synergy with NMDARs at immature glutamatergic synapses to drive their maturation, enabling a neuron to recruit the excitation it needs to develop visual spiking activity. The requirement for depolarising GABAergic inputs may ensure that this process is only available during a limited developmental time window, or alternatively it may point towards a more general role for neuronal Cl^- homeostasis in regulating a neuron's spiking output. This thesis extends previous research on activity-dependent development, which has traditionally focused on how neurons change their response properties once they have already acquired the ability to spike. The unsilencing of tectal neurons represents a novel way for the sensory environment to influence visual system development, allowing non-spiking neurons to break their silence and be heard in the developing circuit.

The onset of vision in Xenopus laevis



Stage	0 - 39	39	40	41	42	43	44	45	46	47	48	49	Adult
Days after fertilisation	0 - 4 days	4 days		5 days		6 days		8 days		12 days		20 days	90+ days
Morphology	Little morphological complexity (Wu et al. 1999)						Small number of distinct morphologies (Wu et al. 1999)	Interneurons and projection neurons can be distinguished (Wu & Cline, 2003)			More complex protoforms of mature cells (Lázár 1973, Wu et al. 1999)		14 distinct cell morphologies (Lázár 1973)
	Continuous neurogenesis and differentiation in caudal tectum												
	Continuous activity-dependent effects on dendritic branching and stabilization, O'Rourke et al. 1994; Rajan & Cline 1998; Ruthazer et al. 2003												
Innervation	Innervation of tectum mostly complete by stage 39 Holt & Harris 1983		Continuous process of updating retinotopic innervation as the tectum expands caudally, Gaze et al. 1974										Complete innervation
Excitability	Neurons are excitable before stage 40 Spitzer & Lamborghini 1976 Baccaglini & Spitzer 1977							Continuous neurogenesis and differentiation in caudal tectum					Mature excitability
Synaptic maturation	Glutamatergic synapses with low AMPA content							Glutamatergic synapses with high AMPA content		Newborn neurons at caudal end of tectum still exhibit immature glutamatergic synapses, Wu et al. 1996			Mature synaptic transmission
GABA reversal	Depolarising GABAergic transmission Akerman & Cine 2006							Hyperpolarising GABAergic synapses Akerman & Cline 2006		More depolarising GABA in caudal tectum, Khakhalin & Aizenman 2012			Mature GABAergic transmission
Eye image formation	Hyperopia		Vision approximates emmetropia								Slight hyperopia in water, slight myopia in air Land & Stirling 1975		Slight hyperopia in water, slight myopia in air Land & Stirling 1975
Visual responses	Absent	Sparse, elicited by high contrast stimuli Holt & Harris 1983	Most neurons have visual synaptic inputs, but some fail to spike						Ubiquitous responses, elicited by high and low contrast stimuli Muldal, Lillicrap & Brodersen, unpublished observations				Responses throughout Gaze et al. 1974
		First retinal responses Witkovsky et al. 1976				Robust retinal responses Witkovsky et al. 1976							
Receptive field size	Spiking: 30-90 degrees Holt & Harris 1983		Glut ~85 degrees; GABA ~80 degrees; Spiking ~ 65 degrees							Spiking: 50-60 degrees Gaze et al. 1974			Spiking: ~15 degrees Gaze et al. 1974
						Glut & GABA: ~75% of visual field Tao & Poo 2005			Glut & GABA: ~40% of visual field Tao & Poo 2005		Glut: ~65 degrees Dong & Aizenman 2012		
						Spiking: 'Up to 180 degrees' Gaze et al. 1974							
Plasticity mechanisms	More spike-independent, permissive? (Chapter 5)		First in vivo demonstration of STDP in retinotectal system Zhang et al. 1998			Spike-dependent induction of direction selectivity, Engert et al. 2002, Mu and Poo 2006			Spike-time-dependent plasticity of recurrent excitation Pratt & Aizenman 2008		More spike-dependent, instructive? (Chapter 5)		Visual responses fully developed
						Instructive spike-time-dependent RF plasticity Vislay-Meltzer et al. 2006, Richards et al. 2010							

Figure legend provided on the next page

Figure A1: The onset of vision in Xenopus laevis
This timeline represents the events that together constitute the development of functional visual responses in the optic tectum of Xenopus laevis at the developmental stages relevant to this thesis (staging according to Nieuwkoop and Faber 1956). The first innervation of the tectum by axons from retinal ganglion cells and the first transmission of visual information take place around stages 39-40, and this thesis is concerned with the developmental stages immediately after these events. This figure is not exhaustive, but aims to provide a context for the developmental stages and events mentioned in this thesis and place some of the more important cited works in this context as well. It should be noted that due to the continuous process of neurogenesis in a proliferative zone at the caudal side of the tectum, tectal neurons of different stages of maturity coexist. This developmental timeline mainly illustrates the status of the most mature (rostrally located) neurons in the tectum, while acknowledging that new neurons with immature properties are still found in the caudal tectum. Black arrows indicate the developmental time window addressed by the experiments conducted in this thesis. Images of developing and adult Xenopus laevis (top row) are reproduced from Nieuwkoop and Faber (1956). Days after fertilisation are reported as under the rearing conditions used for this thesis, i.e. a 10/14h light/dark cycle and a temperature of 18 degrees, which is slightly below the 23 degrees used in the reference work for staging Xenopus (Nieuwkoop and Faber 1956). As Xenopus larvae are not kept until adulthood in the Akerman lab, the developmental time until adulthood is taken from this reference work.

Appendix II

Cell types in the developing optic tectum of Xenopus laevis

The optic tectum of adult Xenopus laevis is a layered structure with a diversity of neuronal morphologies. In his investigations of the adult tectum using the Golgi method (Lázár 1973), Lázár identified 14 morphologically distinct cell types (Figure A2a). Morphological classification of tectal neurons at the early developmental stages considered in this thesis, however, has been a more challenging endeavour. The first stage at which Lázár was able to obtain distinct morphologies using the Golgi method was stage 49 (Nieuwkoop & Faber 1956), already a considerable time after the onset of vision (Figure A2b). This yielded a markedly lower number of morphologically distinct cell types. More recent efforts using in vivo dye labelling methods (Wu et al. 1999; Wu & Cline 2003; Bestman et al. 2012) have shed light on the earlier stages of neuronal differentiation in the developing Xenopus tectum (Figure A2c). At these stages, the tectum can roughly be divided into a cell body-rich layer and a layer with fewer cell bodies, the neuropil, which is where sensory inputs to the tectum converge on the extending dendrites of developing tectal neurons. These studies have confirmed that the variety of morphologies observed in the adult is reduced in the young tectum. It is also important to note that, due to the continuous addition of newborn neurons from a neurogenic proliferative zone at the caudal side of the tectum (Straznicky & Gaze 1972; Wu et al. 1999), there is a rostrocaudal gradient of neuronal maturation. This has as a result that more mature morphologies can be observed rostrally while, simultaneously, more immature morphologies are found at the caudal end.

While such morphological studies have been able to shed light on the distribution of neuronal morphologies in the tectum, the association of morphology with functional attributes has remained tentative. In the zebrafish tectum - a related model system for neuronal development - genetics, morphological studies and functional studies have converged to allow for an association between neuronal morphology and a neuron's function in the tectal circuit (Nevin et al. 2010). Such information is not yet available for Xenopus, though more recent studies

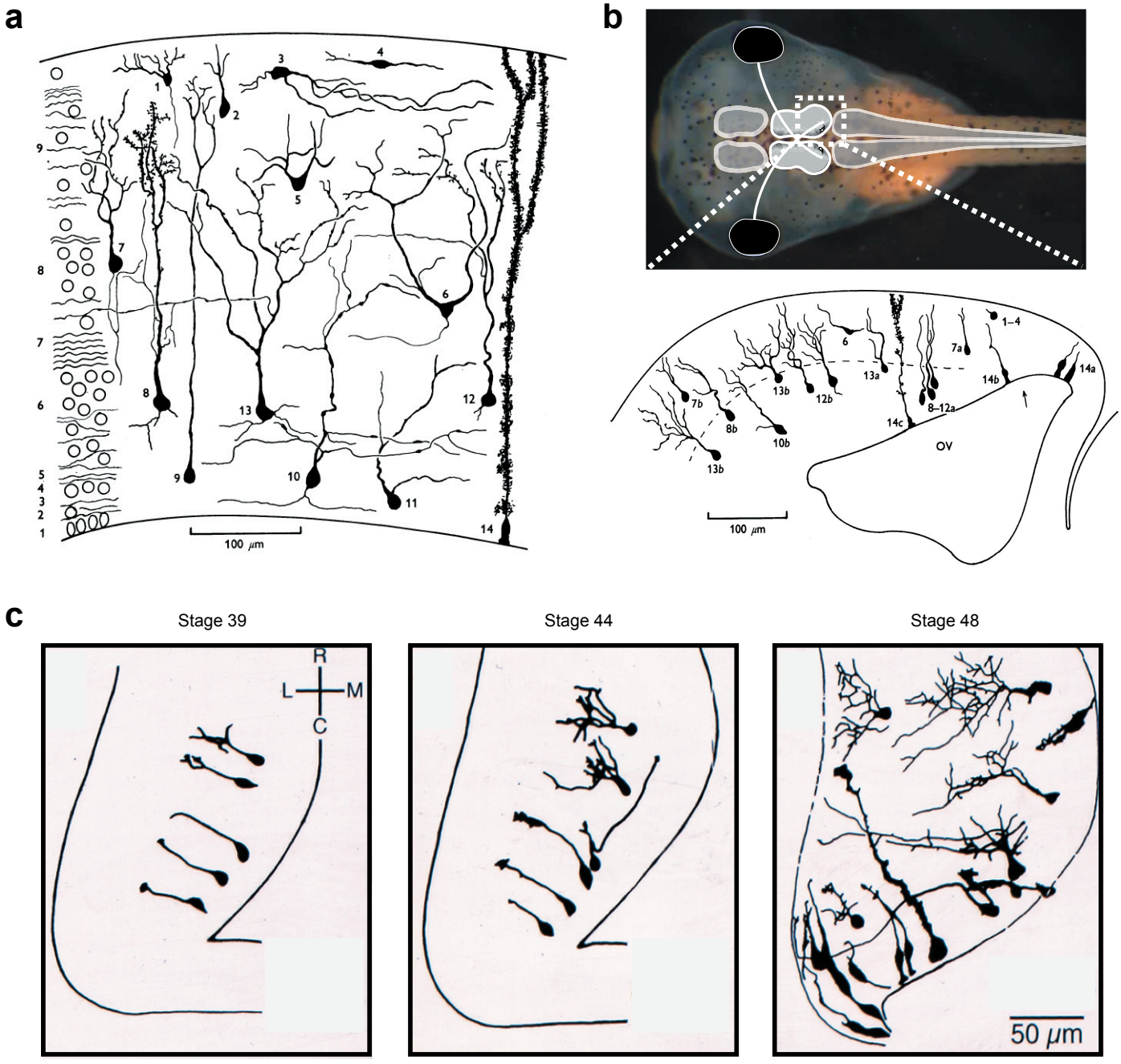


Figure A2: Cell types in the developing optic tectum of Xenopus laevis
a) The main morphologically distinct cell types in the optic tectum of a stage 49 Xenopus laevis tadpole; composite camera lucida drawings made after Golgi stain, reproduced from Lázár 1973. Numbers to the left indicate the different layers of the tectum, numbers next to cells identify different morphologically identified cell types. According to Lázár, 1973: 1) stellate, 2) amacrine, 3) horizontal, 4) fusiform or bipolar, 5) small ganglionic, 6) large ganglionic, 7) small, pear-shaped cell with recurrent axon, 8) pear-shaped cell with ascending axon and narrow dendritic tree, 9) axonless pear-shaped cell, 10) & 11) pear-shaped cells in deep periventricular layers, 12) pear-shaped cell with intratectal horizontal axon, 13) pyramidal cell, 14) ependymal cell. **b)** Morphologically distinct cell types in the optic tectum of a stage 49 tadpole, with numbers indicating a tentative classification of these neurons as one of the 14 cell types described in a), reproduced from Lázár 1973. *'a'* is used to label younger forms of neurons, while *'b'* and *'c'* label more mature forms. OV: optic ventricle. **c)** Tectal cell morphologies obtained from DiL labeling of a stage 39 (left), stage 44 (centre) and stage 48 (right) tadpole, adapted from Wu et al., 1999. Note the marked increases in cell complexity between stages 44 and 48.

have been able to identify functional subtypes of neurons, differentiating projection neurons and interneurons based on whether or not a projecting axon is present (Wu et al. 1999; Wu & Cline 2003; Miraucourt et al. 2012). Studying stage 46 tadpoles, Wu and Cline (Wu & Cline 2003) show that interneurons have densely branched dendritic arbours that extend further away from the cell body (up to 150 μm) and are characterised by consistently high growth rates during early development. Projection neurons, on the other hand, have less dense arbours that extend less far away from the cell body (< 100 μm) and slow down in growth rate as their complexity increases. However, it is interesting to note that young interneurons initially form a projecting axon that is subsequently retracted (Wu & Cline 2003), further complicating the morphological identification of newly generated neurons in the Xenopus tectum. In an effort to further characterise the distribution of functionally distinct cell types in the tectum, Miraucourt et al. (Miraucourt et al. 2012) examined the expression of markers of GABAergic and glutamatergic neurons at early developmental stages, and found that in stage 40-42 and stage 47 tadpoles, GABAergic neurons are found in both the cell body layer and the neuropil. While the cell body layer additionally had a population of GABA-negative neurons, the neurons located in the neuropil layer were predominantly GABA positive. Interestingly, in the youngest (stage 40-42) tadpoles, GABA-positive neurons were found mostly in the rostral area. However, this study left a large population of neuronal cell bodies unaccounted for, indicating that a number of neurons may not yet express the markers that identify mature neurons.

In this thesis, neuronal cell bodies targeted for patch clamping were located in the part of the cell body layer adjacent to the ventricular surface of the *caudal* half of the tectum of stage 40-44 animals. This suggests that these neurons belonged to a mixed population of neurons that is still acquiring distinct morphology as well as functional properties, and therefore it is hard to make a definitive statement about which cell types were sampled.

As a final note, it is discussed in the Introduction that the morphological maturation of a neuron and its functional development may interact, as there is mounting evidence that the process of elaborating and stabilising a dendritic arbour is influenced by neuronal activity and the success or failure of the formation of synaptic connections.

References

Ackman, J.B., Burbridge, T.J. & Crair, M.C., 2012. Retinal waves coordinate patterned activity throughout the developing visual system. *Nature*, 490, pp.219–225.

Ahmari, S.E., Buchanan, J. & Smith, S.J., 2000. Assembly of presynaptic active zones from cytoplasmic transport packets. *Nature Neuroscience*, 3(5), pp.445–451.

Aizenman, C.D. et al., 2003. Visually driven regulation of intrinsic neuronal excitability improves stimulus detection in vivo. *Neuron*, 39(5), pp.831–842.

Akerman, C.J. & Cline, H.T., 2006. Depolarizing GABAergic conductances regulate the balance of excitation to inhibition in the developing retinotectal circuit in vivo. *Journal of Neuroscience*, 26(19), pp.5117–5130.

Akerman, C.J. & Cline, H.T., 2007. Refining the roles of GABAergic signaling during neural circuit formation. *Trends in neurosciences*, 30(8), pp.382–389.

Akerman, C.J., Smyth, D. & Thompson, I.D., 2002. Visual experience before eye-opening and the development of the retinogeniculate pathway. *Neuron*, 36(5), pp.869–879.

Allman, J.M. & Kaas, J.H., 1971. Representation of the visual field in striate and adjoining cortex of the owl monkey (Aotus trivirgatus). *Brain Research*, 35(1), pp.89–106.

Apter, J.T., 1945. Projection of the retina on superior colliculus of cats. *Journal of neurophysiology*, 8, pp.123–134.

Artola, A. & Singer, W., 1987. Long-term potentiation and NMDA receptors in rat visual cortex. *Nature*, 330, pp.649–652.

Baccaglini, P.I. & Spitzer, N.C., 1977. Developmental changes in the inward current of the action potential of Rohon-Beard neurones. *The Journal of physiology*, 271, pp.93–117.

Bean, B.P., 2007. The action potential in mammalian central neurons. *Nature Reviews Neuroscience*, 8(6), pp.451–465.

Bear, M.F. & Malenka, R.C., 1994. Synaptic plasticity: LTP and LTD. *Current opinion in neurobiology*, 4, pp.389–399.

Ben Fredj, N. et al., 2010. Synaptic activity and activity-dependent competition regulates axon arbor maturation, growth arrest, and territory in the retinotectal projection. *Journal of Neuroscience*, 30(32), pp.10939–10951.

Ben-Ari, Y., 2002. Excitatory actions of GABA during development: the nature of the nurture. *Nature Reviews Neuroscience*, 3(9), pp.728–739.

Ben-Ari, Y. et al., 2007. GABA: a pioneer transmitter that excites immature neurons and generates primitive oscillations. *Physiological reviews*, 87(4), pp.1215–1284.

Ben-Ari, Y. et al., 1997. GABAA, NMDA and AMPA receptors: a developmentally regulated "ménage à trois." *Trends in neurosciences*, 20(11), pp.523–529.

Ben-Ari, Y., Cherubini, E. & Corradetti, R., 1989. Giant synaptic potentials in immature rat CA3 hippocampal neurones. *Journal of Physiology*, 416, pp.303–325.

Bestman, J. E., Lee-Osbourne, J., & Cline, H. T., 2012. In vivo time-lapse imaging of cell proliferation and differentiation in the optic tectum of Xenopus laevis tadpoles. *The Journal of Comparative Neurology*, *520*(2), pp.401–433.

Blakemore, C. & Cooper, G.F., 1970. Development of the brain depends on the visual environment. *Nature*, 228(5270), pp.477–478.

Blakemore, C. & Van Sluyters, R.C., 1975. Innate and environmental factors in the development of the kitten's visual cortex. *The Journal of physiology*, 248(3), pp.663–716.

Bliss, T.V.P. & Collingridge, G.L., 1993. A synaptic model of memory: long-term potentiation in the hippocampus. *Nature*, 361, pp.31–39.

Bliss, T.V.P. & Gardner-Medwin, A.R., 1973. Long-lasting potentiation of synaptic transmission in the dentate area of the unanaesthetized rabbit following stimulation of the perforant path. *The Journal of physiology*, 232(2), p.357.

Bliss, T.V.P. & Lømo, T., 1973. Long-lasting potentiation of synaptic transmission in the dentate area of the anaesthetized rabbit following stimulation of the perforant path. *The Journal of physiology*, 232, pp.331–356.

Blomfield, S., 1974. Arithmetical operations performed by nerve cells. *Brain Research*, 69(1), pp.115–124.

Bonhoeffer, F. & Gierer, A., 1984. How do retinal axons find their targets on the tectum? *Trends in neurosciences*, 7(10), pp.378–381.

Bormann, J., 1988. Electrophysiology of GABAA and GABAB receptor subtypes. *Trends in neurosciences*, 11(3), pp.112–116.

Bowery, N., 1989. GABAB receptors and their significance in mammalian pharmacology. *Trends in Pharmacological Sciences*, 10(10), pp.401–407.

Boyden, E.S. et al., 2005. Millisecond-timescale, genetically targeted optical control of neural activity. *Nature Neuroscience*, 8(9), pp.1263–1268.

Brumback, A.C. & Staley, K.J., 2008. Thermodynamic Regulation of NKCC1-Mediated Cl− Cotransport Underlies Plasticity of GABAA Signaling in Neonatal Neurons. *Journal of Neuroscience*, 28(6), pp.1301–1312.

Butts, D.A., 2002. Retinal waves: implications for synaptic learning rules during development. *The Neuroscientist*, 8(3), pp.243–253.

Butts, D.A., Kanold, P.O. & Shatz, C.J., 2007. A burst-based "Hebbian" learning rule at retinogeniculate synapses links retinal waves to activity-dependent refinement. *PLoS biology*, 5(3), p.e61.

Buzsáki, G., 1984. Feed-forward inhibition in the hippocampal formation. *Progress in*

neurobiology, 22, pp.131–153.

Cancedda, L. et al., 2004. Acceleration of visual system development by environmental enrichment. *Journal of neuroscience methods*, 24(20), pp.4840–4848.

Cang, J. et al., 2005. Ephrin-as guide the formation of functional maps in the visual cortex. *Neuron*, 48(4), pp.577–589.

Chalupa, L.M. & Snider, C.J., 1998. Topographic specificity in the retinocollicular projection of the developing ferret: an anterograde tracing study. *The Journal of comparative neurology*, 392(1), pp.35–47.

Chancey, J.H. et al., 2013. GABA depolarization is required for experience-dependent synapse unsilencing in adult-born neurons. *Journal of Neuroscience*, 33(15), pp.6614–6622.

Chen, G., Trombley, P.Q. & van den Pol, A.N., 1996. Excitatory actions of GABA in developing rat hypothalamic neurones. *Journal of Physiology*, 494 (Pt 2), pp.451–464.

Chow, B.Y. et al., 2010. High-performance genetically targetable optical neural silencing by light-driven proton pumps. *Nature*, 463(7277), pp.98–102.

Cline, H.T., 1991. Activity-dependent plasticity in the visual systems of frogs and fish. *Trends in neurosciences*, 14(3), pp.104–111.

Cline, H.T., 2001. Dendritic arbor development and synaptogenesis. *Current opinion in neurobiology*, 11, pp.118–126.

Cline, H.T., 1998. Topographic maps: Developing roles of synaptic plasticity. *Current Biology*, 8(23), pp.R836–R839.

Cline, H.T. & Haas, K., 2008. The regulation of dendritic arbor development and plasticity by glutamatergic synaptic input: a review of the synaptotrophic hypothesis. *The Journal of physiology*, 586(6), pp.1509–1517.

Cohen-Cory, S., 2002. The developing synapse: construction and modulation of synaptic structures and circuits. *Science*, 298(5594), pp.770–776.

Collingridge, G.L. & Bliss, T.V.P., 1987. NMDA receptors - their role in long-term potentiation. *Trends in neurosciences*, 10(7), pp.288–293.

Cooke, S.F. & Bear, M.F., 2010. Visual experience induces long-term potentiation in the primary visual cortex. *Journal of Neuroscience*, 30(48), pp.16304–16313.

Cooper, G.F., Daniel, P.M. & Whitteridge, D., 1953. Nerve impulses in the brainstem and cortex of the goat; spontaneous discharges and responses to visual and other afferent stimuli. *The Journal of physiology*, 120(4), pp.514–527.

Crair, M.C., 1999. Neuronal activity during development: permissive or instructive? *Current opinion in neurobiology*, 9(1), pp.88–93.

Crair, M.C. & Malenka, R.C., 1995. A critical period for long-term potentiation at thalamocortical synapses. *Nature*, 375(6529), pp.325–328.

Daoudal, G. & Debanne, D., 2003. Long-term plasticity of intrinsic excitability: learning rules and mechanisms. *Learning & Memory*, 10(6), pp.456–465.

Davis, G.W. & Bezprozvanny, I., 2001. Maintaining the stability of neural function: a homeostatic hypothesis. *Annual Review of Physiology*, 63, pp.847–869.

Debski, E.A. & Cline, H.T., 2002. Activity-dependent mapping in the retinotectal projection. *Current opinion in neurobiology*, 12(1), pp.93–99.

Delpire, E., 2000. Cation-chloride cotransporters in neuronal communication. *Physiological reviews*, 15, pp.309–312.

Demas, J.A., Payne, H. & Cline, H.T., 2012. Vision drives correlated activity without patterned spontaneous activity in developing Xenopus retina. *Developmental neurobiology*, 72(4), pp.537–546.

Dingledine, R. et al., 1999. The glutamate receptor ion channels. *Pharmacological reviews*, 51(1), pp.7–61.

Dong, W. & Aizenman, C.D., 2012. A competition-based mechanism mediates developmental refinement of tectal neuron receptive fields. *Journal of neuroscience*, 32(47), pp.16872–16879.

Dong, W. et al., 2009. Visual avoidance in Xenopus tadpoles is correlated with the maturation of visual responses in the optic tectum. *Journal of neurophysiology*, 101(2), pp.803–815.

Dunfield, D. & Haas, K., 2009. Metaplasticity Governs Natural Experience-Driven Plasticity of Nascent Embryonic Brain Circuits. *Neuron*, 64, pp.240–250.

Durand, G.M., Kovalchuk, Y. & Konnerth, A., 1996. Long-term potentiation and functional synapse induction in developing hippocampus. *Nature*, 381(6577), pp.71–75.

Easter, S.S., Jr & Nicola, G.N., 1996. The development of vision in the zebrafish (Danio rerio). *Developmental biology*, 180, pp.646–663.

Ebihara, S. et al., 1995. Gramicidin-perforated patch recording: GABA response in mammalian neurones with intact intracellular chloride. *Journal of Physiology*, 484(1), pp.77–86.

Eccles, J., 1961a. The Ferrier lecture: The nature of central inhibition. In Proceedings of the Royal Society of London Series B, Biological Sciences. pp. 445–476.

Eccles, J.C., 1961b. The mechanism of synaptic transmission. *Ergebnisse der Physiologie, biologischen Chemie und experimentellen Pharmakologie*, 51, pp.299–430.

Engert, F. et al., 2002. Moving visual stimuli rapidly induce direction sensitivity of developing tectal neurons. *Nature*, 419, pp.470–475.

Falk, J. et al., 2007. Electroporation of cDNA/Morpholinos to targeted areas of embryonic CNS in Xenopus. *BMC Developmental Biology*, 7(1), p.107.

Fatt, P. & Katz, B., 1953. The effect of inhibitory nerve impulses on a crustacean muscle fibre. *The Journal of physiology*, 121(2), pp.374–389.

Feller, M.B., 1999. Spontaneous correlated activity in developing neural circuits. *Neuron*, 22(4), pp.653–656.

Fernald, R.D. & Wright, S.E., 1983. Maintenance of optical quality during crystalline lens growth. *Nature*, 301(5901), pp.618–620.

Firth, S.I., Wang, C.-T. & Feller, M.B., 2005. Retinal waves: mechanisms and function in visual system development. *Cell calcium*, 37(5), pp.425–432.

Fiumelli, H. & Woodin, M.A., 2007. Role of activity-dependent regulation of neuronal chloride homeostasis in development. *Current opinion in neurobiology*, 17, pp.81–86.

Freeman, R.D. & Lai, C.E., 1978. Development of the optical surfaces of the kitten eye. *Vision Research*, 18, pp.399–407.

Freeman, R.D., Wong, S. & Zezula, S., 1978. Optical development of the kitten cornea. *Vision Research*, 18, pp.409–414.

Friedman, H.V. et al., 2000. Assembly of new individual excitatory synapses: time course and temporal order of synaptic molecule recruitment. *Neuron*, 27(1), pp.57–69.

Froemke, R.C. & Dan, Y., 2002. Spike-timing-dependent synaptic modification induced by natural spike trains. *Nature*, 416(6879), pp.433–438.

Galli, L. & Maffei, L., 1988. Spontaneous impulse activity of rat retinal ganglion cells in prenatal life. *Science*, 242(4875), pp.90–91.

Gao, X., Chen, G. & van den Pol, A.N., 1998. GABA-dependent firing of glutamate-evoked action potentials at AMPA/kainate receptors in developing hypothalamic neurons. *Journal of neurophysiology*, 79, pp.716–726.

Garaschuk, O., Hanse, E. & Konnerth, A., 1998. Developmental profile and synaptic origin of early network oscillations in the CA1 region of rat neonatal hippocampus. *The Journal of physiology*, 507 (Pt 1), pp.219–236.

Gaze, R.M., 1958. The representation of the retina on the optic lobe of the frog. *Experimental brain …*, 43(2), pp.209–214.

Gaze, R.M. et al., 1979. The relationship between retinal and tectal growth in larval Xenopus: implications for the development of the retino-tectal projection. *Journal of embryology and experimental morphology*, 53, pp.103–143.

Gaze, R.M., Chung, S.H. & Keating, M.J., 1972. Development of the retinotectal projection in Xenopus. *Nature*, 236(66), pp.133–135.

Gaze, R.M., Keating, M.J. & Chung, S.H., 1974. The evolution of the retinotectal map during development in Xenopus. *Proceedings of the Royal Society of London Series B …*, 185(80), pp.301–330.

Ge, S. et al., 2005. GABA regulates synaptic integration of newly generated neurons in the adult brain. *Nature*, 439(7076), pp.589–593.

Ghosh, A. & Greenberg, M., 1995. Calcium signaling in neurons: molecular mechanisms and cellular consequences. *Science*, 268(5208), pp.239–247.

Goda, Y. & Davis, G.W., 2003. Mechanisms of synapse assembly and disassembly. *Neuron*, 40(2), pp.243–264.

Gollender, M., Thorn, F. & Erickson, P., 1979. Development of axial ocular dimensions following eyelid suture in the cat. *Vision Research*, 19(2), pp.221–223.

Guillery, R.W., 1973. The effect of lid suture upon the growth of cells in the dorsal lateral geniculate nucleus of kittens. *Journal of Comparative Neurology*, 148, pp.417–422.

Gulledge, A.T. & Stuart, G.J., 2003. Excitatory actions of GABA in the cortex. *Neuron*, 37, pp.299–309.

Gustafsson, B. & Wigström, H., 1988. Physiological mechanisms underlying long-term potentiation. *Trends in neurosciences*, 11(4), pp.156–162.

Gustafsson, B. et al., 1987. Long-term potentiation in the hippocampus using depolarizing current pulses as the conditioning stimulus to single volley synaptic potentials. *Journal of Neuroscience*, 7(3), pp.774–780.

Haas, K., Li, J. & Cline, H.T., 2006. AMPA receptors regulate experience-dependent dendritic arbor growth in vivo. *Proceedings of the National Academy of Sciences*, 103(32), pp.12127–12131.

Hao, J. et al., 2009. An arithmetic rule for spatial summation of excitatory and inhibitory inputs in pyramidal neurons. *Proceedings of the National Academy of Sciences*, 106(51), pp.21906–21911.

Hartenstein, V., 1989. Early neurogenesis in xenopus: The spatio-temporal pattern of proliferation and cell lineages in the embryonic spinal cord. *Neuron*, 3(4), pp.399–411.

He, H.-Y., Hodos, W. & Quinlan, E.M., 2006. Visual deprivation reactivates rapid ocular dominance plasticity in adult visual cortex. *The Journal of neuroscience*, 26(11), pp.2951–2955.

He, S. et al., 2010. Early enriched environment promotes neonatal GABAergic neurotransmission and accelerates synapse maturation. *Journal of Neuroscience*, 30(23), pp.7910–7916.

Hebb, D.O., 1949. *The organization of behavior: A neuropsychological theory*, New York: Wiley.

Hennou, S., Khalilov, I. & Diabira, D., 2002. Early sequential formation of functional GABAA and glutamatergic synapses on CA1 interneurons of the rat foetal hippocampus. *European Journal of Neuroscience*, 16, pp.197–208.

Heynen, A.J. & Bear, M.F., 2001. Long-term potentiation of thalamocortical transmission in the adult visual cortex in vivo. *Journal of Neuroscience*, 21(24), pp.9801–9813.

Hille, B., 2001. *Ion Channels of Excitable Membranes* Third Edition, Sunderland, Massachusetts, U.S.A.: Sinauer.

Hodgkin, A.L. & Huxley, A.F., 1952. A quantitative description of membrane current and its application to conduction and excitation in nerve. *The Journal of physiology*, 117(4), pp.500–544.

Holt, C.E. & Harris, W.A., 1983. Order in the initial retinotectal map in Xenopus: a new technique for labelling growing nerve fibres. *Nature*, 301(5896), pp.150–152.

Hubel, D.H. & Wiesel, T.N., 1965. Binocular interaction in striate cortex of kittens reared with artificial squint. *Journal of neurophysiology*, 28, pp.1041–1059.

Hubel, D.H. & Wiesel, T.N., 1963. Receptive fields of cells in striate cortex of very young, visually inexperienced kittens. *Journal of neurophysiology*, 26, pp.994–1002.

Hubel, D.H. & Wiesel, T.N., 1962. Receptive fields, binocular interaction and functional architecture in the cat's visual cortex. *The Journal of physiology*, 160, pp.106–154.

Huberman, A.D., Feller, M.B. & Chapman, B., 2008. Mechanisms underlying development of visual maps and receptive fields. *Annual review of neuroscience*, 31(1), pp.479–509.

Isaac, J.T., Nicoll, R.A. & Malenka, R.C., 1995. Evidence for silent synapses: implications for the expression of LTP. *Neuron*, 15(2), pp.427–434.

Isaac, J.T.R., 2003. Postsynaptic silent synapses: evidence and mechanisms. *Neuropharmacology*, 45(4), pp.450–460.

Isaac, J.T.R. et al., 1997. Silent Synapses during Development of Thalamocortical Inputs. *Neuron*, 18(2), pp.269–280.

Jeffery, G., 1985. Retinotopic order appears before ocular separation in developing visual pathways. *Nature*, 313(6003), pp.575–576.

Johnston, D. & Wu, S.M.-S., 1999. *Foundations of Cellular Neurophysiology* Fourth Edition, Cambridge, MA, USA: MIT Press.

Kaas, J.H., 1997. Topographic maps are fundamental to sensory processing. *Brain Research Bulletin*, 44(2), pp.107–112.

Kaas, J.H., Guillery, R.W. & Allman, J.M., 1972. Some principles of organization in the dorsal lateral geniculate nucleus. *Brain, Behavior and Evolution*, 6(1-6), pp.283–299.

Kaila, K., 1994. Ionic basis of GABAA receptor channel function in the nervous system. *Progress in neurobiology*, 42, pp.489–537.

Katz, B., 1959. Mechanisms of synaptic transmission. *Reviews of Modern Physics*, 31(2), pp.524–531.

Katz, L.C. & Crowley, J.C., 2002. Development of cortical circuits: lessons from ocular dominance columns. *Nature Reviews Neuroscience*, 3(1), pp.34–42.

Katz, L.C. & Shatz, C.J., 1996. Synaptic activity and the construction of cortical circuits. *Science*, 274(5290), pp.1133–1138.

Kauer, J.A., Malenka, R.C. & Nicoll, R.A., 1988. A persistent postsynaptic modification mediates long-term potentiation in the hippocampus. *Neuron*, 1(10), pp.911–917.

Kelso, S.R., Ganong, A.H. & Brown, T.H., 1986. Hebbian synapses in hippocampus. *Proceedings of the National Academy of Sciences*, 83, pp.5326–5330.

Kerchner, G.A. & Nicoll, R.A., 2008. Silent synapses and the emergence of a postsynaptic

mechanism for LTP. *Nature Reviews Neuroscience*, 9(11), pp.813–825.

Khakhalin, A. S., & Aizenman, C. D., 2012. GABAergic transmission and chloride equilibrium potential are not modulated by pyruvate in the developing optic tectum of Xenopus laevis tadpoles. *PloS One*, *7*(4).

Khazipov, R. et al., 2001. Early development of neuronal activity in the primate hippocampus in utero. *The Journal of neuroscience*, 21(24), pp.9770–9781.

King, A.J., Schnupp, J.W.H. & Thompson, I.D., 1998. Signals from the superficial layers of the superior colliculus enable the development of the auditory space map in the deeper layers. *Journal of Neuroscience*, 18(22), pp.9394–9408.

Kingslake, R., 1951. *Lenses in Photography: The Practical Guide to Optics for Photographers*, Garden City, NY: Garden City Books.

Kiorpes, L. et al., 1987. Effects of early unilateral blur on the macaque's visual system. I. Behavioral observations. *Journal of Neuroscience*, 7(5), pp.1318–1326.

Knudsen, E.I., 1982. Auditory and visual maps of space in the optic tectum of the owl. *The Journal of neuroscience*, 2(9), pp.1177–1194.

Kyrozis, A. & Reichling, D.B., 1995. Perforated-patch recording with gramicidin avoids artifactual changes in intracellular chloride concentration. *Journal of neuroscience methods*, 57, pp.27–35.

Lamborghini, J.E., 1980. Rohon-beard cells and other large neurons in Xenopus embryos originate during gastrulation. *The Journal of comparative neurology*, 189(2), pp.323–333.

Land, M. & Stirling, R.V., 1975. Optics of *Xenopus* eyes during development. *Journal of embryology and experimental morphology*, 33(4), pp.915–940.

Lázár, G., 1973. The development of the optic tectum in Xenopus laevis: a Golgi study. *Journal of anatomy*, 116(Pt 3), pp.347–355.

Leinekugel, X. et al., 1997. Ca2+ oscillations mediated by the synergistic excitatory actions of GABA(A) and NMDA receptors in the neonatal hippocampus. *Neuron*, 18(2), pp.243–255.

Leinekugel, X. et al., 1995. Synaptic GABAA activation induces Ca2+ rise in pyramidal cells and interneurons from rat neonatal hippocampal slices. *The Journal of physiology*, 487 (Pt 2), pp.319–329.

Li, Y. et al., 2008. Experience with moving visual stimuli drives the early development of cortical direction selectivity. *Nature*, 456(7224), pp.952–956.

Li, Y., Fitzpatrick, D. & White, L.E., 2006. The development of direction selectivity in ferret visual cortex requires early visual experience. *Nature Neuroscience*, 9(5), pp.676–681.

Liao, D. et al., 1999. Regulation of morphological postsynaptic silent synapses in developing hippocampal neurons. *Nature Neuroscience*, 2(1), pp.37–43.

Liao, D., Hessler, N.A. & Malinow, R., 1995. Activation of postsynaptically silent synapses during pairing-induced LTP in CA1 region of hippocampal slice. *Nature*, 375(6530),

pp.400–404.

Liao, D., Scannevin, R.H. & Huganir, R., 2001. Activation of silent synapses by rapid activity-dependent synaptic recruitment of AMPA receptors. *Journal of neuroscience*, 21(16), pp.6008–6017.

Lien, C.-C. et al., 2006. Visual stimuli–induced LTD of GABAergic synapses mediated by presynaptic NMDA receptors. *Nature Neuroscience*, 9(3), pp.372–380.

Linden, D.J., 1999. The Return of the Spike: Review Postsynaptic Action Potentials and the Induction of LTP and LTD. *Neuron*, 22(4), pp.661–666.

Lisman, J. & Spruston, N., 2005. Postsynaptic depolarization requirements for LTP and LTD: a critique of spike timing-dependent plasticity. *Nature Neuroscience*, 8(7), pp.839–841.

Lisman, J., Schulman, H. & Cline, H., 2002. The molecular basis of CaMKII function in synaptic and behavioural memory. *Nature Reviews Neuroscience*, 3(3), pp.175–190.

Llinás, R.R., 1988. The intrinsic electrophysiological properties of mammalian neurons: insights into central nervous system function. *Science*, 242(4886), pp.1654–1664.

Lohmann, C., Myhr, K.L. & Wong, R.O.L., 2002. Transmitter-evoked local calcium release stabilizes developing dendrites. *Nature*, 418(6894), pp.177–181.

London, M. & Häusser, M., 2005. Dendritic computation. *Annual review of neuroscience*, 28, pp.503–532.

Lu, W. & Constantine-Paton, M., 2004. Eye opening rapidly induces synaptic potentiation and refinement. *Neuron*, 43(2), pp.237–249.

Lu, W.-Y. et al., 2001. Activation of Synaptic NMDA Receptors Induces Membrane Insertion of New AMPA Receptors and LTP in Cultured Hippocampal Neurons. *Neuron*, 29(1), pp.243–254.

Maffei, L. & Galli-Resta, L., 1990. Correlation in the discharges of neighboring rat retinal ganglion cells during prenatal life. *Proceedings of the National Academy of Sciences*, 87, pp.2861–2864.

Magee, J.C. & Johnston, D., 1997. A synaptically controlled, associative signal for Hebbian plasticity in hippocampal neurons. *Science*, 275(5297), pp.209–213.

Malenka, R.C., 1999. Long-Term Potentiation--A Decade of Progress? *Science*, 285(5435), pp.1870–1874.

Malenka, R.C., Kauer, J.A., Perkel, D.J. & Nicoll, R.A., 1989a. The impact of postsynaptic calcium on synaptic transmission — its role in long-term potentiation. *Trends in neurosciences*, 12(11), pp.444–450.

Malenka, R.C., Kauer, J.A., Perkel, D.J., Mauk, M.D., et al., 1989b. An essential role for postsynaptic calmodulin and protein kinase activity in long-term potentiation. *Nature*, 340, pp.554–557.

Malinow, R. & Malenka, R.C., 2002. AMPA receptor trafficking and synaptic plasticity. *Annual review of neuroscience*, 25, pp.103–126.

Markram, H. et al., 1997. Regulation of synaptic efficacy by coincidence of postsynaptic APs and EPSPs. *Science*, 275(5297), pp.213–215.

Martina, M., Royer, S. & Paré, D., 2001. Cell-type-specific GABA responses and chloride homeostasis in the cortex and amygdala. *Journal of neurophysiology*, 86(6), pp.2887–2895.

Mayer, M.L., Westbrook, G.L. & Guthrie, P.B., 1984. Voltage-dependent block by Mg2+ of NMDA responses in spinal cord neurones. *Nature*, 309(5965), pp.261–263.

McLaughlin, T. & O'Leary, D.D.M., 2005. Molecular gradients and development of retinotopic maps. *Annual review of neuroscience*, 28, pp.327–355.

McLaughlin, T. et al., 2003. Retinotopic map refinement requires spontaneous retinal waves during a brief critical period of development. *Neuron*, 40(6), pp.1147–1160.

Meister, M. et al., 1991. Synchronous bursts of action potentials in ganglion cells of the developing mammalian retina. *Science*, 252(5008), pp.939–943.

Meldrum, B. & Garthwaite, J., 1990. Excitatory amino acid neurotoxicity and neurodegenerative disease. *Trends in Pharmacological Sciences*, 11(9), pp.379–387.

Meyer, M.P. & Smith, S.J., 2006. Evidence from in vivo imaging that synaptogenesis guides the growth and branching of axonal arbors by two distinct mechanisms. *Journal of Neuroscience*, 26(13), pp.3604–3614.

Meyer, M.P., Niell, C.M. & Smith, S.J., 2003. Brain imaging: how stable are synaptic connections? *Current Biology*, 13(5), pp.R180–182.

Miraucourt, L. S., da Silva, J. S., Burgos, K., Li, J., Abe, H., Ruthazer, E. S., & Cline, H. T., 2012. GABA Expression and Regulation by Sensory Experience in the Developing Visual System. *PloS One*, *7*(1), e29086.

Monaghan, D.T. & Bridges, R.J., 1989. The excitatory amino acid receptors: their classes, pharmacology, and distinct properties in the function of the central nervous system. *Annual Review of Pharmacology and Toxicology*, 29, pp.365–402.

Mountcastle, V.B., 1957. Modality and topographic properties of single neurons of cat's somatic sensory cortex. *Journal of neurophysiology*, 20(4), pp.408–434.

Mountcastle, V.B. & Powell, T.P., 1959. Neural mechanisms subserving cutaneous sensibility, with special reference to the role of afferent inhibition in sensory perception and discrimination. *Bulletin of the Johns Hopkins Hospital*, 105, pp.201–232.

Movshon, J.A. & Van Sluyters, R.C., 1981. Visual neural development. *Annual review of psychology*, 32, pp.477–522.

Mu, Y. & Poo, M.-M., 2006. Spike timing-dependent LTP/LTD mediates visual experience-dependent plasticity in a developing retinotectal system. *Neuron*, 50(1), pp.115–125.

Mueller, A.L., Taube, J.S. & Schwartzkroin, P.A., 1984. Development of hyperpolarizing inhibitory postsynaptic potentials and hyperpolarizing response to gamma-aminobutyric acid in rabbit hippocampus studied in vitro. *Journal of Neuroscience*, 4(3), pp.860–867.

Nakanishi, S., 1992. Molecular diversity of glutamate receptors and implications for brain function. *Science*, 258(5082), pp.597–603.

Nevin, L. M., Robles, E., Baier, H., & Scott, E. K., 2010. Focusing on optic tectum circuitry through the lens of genetics. *BMC Biology*, *8*(1), 126.

Niell, C.M., Meyer, M.P. & Smith, S.J., 2004. In vivo imaging of synapse formation on a growing dendritic arbor. *Nature Neuroscience*, 7(3), pp.254–260.

Nieuwkoop, P.D. & Faber, J., 1956. *Normal table of Xenopus laevis (Daudin). A systematical and chronological survey of the development from the fertilized egg till the end of metamorphosis*, Amsterdam: North-Holland Publishing Company.

Nowak, L. et al., 1984. Magnesium gates glutamate-activated channels in mouse central neurones. *Nature*, 307(5950), pp.462–465.

Nusser, Z. et al., 1998. Cell type and pathway dependence of synaptic AMPA receptor number and variability in the hippocampus. *Neuron*, 21(3), pp.545–559.

O'Leary, D.D.M., Crespo, D., et al., 1986a. The effect of intraocular tetrodotoxin on the postnatal reduction in the numbers of optic nerve axons in the rat. *Developmental Brain Research*, 30(1), pp.96–103.

O'Leary, D.D.M., Fawcett, J.W. & Cowan, W.M., 1986b. Topographic targeting errors in the retinocollicular projection and their elimination by selective ganglion cell death. *Journal of Neuroscience*, 6(12), pp.3692–3705.

O'Rourke, N.A., Cline, H.T. & Fraser, S.E., 1994. Rapid remodeling of retinal arbors in the tectum with and without blockade of synaptic transmission. *Neuron*, 12(4), pp.921–934.

Owens, D.F. et al., 1996. Excitatory GABA responses in embryonic and neonatal cortical slices demonstrated by gramicidin perforated-patch recordings and calcium imaging. *Journal of Neuroscience*, 16(20), pp.6414–6423.

Penn, A.A. et al., 1998. Competition in Retinogeniculate Patterning Driven by Spontaneous Activity. *Science*, 279, pp.2108–2112.

Petralia, R.S. et al., 1999. Selective acquisition of AMPA receptors over postnatal development suggests a molecular basis for silent synapses. *Nature Neuroscience*, 2(1), pp.31–36.

Pfeiffenberger, C., Yamada, J. & Feldheim, D.A., 2006. Ephrin-As and patterned retinal activity act together in the development of topographic maps in the primary visual system. *Journal of Neuroscience*, 26(50), pp.12873–12884.

Pouille, F. & Scanziani, M., 2001. Enforcement of temporal fidelity in pyramidal cells by somatic feed-forward inhibition. *Science*, 293, pp.1159–1163.

Pratt, K.G. & Aizenman, C.D., 2007. Homeostatic regulation of intrinsic excitability and synaptic transmission in a developing visual circuit. *Journal of Neuroscience*, 27(31), pp.8268–8277.

Pratt, K.G., Dong, W. & Aizenman, C.D., 2008. Development and spike timing-dependent plasticity of recurrent excitation in the Xenopus optic tectum. *Nature Neuroscience*, 11(4),

pp.467–475.

Raimondo, J.V. et al., 2012. Optogenetic silencing strategies differ in their effects on inhibitory synaptic transmission. *Nature Neuroscience*, 15(8), pp.1102–1104.

Rajan, I. & Cline, H.T., 1998. Glutamate receptor activity is required for normal development of tectal cell dendrites in vivo. *Journal of Neuroscience*, 18(19), pp.7836–7846.

Ramón y Cajal, S., 1909. *Histologie du Systeme Nerveux de l'Homme et des Vertebres* 1st ed, Paris: A. Maloine.

Richards, B., Aizenman, C. & Akerman, C., 2010a. In vivo spike-timing-dependent plasticity in the optic tectum of Xenopus laevis. *Frontiers in Synaptic Neuroscience*, 2, pp.1–11.

Richards, B., Voss, O. & Akerman, C., 2010b. GABAergic circuits control stimulus-instructed receptive field development in the optic tectum. *Nature Neuroscience*, 13(9), pp.1098–1106.

Ruthazer, E. & Cline, H., 2004. Insights into activity-dependent map formation from the retinotectal system: a middle-of-the-brain perspective. *Journal of neurobiology*, 59, pp.134–146.

Ruthazer, E.S., Akerman, C.J. & Cline, H.T., 2003. Control of axon branch dynamics by correlated activity *in vivo*. *Science*, 301(5629), pp.66–70.

Sakaguchi, D.S. & Murphey, R.K., 1985. Map formation in the developing Xenopus retinotectal system: an examination of ganglion cell terminal arborizations. *Journal of Neuroscience*, 5(12), pp.3228–3245.

Sanes, J.R. & Lichtman, J.W., 1999. Development of the vertebrate neuromuscular junction. *Annual review of neuroscience*, 22(1), pp.389–442.

Sanes, J.R. & Lichtman, J.W., 2001. Development: Induction, assembly, maturation and maintenance of a postsynaptic apparatus. *Nature Reviews Neuroscience*, 2(11), pp.791–805.

Sastry, B.R., Goh, J.W. & Auyeung, A., 1986. Associative induction of posttetanic and long-term potentiation in CA1 neurons of rat hippocampus. *Science*, 232(4753), pp.988–990.

Sawtell, N.B. et al., 2003. NMDA receptor-dependent ocular dominance plasticity in adult visual cortex. *Neuron*, 38, pp.977–985.

Schmidt, J.T. & Buzzard, M., 1993. Activity-driven sharpening of the retinotectal projection in goldfish: development under stroboscopic illumination prevents sharpening. *Journal of neurobiology*, 24(3), pp.384–399.

Schmidt, J.T. & Eisele, L.E., 1985. Stroboscopic illumination and dark rearing block the sharpening of the regenerated retinotectal map in goldfish. *Neuroscience*, 14(2), pp.535–546.

Sernagor, E. & Grzywacz, N.M., 1996. Influence of spontaneous activity and visual experience on developing retinal receptive fields. *Current Biology*, 6(11), pp.1503–1508.

Shatz, C.J. & Stryker, M.P., 1988. Prenatal tetrodotoxin infusion blocks segregation of

retinogeniculate afferents. *Science*, 242(4875), pp.87–89.

Shi, S.H. et al., 1999. Rapid spine delivery and redistribution of AMPA receptors after synaptic NMDA receptor activation. *Science*, 284(5421), pp.1811–1816.

Shoham, S., O'Connor, D.H. & Segev, R., 2006. How silent is the brain: is there a "dark matter" problem in neuroscience? *Journal of comparative physiology. A, Neuroethology, sensory, neural, and behavioral physiology*, 192(8), pp.777–784.

Simon, D.K. & O'Leary, D.D.M., 1992. Development of topographic order in the mammalian retinocollicular projection. *The Journal of neuroscience*, 12(4), pp.1212–1232.

Sin, W.C. et al., 2002. Dendrite growth increased by visual activity requires NMDA receptor and Rho GTPases. *Nature*, 419(6906), pp.475–480.

Sivilotti, L. & Nistri, A., 1991. GABA receptor mechanisms in the central nervous system. *Progress in neurobiology*, 36, pp.35–92.

Sperry, R.W., 1963. Chemoaffinity in the orderly growth of nerve fiber patterns and connections. *Proceedings of the National Academy of Sciences*, 50, pp.703–710.

Spitzer, N., 2006. Electrical activity in early neuronal development. *Nature*, 444, pp.707–712.

Spitzer, N., 2002. Outside and in: development of neuronal excitability. *Current opinion in neurobiology*, 12(3), pp.315–323.

Spitzer, N.C., 1991. A developmental handshake: Neuronal control of ionic currents and their control of neuronal differentiation. *Journal of neurobiology*, 22(7), pp.659–673.

Spitzer, N.C. & Lamborghini, J.E., 1976. The development of the action potential mechanism of amphibian neurons isolated in culture. *Proceedings of the National Academy of Sciences of the United States of America*, 73(5), pp.1641–1645.

Spitzer, N.C. & Ribera, A.B., 1998. Development of electrical excitability in embryonic neurons: Mechanisms and roles. *Journal of neurobiology*, 37(1), pp.190–197.

Staley, K.J. & Mody, I., 1992. Shunting of excitatory input to dentate gyrus granule cells by a depolarizing GABAA receptor-mediated postsynaptic conductance. *Journal of neurophysiology*, 68(1), pp.197–212.

Stellwagen, D. & Shatz, C.J., 2002. An Instructive Role for Retinal Waves in the Development of Retinogeniculate Connectivity. *Neuron*, 33(3), pp.357–367.

Straznicky, K., & Gaze, R. M., 1972. The development of the tectum in Xenopus laevis: an autoradiographic study. *Journal of Embryology and Experimental Morphology*, *28*(1), pp.87–115.

Stryker, M.P. & Harris, W.A., 1986. Binocular impulse blockade prevents the formation of ocular dominance columns in cat visual cortex. *Journal of Neuroscience*, 6(8), pp.2117–2133.

Takahashi, T., Svoboda, K. & Malinow, R., 2003. Experience strengthening transmission by driving AMPA receptors into synapses. *Science*, 299(5612), pp.1585–1588.

Talbot, S.A. & Marshall, W.A., 1941. Physiological studies on neural mechanisms of visual location and discrimination. *American Journal of Opthalmology*, 24, pp.1255–1264.

Tao, H. & Poo, M., 2005. Activity-dependent matching of excitatory and inhibitory inputs during refinement of visual receptive fields. *Neuron*, 45, pp.829–836.

Tao, H.W. et al., 2001. Emergence of input specificity of ltp during development of retinotectal connections in vivo. *Neuron*, 31(4), pp.569–580.

Thorn, F., Gollender, M. & Erickson, P., 1976. The development of the kitten's visual optics. *Vision Research*, 16(10), pp.1145–1149.

Tian, N. & Copenhagen, D.R., 2003. Visual stimulation is required for refinement of ON and OFF pathways in postnatal retina. *Neuron*, 39(1), pp.85–96.

Troilo, D., 1992. Neonatal eye growth and emmetropisation—A literature review. *Eye (London, England)*, 6(2), pp.154–160.

Troilo, D. & Wallman, J., 1991. The regulation of eye growth and refractive state: an experimental study of emmetropization. *Vision Research*, 31(7-8), pp.1237–1250.

Turrigiano, G., Abbott, L.F. & Marder, E., 1994. Activity-dependent changes in the intrinsic properties of cultured neurons. *Science*, 264, pp.974–977.

Turrigiano, G.G. & Nelson, S.B., 2004. Homeostatic plasticity in the developing nervous system. *Nature Reviews Neuroscience*, 5(2), pp.97–107.

Turrigiano, G.G., Desai, N.S. & Rutherford, L.C., 1999. Plasticity in the intrinsic excitability of cortical pyramidal neurons. *Nature Neuroscience*, 2(6), pp.515–520.

Tyzio, R. et al., 1999. The establishment of GABAergic and glutamatergic synapses on CA1 pyramidal neurons is sequential and correlates with the development of the apical dendrite. *Journal of Neuroscience*, 19(23), pp.10372–10382.

Vaughn, J.E., 1989. Review: Fine structure of synaptogenesis in the vertebrate central nervous system. *Synapse*, 3(3), pp.255–285.

Vislay-Meltzer, R.L., Kampff, A.R. & Engert, F., 2006. Spatiotemporal specificity of neuronal activity directs the modification of receptive fields in the developing retinotectal system. *Neuron*, 50(1), pp.101–114.

Voronin, L.L. & Cherubini, E., 2004. "Deaf, mute and whispering" silent synapses: their role in synaptic plasticity. *The Journal of physiology*, 557(Pt 1), pp.3–12.

Wallman, J., Adams, J.I. & Trachtman, J.N., 1981. The eyes of young chickens grow toward emmetropia. *Investigative ophthalmology & visual science*, 20(4), pp.557–561.

Walter, J., Henke-Fahle, S. & Bonhoeffer, F., 1987a. Avoidance of posterior tectal membranes by temporal retinal axons. *Development*, 101, pp.909–913.

Walter, J., Kern-Veits, B., et al., 1987b. Recognition of position-specific properties of tectal cell membranes by retinal axons in vitro. *Development*, 101, pp.685–696.

Wang, D.D. & Kriegstein, A.R., 2011. Blocking early GABA depolarization with bumetanide

results in permanent alterations in cortical circuits and sensorimotor gating deficits. *Cerebral Cortex*, 21(3), pp.574–587.

Wang, D.D. & Kriegstein, A.R., 2008. GABA regulates excitatory synapse formation in the neocortex via NMDA receptor activation. *Journal of Neuroscience*, 28(21), pp.5547–5558.

Washbourne, P., 2004. Cell Adhesion Molecules in Synapse Formation. *Journal of Neuroscience*, 24(42), pp.9244–9249.

Washbourne, P., Bennett, J.E. & McAllister, A.K., 2002. Rapid recruitment of NMDA receptor transport packets to nascent synapses. *Nature Neuroscience*, 5(8), pp.751–759.

Wei, H.-P. et al., 2012. Activity-induced long-term potentiation of excitatory synapses in developing zebrafish retina in vivo. *Neuron*, 75(3), pp.479–489.

White, L.E., Coppola, D.M. & Fitzpatrick, D., 2001. The contribution of sensory experience to the maturation of orientation selectivity in ferret visual cortex. *Nature*, 411(6841), pp.1049–1052.

Wiesel, T.N. & Hubel, D.H., 1965. Comparison of the effects of unilateral and bilateral eye closure on cortical unit responses in kittens. *Journal of neurophysiology*, 28(6), pp.1029–1040.

Wiesel, T.N. & Hubel, D.H., 1963a. Effects of visual deprivation on morphology and physiology of cells in the cat's lateral geniculate body. *Journal of neurophysiology*, 26, pp.978–993.

Wiesel, T.N. & Hubel, D.H., 1963b. Single-cell responses in striate cortex of kittens deprived of vision in one eye. *Journal of neurophysiology*, 26, pp.1003–1017.

Wiesel, T.N. & Raviola, E., 1977. Myopia and eye enlargement after neonatal lid fusion in monkeys. *Nature*, 266(5597), pp.66–68.

Wilhelm, M., & Gabriel, R., 1999. Functional anatomy of the photoreceptor and second-order cell mosaics in the retina of Xenopus laevis. *Cell and Tissue Research*, *297*(1), pp.35–46.

Willshaw, D.J. & Malsburg, Von Der, C., 1976. How patterned neural connections can be set up by self-organization. *Proceedings of the Royal Society of London Series B, Biological Sciences*, 194, pp.431–445.

Witkovsky, P. et al., 1976. Photoreceptor thresholds and visual pigment levels in normal and vitamin A-deprived Xenopus tadpoles. *Journal of neurophysiology*, 39(6), pp.1272–1287.

Wong, R., 1999. Retinal waves and visual system development. *Annual review of neuroscience*, 22, pp.29–47.

Wong, R., Meister, M. & Shatz, C.J., 1993. Transient period of correlated bursting activity during development of the mammalian retina. *Neuron*, 11, pp.923–938.

Wu, G. Y. & Cline, H.T., 1998. Stabilization of dendritic arbor structure in vivo by CaMKII. *Science*, 279, pp.222–226.

Wu, G.Y. & Cline, H.T., 2003. Time-lapse in vivo imaging of the morphological development of Xenopus optic tectal interneurons. *The Journal of Comparative Neurology*, *459*(4), pp.392–406.

Wu, G.Y., Malinow, R. & Cline, H.T., 1996. Maturation of a central glutamatergic synapse. *Science*, 274(5289), pp.972–976.

Wu, G.Y., Zou, D.J., Rajan, I., & Cline, H.T., 1999. Dendritic dynamics in vivo change during neuronal maturation. *Journal of Neuroscience*, *19*(11), pp.4472–4483.

Xiao, M.-Y. et al., 2004. Creation of AMPA-silent synapses in the neonatal hippocampus. *Nature Neuroscience*, 7(3), pp.236–243.

Yamagata, M., Sanes, J.R. & Weiner, J.A., 2003. Synaptic adhesion molecules. *Current Opinion in Cell Biology*, 15(5), pp.621–632.

Zhang, L.I. et al., 1998. A critical window for cooperation and competition among developing retinotectal synapses. *Nature*, 395, pp.37–44.

Zhang, L.I., Tao, H.W. & Poo, M.-M., 2000. Visual input induces long-term potentiation of developing retinotectal synapses. *Nature Neuroscience*, 3(7), pp.708–715.

Zhang, W. & Linden, D.J., 2003. The other side of the engram: experience-driven changes in neuronal intrinsic excitability. *Nature Reviews Neuroscience*, 4(11), pp.885–900.

Zhang, Z.-W., Peterson, M. & Liu, H., 2013. Essential role of postsynaptic NMDA receptors in developmental refinement of excitatory synapses. *Proceedings of the National Academy of Sciences of the United States of America*, 110(3), pp.1095–1100.

Zhou, Q., Tao, H.W. & Poo, M.-M., 2003. Reversal and stabilization of synaptic modifications in a developing visual system. *Science*, 300(5627), pp.1953–1957.

Zito, K. & Svoboda, K., 2002. Activity-dependent synaptogenesis in the adult Mammalian cortex. *Neuron*, 35(6), pp.1015–1017.